Verification and Validation of Selected Fire Models for Nuclear Power Plant Applications

Volume 3:
Fire-Induced Vulnerability Evaluation (FIVE-Rev1)

January 2006

U.S. Nuclear Regulatory Commission
Office of Nuclear Regulatory Research
Washington, DC 20555-0001

Electric Power Research Institute
3412 Hillview Avenue
Palo Alto, CA 94303

Verification & Validation of Selected Fire Models for Nuclear Power Plant Applications

Volume 3: Fire-Induced Vulnerability Evaluation (FIVE-Rev1)

NUREG-1824 **EPRI 1011999**

January 2006

U.S. Nuclear Regulatory Commission
Office of Nuclear Regulatory Research (RES)
Division of Risk Analysis and Applications
Two White Flint North, 11545 Rockville Pike
Rockville, MD 20852-2738

U.S. NRC-RES Project Manager
M. H. Salley

Electric Power Research Institute (EPRI)
3412 Hillview Avenue
Palo Alto, CA 94303

EPRI Project Manager
R. P. Kassawara

DISCLAIMER OF WARRANTIES AND LIMITATION OF LIABILITIES

ORGANIZATION(S) THAT PREPARED THIS DOCUMENT:

U.S. Nuclear Regulatory Commission, Office of Nuclear Regulatory Research

Science Applications International Corporation

National Institute of Standards and Technology

ORDERING INFORMATION

Requests for copies of this report should be directed to EPRI Orders and Conferences, 1355 Willow Way, Suite 278, Concord, CA 94520, (800) 313-3774, press 2 or internally x5379, (925) 609-9169, (925) 609-1310 (fax).

COMMENTS ON DRAFT NUREG-1824 REPORT

This report is being published jointly by the U.S. Nuclear Regulatory Commission (NRC) and the Electric Power Research Institute (EPRI). Any interested party may submit comments on this report for consideration by the NRC and EPRI staffs. Comments may be accompanied by additional relevant information or supporting data. Please specify both the report number (Draft NUREG-1824) and the volume number in your comments, and send them by March 31, 2006, to the following address:

Chief Rules Review and Directives Branch
U.S. Nuclear Regulatory Commission
Mail Stop T-6D59
Washington, DC 20555-0001

For any questions about the material in this report, please contact:

Mark Henry Salley
Mail Stop T-10E50
U.S. Nuclear Regulatory Commission
Washington, DC 20555-0001
Phone: (301) 415-2840
Email: MXS3@nrc.gov

If EPRI members also wish to provide comments to EPRI, they may send them to the following address:

R.P. Kassawara
Electric Power Research Institute
3412 Hillview Avenue
Palo Alto, CA 94304
Phone: (650) 855-2775
Email: RKASSAWA@epri.com

CITATIONS

This report was prepared by

U.S. Nuclear Regulatory Commission,
Office of Nuclear Regulatory Research (RES)
Two White Flint North, 11545 Rockville Pike
Rockville, MD 20852-2738

Principal Investigators:
K. Hill
J. Dreisbach

Electric Power Research Institute (EPRI)
3412 Hillview Avenue
Palo Alto, CA 94303

Science Applications International Corp (SAIC)
4920 El Camino Real
Los Altos, CA 94022

Principal Investigators:
F. Joglar
B. Najafi

National Institute of Standards and Technology
Building Fire Research Laboratory (BFRL)
100 Bureau Drive, Stop 8600
Gaithersburg, MD 20899-8600

Principal Investigators:
K McGrattan
R. Peacock
A. Hamins

Volume 1, Main Report: B. Najafi, M.H. Salley, F. Joglar, J. Dreisbach
Volume 2, FDT^S: K. Hill, J. Dreisbach
Volume 3, FIVE-REV. 1: F. Joglar
Volume 4, CFAST: R. Peacock, J. Dreisbach, P. Reneke (NIST)
Volume 5, MAGIC: F. Joglar, B. Guatier (EdF), L. Gay (EdF), J. Texeraud (EdF)
Volume 6, FDS: K. McGrattan, J. Dreisbach
Volume 7, Experimental Uncertainty: A. Hamins, K. McGrattan

This report describes research sponsored jointly by U.S. Nuclear Regulatory Commission, Office of Nuclear Regulatory Research (RES) and Electric Power Research Institute (EPRI).

The report is a corporate document that should be cited in the literature in the following manner:

Verification and Validation of Selected Fire Models for Nuclear Power Plant Applications, Volume 3: Fire-Induced Vulnerability Evaluation (FIVE-Rev1), U.S. Nuclear Regulatory Commission, Office of Nuclear Regulatory Research (RES), Rockville, MD: 2005 and Electric Power Research Institute (EPRI), Palo Alto, CA. NUREG-1824 and EPRI 1011999.

ABSTRACT

There is a movement to introduce risk- and performance-based analyses into fire protection engineering practice, both domestically and worldwide. This movement exists in the general fire protection community, as well as the nuclear power plant (NPP) fire protection community.

In 2002, the National Fire Protection Association (NFPA) developed NFPA 805, *Performance-Based Standard for Fire Protection for Light-Water Reactor Electric Generating Plants, 2001 Edition.* In July 2004, the U.S. Nuclear Regulatory Commission (NRC) amended its fire protection requirements in Title 10, Section 50.48, of the *Code of Federal Regulations* (10 CFR 50.48) to permit existing reactor licensees to voluntarily adopt fire protection requirements contained in NFPA 805 as an alternative to the existing deterministic fire protection requirements. In addition, the nuclear fire protection community wants to use risk-informed, performance-based (RI/PB) approaches and insights to support fire protection decision-making in general.

One key tool needed to support RI/PB fire protection is the availability of verified and validated fire models that can reliably predict the consequences of fires. Section 2.4.1.2 of NFPA 805 requires that only fire models acceptable to the Authority Having Jurisdiction (AHJ) shall be used in fire modeling calculations. Further, Sections 2.4.1.2.2 and 2.4.1.2.3 of NFPA 805 state that fire models shall only be applied within the limitations of the given model, and shall be verified and validated.

This report is the first effort to document the verification and validation (V&V) of five fire models that are commonly used in NPP applications. The project was performed in accordance with the guidelines that the American Society for Testing and Materials (ASTM) set forth in *Standard E1355, "Evaluating the Predictive Capability of Deterministic Fire Models."* The results of this V&V are reported in the form of ranges of accuracies for the fire model predictions.

CONTENTS

FIGURES

TABLES

REPORT SUMMARY

This report documents the verification and validation (V&V) of five selected fire models commonly used in support of risk-informed and performance-based (RI/PB) fire protection at nuclear power plants (NPPs).

Background

Over the past decade, there has been a considerable movement in the nuclear power industry to transition from prescriptive rules and practices towards the use of risk information to supplement decision-making. In the area of fire protection, this movement is evidenced by numerous initiatives by the U.S. Nuclear Regulatory Commission (NRC) and the nuclear community worldwide. In 2001, the National Fire Protection Association (NFPA) completed the development of NFPA Standard 805, "Performance-Based Standard for Fire Protection for Light Water Reactor Electric Generating Plants 2001 Edition." Effective July, 16, 2004, the NRC amended its fire protection requirements in 10 CFR 50.48(c) to permit existing reactor licensees to voluntarily adopt fire protection requirements contained in NFPA 805 as an alternative to the existing deterministic fire protection requirements. RI/PB fire protection relies on fire modeling for determining the consequence of fires. NFPA 805 requires that the "fire models shall be verified and validated," and "only fire models that are acceptable to the Authority Having Jurisdiction (AHJ) shall be used in fire modeling calculations."

Objectives

The objective of this project is to examine the predictive capabilities of selected fire models. These models may be used to demonstrate compliance with the requirements of 10 CFR 50.48(c) and the referenced NFPA 805, or support other performance-based evaluations in NPP fire protection applications. In addition to NFPA 805 requiring that only verified and validated fire models acceptable to the AHJ be used, the standard also requires that fire models only be applied within their limitations. The V&V of specific models is important in establishing acceptable uses and limitations of fire models. Specific objectives of this project are:

- Perform V&V study of selected fire models using a consistent methodology (ASTM E1355) and issue a report to be prepared by U.S. Nuclear Regulatory Commission Office of Nuclear Regulatory Research (RES) and Electric Power Research Institute (EPRI).
- Investigate the specific fire modeling issues of interest to the NPP fire protection applications.
- Quantify fire model predictive capabilities to the extent that can be supported by comparison with selected and available experimental data.

The following fire models were selected for this evaluation: (i) NRC's NUREG-1805 Fire Dynamics Tools (FDT^s), (ii) EPRI's Fire-Induced Vulnerability Evaluation Revision 1 (FIVE-Rev. 1), (iii) National Institute of Standards and Technology's (NIST) Consolidated Model of Fire Growth and Smoke Transport (CFAST), (iv) Electricite de France's (EdF) MAGIC, and (v) NIST's Fire Dynamics Simulator (FDS).

Approach

This program is based on the guidelines of the ASTM E1355, "Evaluating the Predictive Capability of Deterministic Fire Models," for verification and validation of the selected fire models. The guide provides four areas of evaluation:

- Defining the model and scenarios for which the evaluation is to be conducted,
- Assessing the appropriateness of the theoretical basis and assumptions used in the model,
- Assessing the mathematical and numerical robustness of the model, and
- Validating a model by quantifying the accuracy of the model results in predicting the course of events for specific fire scenarios.

Traditionally, a V&V study reports the comparison of model results with experimental data, and therefore, the V&V of the fire model is for the specific fire scenarios of the test series. While V&V studies for the selected fire models exist, it is necessary to ensure that technical issues specific to the use of these fire models in NPP applications are investigated. The approach below was followed to fulfill this objective.

1. A set of fire scenarios were developed. These fire scenarios establish the "ranges of conditions" for which fire models will be applied in NPPs.
2. The next step summarizes the same attributes or "range of conditions" of the "fire scenarios" in test series available for fire model benchmarking and validation exercises.
3. Once the above two pieces of information were available, the validation test series, or tests within a series, that represent the "range of conditions" was mapped for the fire scenarios developed in Step 1. The range of uncertainties in the output variable of interest as predicted by the model for a specific "range of conditions" or "fire scenario" are calculated and reported.

The scope of this V&V study is limited to the capabilities of the selected fire models. There are potential fire scenarios in NPP fire modeling applications that do not fall within the capabilities of these fire models and therefore are not covered by this V&V study.

Results

The results of this study are presented in the form of relative differences between fire model predictions and experimental data for fire modeling attributes important to NPP fire modeling applications, e.g., plume temperature. The relative differences sometimes show agreement, but may also show both under-prediction and over-prediction. These relative differences are affected by the capabilities of the models, the availability of accurate applicable experimental data, and the experimental uncertainty of this data. The relative differences were used, in combination with some engineering judgment as to the appropriateness of the model and the

agreement between model and experiment, to produce a graded characterization of the fire model's capability to predict attributes important to NPP fire modeling applications.

This report does not provide relative differences for all known fire scenarios in NPP applications. This incompleteness is due to a combination of model capability and lack of relevant experimental data. The first can be addressed by improving the fire models while the second needs more applicable fire experiments.

EPRI Perspective

The use of fire models to support fire protection decision-making requires that their limitations and confidence in their predictive capability is well understood. While this report makes considerable progress towards that goal, it also points to ranges of accuracies in the predictive capability of these fire models that could limit their use in fire modeling applications. Use of these fire models present challenges that should be addressed if the fire protection community is to realize the full benefit of fire modeling and performance-based fire protection. This requires both short term and long term solutions. In the short term a methodology will be to educate the users on how the results of this work may affect known applications of fire modeling. This may be accomplished through pilot application of the findings of this report and documentation of the insights as they may influence decision-making. Note that the intent is not to describe how a decision is to be made, but rather to offer insights as to where and how these results may, or may not be used as the technical basis for a decision. In the long term, additional work on improving the models and performing additional experiments should be considered.

Keywords

Fire	Fire Modeling	Verification and Validation (V&V)
Performance-based	Risk-informed regulation	Fire Hazard Analysis (FHA)
Fire safety	Fire protection	Nuclear Power Plant
Fire Probabilistic Risk Assessment (PRA)		Fire Probabilistic Safety Assessment (PSA)

PREFACE

This report is presented in seven volumes. Volume 1, the Main Report, provides general background information, programmatic and technical overviews, and project insights and conclusions. Volumes 2 through 6 provide detailed discussions of the verification and validation (V&V) of the following five fire models:

Volume 2 Fire Dynamics Tools (FDT^s)

Volume 3 Fire-Induced Vulnerability Evaluation, Revision 1 (FIVE-Rev1)

Volume 4 Consolidated Model of Fire Growth and Smoke Transport (CFAST)

Volume 5 MAGIC

Volume 6 Fire Dynamics Simulator (FDS)

Finally, Volume 7 quantifies the uncertainty of the experiments used in the V&V study of these five fire models.

FOREWORD

Fire modeling and fire dynamics calculations are used in a number of fire hazards analysis (FHA) studies and documents, including fire risk analysis (FRA) calculations; compliance with, and exemptions to the regulatory requirements for fire protection in 10 CFR Part 50; the Significance Determination Process (SDP) used in the inspection program conducted by the U.S. Nuclear Regulatory Commission (NRC); and, most recently, the risk-informed performance-based (RI/PB) voluntary fire protection licensing basis established under 10 CFR 50.48(c). The RI/PB method is based on the National Fire Protection Association (NFPA) Standard 805, "Performance-Based Standard for Fire Protection for Light-Water Reactor Generating Plants."

The seven volumes of this NUREG-series report provide technical documentation concerning the predictive capabilities of a specific set of fire dynamics calculation tools and fire models for the analysis of fire hazards in nuclear power plant (NPP) scenarios. Under a joint memorandum of understanding (MOU), the NRC Office of Nuclear Regulatory Research (RES) and the Electric Power Research Institute (EPRI) agreed to develop this technical document for NPP application of these fire modeling tools. The objectives of this agreement include creating a library of typical NPP fire scenarios and providing information on the ability of specific fire models to predict the consequences of those typical NPP fire scenarios. To meet these objectives, RES and EPRI initiated this collaborative project to provide an evaluation, in the form of verification and validation (V&V), for a set of five commonly available fire modeling tools.

The road map for this project was derived from NFPA 805 and the American Society for Testing and Materials (ASTM) Standard E1355-04, "Evaluating the Predictive Capability of Deterministic Fire Models." These industry standards form the methodology and process used to perform this study. Technical review of fire models is also necessary to ensure that those using the models can accurately assess the adequacy of the scientific and technical bases for the models, select models that are appropriate for a desired use, and understand the levels of confidence that can be attributed to the results predicted by the models. This work was performed using state-of-the-art fire dynamics calculation methods/models and the most applicable fire test data. Future improvements in the fire dynamics calculation methods/models and additional fire test data may impact the results presented in the seven volumes of this report.

This document does not constitute regulatory requirements, and RES participation in this study neither constitutes nor implies regulatory approval of applications based on the analysis contained in this text. The analyses documented in this report represent the combined efforts of individuals from RES and EPRI, both of which provided specialists in the use of fire models and other FHA tools. The results from this combined effort do not constitute either a regulatory position or regulatory guidance. Rather, these results are intended to provide technical analysis, and they may also help to identify areas where further research and analysis are needed.

Carl J. Paperiello, Director
Office of Nuclear Regulatory Research
U.S. Nuclear Regulatory Commission

ACKNOWLEDGMENTS

The work documented in this report benefited from contributions and considerable technical support from several organizations.

The verification and validation (V&V) studies for FDT^s (Volume 2), CFAST (Volume 4), and FDS (Volume 6) were conducted in collaboration with the U.S. Department of Commerce, National Institute of Standards and Technology (NIST), Building and Fire Research Laboratory (BFRL). Since the inception of this project in 1999, the NRC has collaborated with NIST through an interagency memorandum of understanding (MOU) and conducted research to provide the necessary technical data and tools to support the use of fire models in nuclear power plant fire hazard analysis (FHA).

We appreciate the efforts of Doug Carpenter and Rob Schmidt of Combustion Science Engineers, Inc. for their comments and contribution to Volume 2.

In addition, we acknowledge and appreciate the extensive contributions of Electricité de France (EdF) in preparing Volume 5 for MAGIC.

We also appreciate the efforts of organizations participating in the International Collaborative Fire Model Project (ICFMP) to Evaluate Fire Models for Nuclear Power Plant Applications, which provided experimental data, problem specifications, and insights and peer comment for the international fire model benchmarking and validation exercises, and jointly prepared the panel reports used and referred to in this study. We specifically appreciate the efforts of the Building Research Establishment (BRE) and the Nuclear Installations Inspectorate in the United Kingdom, which provided leadership for ICFMP Benchmark Exercise (BE) #2, as well as Gesellschaft fuer Anlagen-und Reaktorsicherheit (GRS) and Institut fuer Baustoffe, Massivbau und Brandschutz (iBMB) in Germany, which provided leadership and valuable experimental data for ICFMP BE #4 and BE #5. In particular, ICFMP BE #2 was led by Stewart Miles at BRE; ICFMP BE #4 was led by Walter Klein-Hessling and Marina Rowekamp at GRS, and R. Dobbernack and Olaf Riese at iBMB; and ICFMP BE #5 was led by Olaf Riese and D. Hosser at iBMB, and Marina Rowekamp at GRS. We acknowledge and sincerely appreciate all of their efforts.

We greatly appreciate Paula Garrity, Technical Editor for the Office of Nuclear Regulatory Research, and Linda Stevenson, agency Publication Specialist, for providing editorial and publishing support for this report. We also greatly appreciate Dariusz Szwarc, Nuclear Safety Professional Development Program participant, for his assistance finalizing this report.

LIST OF ACRONYMS

AGA	American Gas Association
AHJ	Authority Having Jurisdiction
ASME	American Society of Mechanical Engineers
ASTM	American Society for Testing and Materials
BE	Benchmark Exercise
BFRL	Building and Fire Research Laboratory
BRE	Building Research Establishment
CFAST	Consolidated Fire Growth and Smoke Transport Model
CFR	*Code of Federal Regulations*
EdF	Electricité de France
EPRI	Electric Power Research Institute
FDS	Fire Dynamics Simulator
FDT^s	Fire Dynamics Tools (NUREG-1805)
FHA	Fire Hazard Analysis
FIVE-Rev1	Fire-Induced Vulnerability Evaluation, Revision 1
FM-SNL	Factory Mutual & Sandia National Laboratories
FPA	Foote, Pagni, and Alvares
FRA	Fire Risk Analysis
GRS	Gesellschaft fuer Anlagen-und Reaktorsicherheit (Germany)
HRR	Heat Release Rate
IAFSS	International Association of Fire Safety Science
iBMB	Institut für Baustoffe, Massivbau und Brandschutz
ICFMP	International Collaborative Fire Model Project
IEEE	Institute of Electrical and Electronics Engineers
MCC	Motor Control Center
MQH	McCaffrey, Quintiere, and Harkleroad

MOU	Memorandum of Understanding
NBS	National Bureau of Standards (now NIST)
NFPA	National Fire Protection Association
NIST	National Institute of Standards and Technology
NPP	Nuclear Power Plant
NRC	U.S. Nuclear Regulatory Commission
NRR	Office of Nuclear Reactor Regulation (NRC)
RES	Office of Nuclear Regulatory Research (NRC)
RI/PB	Risk-Informed, Performance-Based
SDP	Significance Determination Process
SFPE	Society of Fire Protection Engineers
V&V	Verification & Validation

1
INTRODUCTION

As the use of fire modeling tools increases in support of day-to-day nuclear power plant (NPP) applications including fire risk studies, the importance of verification and validation (V&V) studies for these tools also increases. V&V studies afford fire modeling analysts confidence in the application of analytical tools by quantifying and discussing the performance of the given model in predicting the fire conditions measured in a particular experiment. The underlying assumptions, capabilities and limitations of the model are discussed and evaluated as part of the V&V study.

In August 2002, the Electric Power Research Institute (EPRI) published for the first time the *Fire Modeling Guide for Nuclear Power Plant Applications* (EPRI TR-1002981) [Ref. 1]. This fire modeling guide provides fire protection engineers in the commercial nuclear industry a broad overview of fire modeling theory and applications, including representative calculations performed with various state-of-the-art fire models. With the guide, EPRI included a library of pre-programmed equations in Microsoft® Excel®, which are used to estimate some aspects of fire-generated conditions. This collection of hand calculations is referred as Revision 1 of the Fire-Induced Vulnerability Evaluation model (FIVE-Rev1).

In general, the equations in the library are closed-form analytical expressions that can be solved by hand. The capabilities of the various equations in the library include predicting temperature and convective heat fluxes in the fire plume or ceiling jet, irradiated heat flux, upper layer temperature, time to detection, and target heating, among others.

The main objective of this study is to document a V&V study for selected models in the FIVE-Rev1 library, in accordance with ASTM E1355, *Standard Guide for Evaluating the Predictive Capability of Deterministic Fire Models* [Ref. 2]. As such, this report is structured to follow the guidance provided in the ASTM standard:

- Chapter 2 provides qualitative background information about FIVE-Rev1 and the V&V process.
- Chapter 3 presents a technical description of FIVE-Rev1, which includes the underlying physics and chemistry inherent in the model. The description includes assumptions and approximations, an assessment of whether the open literature provides sufficient scientific evidence to justify the approaches and assumptions used, and an assessment of empirical or reference data used for constant or default values in the context of the model.
- Chapter 4 documents the mathematical and numerical robustness of FIVE-Rev1, which involves verifying that the implementation of the model matches the stated documentation.
- Chapter 5 presents a sensitivity analysis, for which the researchers defined a base case scenario and varied selected input parameters in the FIVE-Rev1 equations.

- Chapter 6 presents the results of the V&V study, in the form of accuracies classified on the basis of NPP configurations and relevant attributes of enclosure fires in NPPs. The calculated accuracies are based on both "blind" and "open" calculations. Blind calculations refer to those conducted before the experimental data were available. In contrast, open calculations refer to those conducted with the experimental data available.
- Appendix A lists the calculated accuracies which for the basis for the evaluation results discussed in Chapter 6.

2
MODEL DEFINITION

This chapter provides qualitative background information about FIVE-Rev1 and the V&V process, as required by ASTM E1355.

2.1 Name and Version of the Model

This V&V study focused on Revision 1 of the Fire-Induced Vulnerability Evaluation model (FIVE-Rev1). The latest version of FIVE-Rev1 was released in August 2002.

2.2 Type of Model

In August 2002, EPRI published for the first time the *Fire Modeling Guide for Nuclear Power Plant Applications* (EPRI TR-1002981) [Ref. 1]. This fire modeling guide provides fire protection engineers in the commercial nuclear industry a broad overview of fire modeling theory and applications, including representative calculations performed with various state-of-the-art fire models. With the guide, EPRI included a library of pre-programmed equations in Microsoft® Excel®, which are used to estimate some aspects of fire-induced conditions. This collection of hand calculations is referred as FIVE-Rev1.

In general, the equations in the library are closed-form analytical expressions that can be solved by hand. The capabilities of the various equations in the library include predicting temperature and convective heat fluxes in the fire plume or ceiling jet, irradiated heat flux, upper layer temperature, time to detection, and target heating, among others.

NOTE: This study did not address all of the equations in the FIVE-Rev1 library; those subjected to the V&V process are identified throughout this report.

2.3 Model Developers

The FIVE-Rev1 model was compiled and is maintained by the Electric Power Research Institute, EPRI.

2.4 Relevant Publications

Technical descriptions of FIVE-Rev1 are provided in EPRI's *Fire Modeling Guide for Nuclear Power Plant Applications* (EPRI TR-1002981) [Ref. 1] and in Chapter 3 of this report. In addition, EPRI's *Methods of Quantitative Fire Hazard Analysis* (EPRI TR-100443) [Ref. 3] documents the quantitative fire modeling methods used in FIVE.

2.5 Governing Equations and Assumptions

As mentioned above, FIVE-Rev1 is a library of equations for use in estimating various aspects of fire-induced conditions. Each equation has its own assumptions, as detailed in Chapter 3 of this report.

2.6 Input Data Required To Run the Model

The various equations in the FIVE-Rev1 library require different inputs, as detailed in Chapter 3 of this report. However, the following data are generally necessary to use the equations in the FIVE-Rev1 library:

(1) The following parameters describe the compartment geometry and ventilation conditions:

- The compartment (or each compartment in a multi-room scenario) is assumed to have a rectangular floor base and flat ceiling. Its compartment geometry is defined by its length, width, and height.
- The material properties of the floor, ceiling, and walls include density, specific heat, and thermal conductivity. Depending on the selected material, this information may be available in generic fire protection engineering handbooks or similar references.
- Natural ventilation is determined by the height and width of doors; height, width, and elevation of windows; time to open/close doors and windows during a fire simulation; and leakage paths.
- Mechanical ventilation is determined by supply and return rates, vent elevations, and time to start/stop the system.

(2) The following parameters describe the characteristics of the fire:

- Fuel type and fire heat release rate profile: The heat release rate profile is specified using the heat of combustion and the mass loss rate of the fuel.
- Fire location (elevation, near a wall, near a corner, or center of room)
- Footprint area of the fire: circular (e.g., pool fires specified by diameter) or rectangular (e.g., bounded pool fires, electrical cabinets specified by length and width)
- Fuel mass, irradiated fraction, and stochiometric fuel-oxygen ratio.

(3) Two sets of parameters (thermo-physical properties and location) describe targets. Thermo-physical properties include the density, specific heat, and thermal conductivity of the material. Location refers to where the target is with respect to the fire (expressed in tri-dimensional coordinates).

(4) The inputs for sprinklers and detectors are (a) the device's location with respect to the fire and (b) its response characteristics, including activation temperature and response time index.

2.7 Property Data

Some of the equations in the FIVE-Rev1 library require the following property data:

- For walls, ceiling, and floor: density, thermal conductivity, and specific heat.
- For targets: damage temperature, density, thermal conductivity, and specific heat.

- For fuels: heat of combustion, mass loss rate, stochiometric fuel-oxygen ratio, specific area, and radiated fraction.

These properties may be available in fire protection engineering handbooks or similar references. However, depending on the application, properties for specific materials may not be readily available.

2.8 Model Results

Each equation in the FIVE-Rev1 library provides a single numerical output.

3
THEORETICAL BASIS FOR FIVE-REV1

This chapter presents a technical description of the FIVE-Rev1, including theoretical background and the underlying physics and chemistry inherent in the different models. In so doing, this chapter addresses the ASTM E1355 requirement to "verify the appropriateness of the theoretical basis and assumptions used in the model."

The description provided in this chapter includes assumptions and approximations, an assessment of whether the open literature provides sufficient scientific evidence to justify the approaches and assumptions used, and an assessment of empirical or reference data used for constant or default values in the context of the models.

The models included in the FIVE-Rev1 library have been developed, reviewed, and documented over the past 30 years. In addition, most of the engineering calculations in the FIVE-Rev1 library are available in the open fire protection engineering literature, particularly in the *Society of Fire Protection Engineers [SFPE] Handbook of Fire Protection Engineering* (3rd Edition) [Ref. 4]. As a result, this chapter references previous publications describing assumptions and theoretical bases of some of the models included in the V&V process.

3.1 Theoretical Basis for FIVE-Rev1

FIVE-Rev 1 is actually a collection of engineering equations (hand calculations) that have been developed over the past 30 years, which are pre-programmed and automated in a Microsoft® Excel® workbook. As FIVE-Rev1 is not actually a model itself, its advantages are not attributed to its modeling capabilities. Instead, FIVE-Rev1 provides a collection of models in a single file, with a graphical interface that simplifies (as much as possible) the process of manually solving mostly algebraic equations

The modeling capabilities of FIVE-Rev1 are restricted to the individual capabilities and limitations of each model in the library. That is, each model was developed based on specific assumptions and conditions, which restrict its application. This section provides the mathematical formulation of the FIVE-Rev1 models and a summary of the assumptions and limitations related to their use.

As suggested by Karlsson and Quintierre [Ref. 6], the hand calculations compiled in the FIVE-Rev1 library can be broadly classified as those that deal with (1) combustion, (2) resulting environmental conditions, and (3) heat transfer. The following sections present technical details about each of these model classifications.

3.1.1 Hand Calculations Dealing with Combustion

Hand calculations dealing with the combustion process relate specifically to determination of the heat release rate, $\dot{Q}$. Two models in the FIVE-Rev1 library serve this purpose.

3.1.1.1 Fire Heat Release Rate

In general, the heat release rate of a fire, $\dot{Q}_f$, is calculated using the flammability properties of the fuel, including the heat of combustion (ΔH_c, kJ/kg) and the specific burning rate ($\dot{m}''$, kg/sec-m^2). Using these two parameters, together with the burning area, we can estimate the heat release rate of the fire using the following equation (model), as described by Drysdale [Ref. 6]:

$$\dot{Q}_f = \Delta H_c \cdot \dot{m}'' \cdot A$$

This approach is easily applied in the case of liquid and some plastic combustibles. Unfortunately, mathematical modeling of the physical and chemical transformations of materials as they burn is still the subject of research and, therefore, the model presented above cannot calculate the heat output of a fire as a function of time for many combustibles under actual configurations and scenario conditions.

3.1.1.2 Cable Tray Heat Release Rate

The fire protection literature [see for example Ref. 7, and Vol 2 of this report] offers the following correlation for estimating the heat release rate generated by burning cable trays, $\dot{Q}_{ct}$:

$$\dot{Q}_{ct} = 0.45 \cdot \dot{q}_{bs} \cdot A(t) \text{ (kW)}$$

$$A(t) = A_o + \frac{dA}{dt} t \text{ (m}^2\text{)}$$

$$\frac{dA}{dt} \approx 5 \cdot 10^{-3} \dot{q}_{bs} - 0.6. \text{ (m}^2\text{)}$$

where:

A_o = initial cable tray burning area (m^2)

T = time (min)

q_{bs} = experimental bench scale heat release rate value (kW/m^2)

Notice that the equation for estimating heat release rate is identical to the one discussed above at t = 0 min.

Unfortunately, this correlation is based on experimental results only and should be used with caution. Moreover, the fire propagation model (second and third equations above) should not be used for a single cable tray. It applies only to a stack of trays subjected to a constant heat release rate from the ignition source, since the experimental measurements used to develop the correlation involve the area of fire involvement in all trays. Specifically, the experiments involved two parallel stacks of six horizontal cable trays on a load cell using a pan of heptane as the ignition source between the two stacks. The stacks were 15 cm (6 in.) apart. Of the 17 tests, 3 tests used

an arrangement of 3 vertical cable trays in addition to the 12 horizontal trays (2 stacks of 6 trays). The 96″ x 10″ x 3″ cable trays had a vertical separation of approximately 25 cm (10 in.). The experiments measured the mass loss rate from the cable trays, as well as the estimated area of fire involvement in the trays at the time of extinguishment. The data collected from these experiments was correlated with bench scale heat release rate data. Reference 7 provides further technical details on the model and the experiments.

3.1.2 Hand Calculations Dealing with Resulting Environmental Conditions

Numerous models are available for use in predicting resulting environmental conditions. The FIVE-Rev1 library includes models for predicting fire plume temperature and heat flux, ceiling jet temperature and heat flux, room temperature, and flame height.

3.1.2.1 Flame Height

According to Heskestad, the flame height marks the level where the combustion reaction is complete and the inert plume can be considered to begin [Ref. 8]. The flame height is estimated using the following equation:

$$L = 0.235\dot{Q}_f^{2/5} - 1.02D \text{ (m)}$$

where:

Q_f = fire heat release rate (kW)

D = fire diameter (m)

Based on its formulation, the FIVE-Rev1 model for flame height is not appropriate for estimating jet flame lengths or for scenarios where atmospheric conditions deviate significantly from normal. Furthermore, the above equation is valid for combustibles in which the heat liberated per unit mass of air entering the combustion reaction ranges between 2,900 and 3,200 kJ/kg. That is, the equation is not valid for very small heat release rate values where the resulting length is a negative.

The above equation correlates well data for L/D values up to 20 (note that L/D is a dimensionless term), and Q_D^* up to 100 [Ref. 8]. Q_D^* is also a dimensionless term, which is defined as follows:

$$Q_D^* = \frac{\dot{Q}_f}{\rho_\infty c_p T_\infty \sqrt{gD} D^2}$$

Beyler [Ref. 9] indicates that a flame height determination based on a circular fuel source with an area equal to the real source may overestimate the flame height. The above correlation is intended for horizontal pool-type sources, but is likely to work reasonably well for more complex sources if the calculated flame height is large relative to the diameter of the source.

3.1.2.2 Fire Plumes

The FIVE-Rev1 library includes three semi-empirical correlations for estimating fire plume temperatures. These three correlations have essentially the same underlying assumptions, limitations, and input parameters. In general, these correlations predict the average temperature at some predetermined height above the fire. In each case, the temperature estimate is derived by applying the principles of conservation of mass, momentum and energy in the fire plume, combined with experimental observations. Heskestad fundamentally analyzed the problem in terms of the total mass, momentum, and energy integrated across the plume cross-section, assuming that the entrainment velocity is proportional to the plume velocity, with the constant of proportionality being the entrainment constant [Ref. 9].

Results from these three semi-empirical correlations are expected to be adequate for unobstructed vertical plumes. Nonetheless, it should be noted that the correlations do not consider hot gas layer effects, which are discussed in Section 3.1.2.5. The following table lists the plume temperature models.

Table 3-1: Summary of Plume Temperature Correlations

Heskestad [Ref. 8]	**McCaffrey [Ref. 5]**	**Alpert [Ref. 10]**
$T_{pl} = T_{amb} + 25\left(\frac{\left(k_f \dot{Q}_f (1-\chi_r)\right)^{2/5}}{\left((H_p - F_e) - z_o\right)}\right)^{5/3}$	$T_{pl} = \left(\frac{\kappa}{0.9\sqrt{2g}}\right)^2 \left(\frac{H_p - F_e}{\left(k_f \dot{Q}_f\right)^{2/5}}\right)^{2\eta-1} T_{amb}$	$T_{pl} = T_{amb} + 16.9\left(\frac{\left(k_f \dot{Q}_f\right)^{2/3}}{\left(H_p - F_e\right)^{5/3}}\right)$
$z_o = 0.083\dot{Q}_f^{\,2/5} - 1.02D$	$\kappa = 1.1,\ \eta = -1/3$	

Where:

T_{amb} = ambient temperature (°C)

k_f = fire location factor

Q_f = fire heat release rate (kW)

F_e = fire elevation (m)

H_p = target height measured from the floor (m)

X_r = irradiated fraction of the heat release rate
(FIVE-Rev1 recommends 0.4 as a conservative estimate)

D = plume diameter (m)

Models for plume velocity were also developed as part of the same set of correlations. Table 3-2 lists the associated equations.

Table 3-2: Plume Velocity Correlations

Heskestad's [Ref. 8]	McCaffrey [Ref. 5]	Alpert [Ref. 10]
$V_{pl} = \left(\frac{Q_f (1-\chi_r)}{(H_p - F_e) - z_o} \right)^{1/3}$ $z_o = 0.083 \dot{Q}_f^{2/5} - 1.02D$	$V_{pl} = \kappa \left(\frac{(H_p - F_e)}{\dot{Q}_f^{2/5}} \right)^{\eta} \dot{Q}_f^{1/5}$ $\kappa = 1.1, \eta = -1/3$	$V_{pl} = 0.96 \left(\frac{\dot{Q}_f}{H_p - F_e} \right)^{1/3}$

Heskestad also developed the following model for plume diameter as part of the formulation for the plume temperature and velocity models:

$$D = 0.12 \left(\frac{T_{pl}}{T_{amb}} \right)^{1/2} (H_p - F_e - z_o) \text{ (m)}$$

In addition, three models are available for estimating air entrainment into the fire plume, as listed in Table 3-3. Note that the Thomas and Zukoski models are not part of the set of correlations previously discussed in this section.

Table 3-3: Plume Entrainment Correlations

Heskestad's [Ref. 8]	Zukoski [Ref. 5]	Thomas [Ref. 5]
$\dot{m} = \frac{0.071}{k_f} \left(k_f \cdot \dot{Q}_f (1-\chi_r) \right)^{1/3} (H_p - F_e - z_o$ $+ 1.85 \cdot 10^{-3} \cdot \left(k_f \cdot \dot{Q}_f (1-\chi_r) \right)$ $z_o = 0.083 \dot{Q}_f^{2/5} - 1.02D$	$m_p = \frac{0.071}{k_f} \cdot \left(k_f \cdot \dot{Q}_f \right)^{1/3} (H_p - F_e$	$m_p = 0.188 \cdot P \cdot (H_p - F_e)^3$ p = fire perimeter

3.1.2.3 Ceiling Jet

Alpert developed the ceiling jet temperature correlation [Ref. 10] for unobstructed flat ceilings without the effect of a smoke layer. This correlation is an extension of Alpert's correlation for plume temperature. That is, the temperature at the ceiling above a fire source is determined using Alpert's correlation for plume temperature. Thus, the ceiling jet correlation predicts gas temperatures as the hot gases spread radially from the plume. The mathematical form of the correlation is as follows:

$$T_{cj} = \frac{5.38\left(k_f \cdot \dot{Q}_f / R\right)^{2/3}}{h - Fe} + T_{amb} \quad (^{\circ}\mathrm{C})$$

Where:

T_{amb} = ambient temperature ($^{\circ}$C)

k_f = fire location factor

Q_f = fire heat release rate (kW)

h = room height (m)

F_e = fire elevation (m)

R = horizontal radial distance from the centerline of the fire to where the temperature is reported (m)

The experimental data collected for developing the correlation consisted of various types of solid and liquid fuels with energy release rates ranging from roughly 500 kW to 100 MW under ceiling heights ranging from 4.6 to 15.5 m (15.09 ft to 50.85 ft). The correlation has good agreement with the data in the range of R/H from 1 to 2 (note that R/H is a dimensionless term) and $\Delta T_{cj} / \left(T_{amb}\left(Q^*\right)^{1/3}\right)$, another dimensionless term, ranging from 1 to 6.

The following equation resulted from the analysis of ceiling jet flows that produced the temperature model shown above.

$$V_{cj} = \frac{0.195 \cdot \left(k_f \dot{Q}_f\right)^{1/3} \left(h - F_e\right)^{1/2}}{R^{5/6}} \quad (\mathrm{m/s})$$

The above correlations assume that no walls exist to channel the flow of gases or cause the formation of a hot gas layer. The presence of walls or a hot gas layer will always increase the temperature of the ceiling jet flow [Ref. 10].

Delichatsios [Ref. 10] developed the following model for confined ceiling jets:

$$\frac{T_{cj} - T_{amb}}{T_{pl}} = 0.29 \cdot \left(\frac{h - F_e}{l_b} \right)^{1/3} \exp\left[-0.20 \left(\frac{R}{h - F_e} \right) \cdot \left(\frac{l_b}{h - F_e} \right)^{1/3} \right] \ (^{\circ}\mathrm{C})$$

where:

T_{amb} = ambient temperature ($^{\circ}$C)

k_f = fire location factor

Q_f = fire heat release rate (kW)

h = room height (m)

F_e = fire elevation (m)

R = horizontal radial distance from the centerline of the fire to where the temperature is reported (m)

l_b = corridor half width (m)

This correlation applies after the ceiling jet has impinged on the corridor walls. The equation was developed in cases where the corridor half width, l_b, is greater than 20 percent of the ceiling height above the fire source. The model assumes that the ceiling jet is confined without spillage, such that the flow occurs only in the primary channel. This is an important assumption for cases where the ceiling jet is confined by beams that may not fully confine the flows.

3.1.2.4 Room Temperatures

The first model in this section, developed by McCaffrey, Quintiere, and Harkleroad [Ref. 5, 11] (commonly known as the MQH model), estimates the average room temperature, as follows:

$$T = T_{amb} + 6.85 \cdot \left(\frac{\dot{Q}_f^2}{A_o \sqrt{H_o} h_k A_T} \right)^{1/3} \ (^{\circ}\mathrm{C})$$

$$h_k = \begin{cases} \sqrt{\dfrac{k \cdot d_m \cdot c_p}{t}} & t < t_p \\ \dfrac{k}{th} & t \geq t_p \end{cases} \qquad t_p = \frac{th^2}{4 \cdot \left(k / \left(d_m \cdot c_p \right) \right)}$$

where:

T_{amb} = ambient temperature ($^{\circ}$C)

Q_f = fire heat release rate (kW)

A_o = opening area (or sum of opening areas) (m^2)

H_o = height of opening [m]

A_T = internal surface area of the room (not including opening area) (m^2)

k = thermal conductivity of wall material (kW/m-$^{\circ}$C)

d_m = density of wall material (kg/m^3)

c_p = specific heat of wall material (kJ/kg-°C)

th = wall thickness (m)

t = time value (sec)

The following additional considerations also apply to the use of the MQH model [Ref. 9]:

- The rise in temperature must be between 20 °C and 600 °C (68°F and 1112°F).
- The model applies to both transient and steady fire growths.
- The model attributes heat loss to mass flowing out through openings. Therefore, the model does not apply to situations where significant time passes before hot gases begin leaving the compartment through openings (for example, large enclosures with relatively small fires, where it may take the smoke layer some time to reach the opening height).
- The model assumes that the fire is fuel-controlled.

Following the basic correlation of the MQH model, Foote, Pagni, and Alvares developed a model [Ref. 11] for use in estimating temperatures in mechanically ventilated rooms. The mathematical expression for this formulation is as follows:

$$\frac{\Delta T_g}{T_\infty} = 0.63\left(\frac{\dot{Q}}{\dot{m}_g c_p T_\infty}\right)^{0.72}\left(\frac{h_k A_T}{\dot{m}_g c_p}\right)^{-0.36}$$

where m_g is the compartment mass ventilation rate. The following additional considerations also apply to the use of the Foote, Pagni, and Alvares model [Ref. 11]:

- The expression for doorway flow is not considered.
- The coefficients and exponents are based on data from well-ventilated fire tests.
- The experimental compartment size is 6 x 4 x 4.5 m^3 (19.7 x 13.1 x 14.7 ft^3).
- Experimental ventilation rates range from 110 to 325 g/s (0.25 to 0.7 lb/sec).
- Experimental heat release rates range from 150 to 490 kW (142 to 465 Btu/sec).

3.1.2.5 Plume and Ceiling Jet Temperatures in Hot Gas Layer Environments

The correlations for plume and ceiling jet temperatures (discussed in Sections 3.1.2.2 and 3.1.2.3) were developed using experimental data collected from controlled environments with no hot gas layer effects. If such correlations are used to analyze fire scenarios involving a hot gas layer, a correction is recommended to account for the thermal effects of the hot gas layer in the plume or ceiling jet temperature. In the case of fire plume temperatures, the correlations can be used without the correction if the target elevation above the fire source is below the hot gas layer interface. By contrast, in the case of ceiling jet temperatures, hot gas layer effects may not be important (1) in the early phases of the fire event, when a hot gas layer has not been established, and (2) in relatively large rooms with relatively small fires, where the hot gas layer temperature is close to ambient.

Zone models like MAGIC model the hot gas layer effects in the fire plume temperature using the research documented by Cooper [Ref. 12]. This approach is based on the premise that above the hot gas layer interface, the fire plume entrains hot gases from the upper layer instead of fresh air at ambient temperature.

In the first version of FIVE [Ref. 3], the hot gas layer effects were included in the analysis by adding the calculated temperature rise in the fire plume to the hot gas layer temperature using the following equation:

$$T_{P-HGL} = T_{HGL} + \Delta T_P = T_{HGL} + T_P - T_{amb}$$

In most cases, this simplification produces conservative estimates of plume temperature in the hot gas layer.

This V&V study used the FIVE model described above to calculate plume temperatures inside the hot gas layer. The fire plume temperature data for this study were collected in rooms where the hot gas layer effects appeared to be significant. Therefore, the calculated accuracies include such effects.

3.1.2.6 Visibility

Mulholland documented the model for estimating the visibility distance through smoke [Ref. 13]. Toward that end, the FIVE-Rev1 library uses the following equations to calculate the visibility distance from a light-reflecting object, assuming that the burned fuel mass is well-mixed in the volume of the room:

$$Dist = \frac{3}{K} \text{ (m)}$$

$$K = \frac{2.3}{D} \text{ (m}^{-1}\text{)} \quad D = \frac{D_m M}{V} \text{ (m}^{-1}\text{)}$$

where:

K = light extinction coefficient (m^{-1})

D = optical density per meter (m^{-1})

D_m = mass optical density (m^2/g) [Ref. 13 lists D_m values for different materials]

M = burned fuel mass (g)

V = enclosure volume (m^3)

3.1.3 Hand Calculations Dealing with Heat Transfer

This section discusses four models that use hand calculations dealing with heat transfer, including (1) the point source model for flame radiation, (2) a model for predicting incident heat flux in the fire plume, (3) a model for predicting incident heat flux in the ceiling jet, and (4) a model for estimating surface temperature at a target.

3.1.3.1 Point Source Model for Flame Radiation

As described by Karlsson and Quintiere, the point source model for flame radiation assumes a fire as a point source of heat release [Ref. 5]. Therefore, this model is appropriate for remote targets, which "see" the fire as a point in space. A distance of twice the diameter of the fire is probably appropriate. The critical distance from the target to a burning fuel can then be obtained by solving the following equation for R and providing a critical heat flux required for target damage:

$$\dot{q}''_{irr} = \frac{\dot{Q}_f \chi_r}{4\pi R^2} \text{ (kW/m}^2\text{)}$$

where:

Q_f = fire heat release rate (kW)

R = distance from flames (m)

X_r = irradiated fraction of the heat release rate (FIVE recommends 0.4)

D = fire diameter (m)

3.1.3.2 Incident Heat Flux in the Fire Plume

The incident heat flux to a target in the fire plume equals the sum of the convective flux of hot gases and thermal radiation from the flame zone. Within the flame, thermal radiation is the dominant heat flux, and the expected radiant heat flux from the flame is approximately 160 kW/m^2. However, the contribution from convective heat flux cannot be neglected. That contribution is obtained from the following equation, substituting $H_p - F_e$ by the flame height. However, if the target is outside the flame zone, but within the plume, the contribution of thermal radiation from the flame can be neglected compared to convection. The incident heat flux is then given by the following equation [Ref. 14].

$$\dot{q}''_{pl} = 0.3\left(\frac{k_f \dot{Q}_f}{(H_p - F_e)^2}\right) \text{ (kW/m}^2\text{)}$$

where:

Q_f = fire heat release rate (kW)

k_f = fire location factor

H_p = target height measured from the floor (m)

F_e = fire elevation (m)

3.1.3.3 Incident Heat Flux in the Ceiling Jet

The incident heat flux to a target in the ceiling jet is, for the most part, the convective flux of hot gases transferred to the target. The following model estimates the convective heat flux in the ceiling jet [Ref. 5]:

$$\dot{q}_c'' = \frac{0.04 \cdot \dot{Q}_f}{\left(R/\left(h - F_e\right)\right)^{1/3}\left(h - F_e\right)^2} \text{ (kW/m}^2\text{)}$$

where:

Q_f = fire heat release rate (kW)

R = horizontal radial distance (m)

h = ceiling height (m)

F_e = fire elevation (m)

This correlation models well data with the dimensionless parameter R/h ranging from 0.1 to around 2.0.

3.1.3.4 Surface Temperature at the Target

The following equation estimates the surface temperature for a semi-infinite solid[1] subjected to a constant heat flux [Ref. 3]:

$$T = T_{amb} + 2 \cdot \dot{q}'' \sqrt{\frac{t}{\pi\left(k \cdot d_m \cdot c_p\right)}} \text{ (}^{\circ}\text{C)}$$

The same equation can be solved for the time to target damage, as follows:

$$t_d = \frac{\pi}{4}\left(k \cdot d_m \cdot c_p\right)\left(\frac{T_{dam} - T_{amb}}{\dot{q}''}\right)^2 \text{ (sec)}$$

where:

T_{amb} = ambient temperature ($^{\circ}$C)

q'' = constant incident heat flux (kW/m^2)

t = time (sec)

k = thermal conductivity of wall material (kW/m-$^{\circ}$C)

d_m = density of wall material (kg/m^3)

c_p = specific heat of wall material (kJ/kg-$^{\circ}$C)

[1] Semi-infinite solids refer to targets where the temperature remains ambient in the surface opposite the one receiving the heat flux.

3.1.4 Additional Models in the FIVE-Rev1 Library

Sections 3.1.1 – 3.1.3 provided a brief summary of the technical basis and reference material for several models in the FIVE-Rev1 library. However, this study did not subject all of the FIVE-Rev1 models to the V&V process for two main reasons:

(1) Experience in performing fire modeling studies in commercial nuclear plants suggests that the models subjected to the V&V process are the most commonly used in plant applications.

(2) The experimental evidence available and selected for this study does not support the V&V analysis for some models.

It is important to mention, however, that most of the models in the FIVE-Rev1 library are available in the open fire protection engineering literature and are used in other applications, as illustrated by the following examples:

- DETACT is a commonly used model for estimating time to heat detection, and the SFPE has published a V&V study for this model [Ref. 15].
- ASET is a commonly used model for estimating smoke layer descent.
- Models for the velocity of plume and ceiling jet gases result from the same formulation used to develop the models for gas temperature. In other words, they are part of the same set of correlations used to describe the thermo-dynamic conditions in the plume or ceiling jet.
- The t^2 model for the heat release rate growth profile is a tool for describing a known or assumed fire development. Although it does not predict fire conditions, it is a mathematical framework for providing the fire intensity input to the model.

4
MATHEMATICAL AND NUMERICAL ROBUSTNESS

This chapter documents the mathematical and numerical robustness of FIVE-Rev1, which involves verifying that the implementation of the model matches the stated documentation. Specifically, ASTM E1355 requires the following analyses to address the mathematical and numerical robustness of models:

- Analytical tests involve testing the correct functioning of the model. In other words, these tests use the code to solve a problem with a known mathematical solution. However, there are relatively few situations for which analytical solutions are known.
- Code checking refers to verifying the computer code on a structural basis. This verification can be achieved manually or by using a code-checking program to detect irregularities and inconsistencies within the computer code.
- Numerical tests investigate the magnitude of the residuals from the solution of a numerically solved system of equations (as an indicator of numerical accuracy) and the reduction in residuals (as an indicator of numerical convergence).

In general, the series of analyses that ASTM E1355 requires to address the mathematical and numerical robustness of models do not apply to the models in the FIVE-Rev1 library within the scope of this V&V study, for the following reasons:

- Analytical tests: The models in the FIVE-Rev1 library do not solve problems with known mathematical solutions. Therefore, the model results cannot be compared to assess the correct functioning of the models.
- Code checking: The models in the FIVE-Rev1 library are pre-programmed as user-defined functions in a Microsoft® Excel® workbook. Like any typical built-in Excel® function, each of these functions requires a set of inputs and returns a single value. In this case, the returned value is the solution of the model. (Section 3.1 discusses the models and their required inputs.) The user-defined Excel® functions programmed in the FIVE-Rev1 library are relatively brief. The structure of each function includes a variable declaration section and the mathematical solution of the equation. In addition, all of the models are consistent in their use of input variable names. Therefore, no problems are expected with regard to irregularities and inconsistencies within the computer code.
- Numerical tests: These models in the FIVE-Rev1 library are closed-form mathematical expressions that are not solved using numerical methods. As a result, there are no numerical instabilities or convergence issues associated with the solution of the models.

The FIVE-Rev1 library passed the EPRI software usability tests, which are intended to ensure that the computer program can be installed on and uninstalled from a computer, the user's guide is adequate for a first-time user, error messages are clear and displayed when required, and examples in the user's guide can be reproduced. More details on the EPRI software usability tests are available at www.epri.com.

5
MODEL SENSITIVITY

This chapter presents a sensitivity analysis, for which the researchers defined a base case scenario and varied selected input parameters in the FIVE-Rev1 equations. According to ASTM E1355, a sensitivity analysis of a model is a study of how changes in model parameters affect the results. In other words, sensitivity refers to the rate of change of the model output with respect to input variations. The standard also indicates that model predictions may be sensitive to (1) uncertainties in input data, (2) the level of rigor employed in modeling the relevant physics and chemistry, and (3) the accuracy of numerical treatments. Thus, the purpose of a sensitivity analysis is to assess the extent to which uncertainty in the model inputs is manifested as uncertainty in the model results of interest.

Conducting a sensitivity analysis involves defining a base case scenario, and varying selected input parameters. The resultant variations in the model output are then measured with respect to the base case scenario.

5.1 Definition of the Base Case Scenario for Sensitivity Analysis

Benchmark Exercise #1 exercised the base case scenario for this study as part of an ongoing International Collaborative Fire Modeling Project [Ref. 16]. (Note that only Part 1 of the Benchmark Exercise #1 was selected for the base case scenario.) This section summarizes the technical description of the base case scenario, which involved a trash can fire in a switchgear room affecting elevated cable trays. Three fire locations were selected for this study. The following parameters characterize the base case scenario:

- Room
  - Length: 15.2 m (50 ft)
  - Width: 9.1 m (30 ft)
  - Height: 4.6 m (15 ft)
  - Walls: 0.15 m thick concrete (0.5 ft)
  - Door: 2.4 m x 2.4 m (7.9 x 7.9 ft)
  - Mechanical ventilation: 5 air changes per hour
  - Vent size: 0.5 m^2 (5.4 ft^2)
  - Vent elevation: 2.4 m (7.9 ft)
- Target
  - Cable tray A: 0.6 m (2 ft) wide, 0.08 m (0.3 ft) deep
  - Elevation (cable tray A): 2.3 m (7.5 ft), 0.9 m (3 ft) off the right wall of the room
  - Cable tray B: 0.6 m (2 ft) wide, 0.08 m (0.3 ft) deep
  - Elevation (cable tray B): 2.3 m (7.5 ft), along the left wall of the room

- Material properties for concrete
  - Specific heat: 1,000 J/kg-K
  - Thermal conductivity: 1.5 W/m-K
  - Density: 2,200 kg/m^3
  - Emissivity: 0.94
- Material properties for cables (targets)
  - Specific heat: 1,040 J/kg-K
  - Thermal conductivity: 0.092 W/m-K
  - Density: 1,710 kg/m^3
  - Emissivity: 0.8
  - Heat of combustion: 16 MJ/kg
  - Radiative fraction: 0.48
- Ambient conditions
  - Temperature: 27 °C (80 ^oF)
  - Relative humidity: 50%
  - Pressure: 101,300 Pa
  - Elevation: 0
  - Wind speed: 0
- Fire (Heat release rate)
  - Fire type: transient (trash bag)
  - Location: horizontal distance from cable tray: 0.3 m (1.0 ft), 0.5 m (1.64 ft), 1.5 m (4.9 ft)
  - Radiative fraction: 0.30
  - Diameter: 0.5 m (1.64 ft)
  - Trash can height: 0.62 m
  - Heat of combustion: 24.1 MJ/kg
  - Heat release rate profile

-

Table 5-1: Base Case Heat Release Rate

Time [min]	HRR [kW]
1	200
2	350
3	340
4	200
5	150
6	100
7	100
8	80
9	75
10	100
Average HRR:	**170**
St. Deviation:	**103**
Peak HRR:	**350**

5.2 Sensitivity Analysis for FIVE-Rev1

This section describes a sensitivity analysis performed using the models listed in Chapter 3, as included in the scope of this V&V study.

5.2.1 Point Source Model for Flame Radiation

The distance from the fire to the cable tray in the base case is $\sqrt{0.3^2 + 0.5^2 + 1.5^2} = 1.6$ m (5.2 ft). A peak heat release rate of 350 kW with a 30-percent radiation fraction will result in a radiated heat flux of 3.27 kW/m^2. This result is in the lower range of results that can be predicted with this model if compared with values plotted in Figure 5-1. Figure 5-1 presents the sensitivity analysis for the point source model. Note that heat fluxes of 20 kW/m^2 or higher are predicted for distances of 3 m (9.8 ft) with heat release rates up to 8.0 MW. 20 kW/m^2 is considered in the fire protection engineering literature as the threshold of flashover [Ref. 5], which in practical terms means that any predicted incident heat flux above 20 kW/m^2 is an indication of damage for most types of targets. Note that in the context of this discussion the value of 20 kW/m^2 does not refer to the damage criteria for any particular type of cable. This value only provides a limit to the range of sensitivity analysis performed.

It can be observed from Figure 5-1 that predicted radiative heat fluxes increase as the fire intensity increase and the distance from the flames also increases. For relatively high heat release rates, in the order of 8 MW, the heat flux is over 15 kW/m^2 within 3 m (9.8 ft) from the flames. In contrast, for fires in the order of 1 MW and lower, the predicted heat flux is relatively lower. Damaging heat fluxes generated by these fire intensities may only be observed less than 1 m away from the fire.

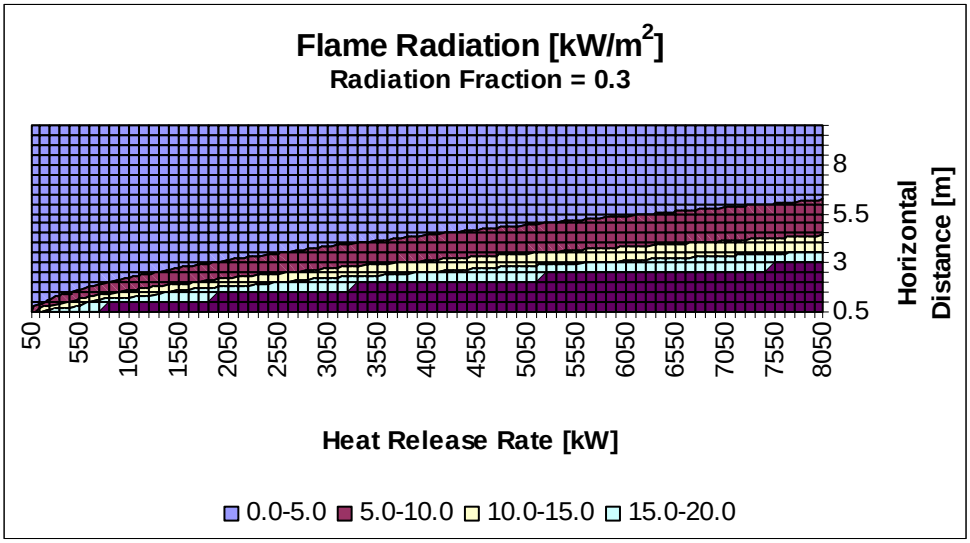

Figure 5-1: Sensitivity Analysis for the Point Source Radiation Model

Variations in the radiated fraction may significantly impact the estimated heat fluxes since it multiplies the heat release rate term in the point source model. Variations of around 10% in the resulting heat flux are expected if the fraction is varied from 30% to 40%, which is the range typically recommended.

5.2.2 Heskestad's Model for Flame Height

The peak fire intensity in the base case scenario is 350 kW. The fire diameter is 0.5 m (1.6 ft). Such fire is expected to generate a flame height of 1.95 m (6.4 ft) based on Heskestad's flame height model.

The sensitivity analysis presented in Figure 5-2 suggests that the highest flame heights are observed with the combination of relatively large heat release rates (above 5 MW) and relatively small to medium fire diameters (less than 2 m, 6.6 ft). It is difficult to determine a typical range of fire diameters and fire intensities for nuclear power plant applications in order to bound the sensitivity analysis for flame height. Such ranges depend on the nature of the ignition source (oils spills, electrical cabinets, etc), and the geometric characteristics of the scenario. Notice that the flame height in the base case scenario is the lower limit of flame height. Heat release rates just larger than the peak 350 kW in the base case scenario will generate flame heights above 2 m (6.6 ft).

Probably the largest flame-heights are associated with high heat release rates and very small diameters (4.0 MW fires with diameters of ~ 0.5 m, 1.6 ft), which likely are unrealistic scenarios for diffusion flame fires. Note that as the fire diameter increases, higher heat release rates are necessary for generating flames above 2 m (6.6 ft) high.

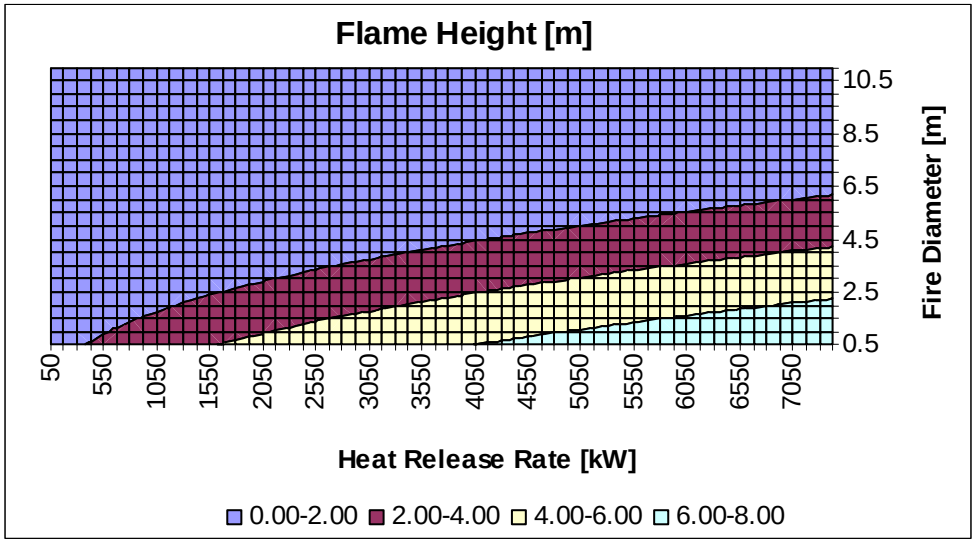

Figure 5-2: Sensitivity Analysis for Heskestad's Model for Flame Height

5.2.3 Fire Plume Temperature

Table 5-2 summarizes the relevant input data and results associated with the plume temperature calculations for the base case scenario. The temperatures are estimated at the ceiling height of 4.6 m above the fire. Results indicate that plume temperatures will be in the range of 80 °C to 110 °C (176 to 230 °F).

Table 5-2: Plume Temperature Analysis Using Plume Temperature Correlations

EPRI's FIVE-Rev1 Analysis		**EPRI's FIVE-Rev1 Analysis**		**EPRI's FIVE-Rev1 Analysis**	
Heskestad's Plume Temp Correlation		McCaffrey's Plume Temp Correlation		Alpert's Plume Temp Correlation	
Inputs		**Inputs**		**Inputs**	
Ambient temperature [°C]	20	Ambient temperature [°C]	20	Ambient temperature [°C]	20
Fire location factor	1	Fire location factor	1	Fire location factor	1
HRR [kW]	350	HRR [kW]	350	HRR [kW]	350
Fire elevation [m]	0	Fire elevation [m]	0	Fire elevation [m]	0
Target Elevation [m]	4.6	Target Elevation [m]	4.6	Target Elevation [m]	4.6
Radiation Fraction	0.3				
Fire Diameter [m]	0.5				
Results		**Results**		**Results**	
Plume Temp [°C]	**106**	Plume Temp [°C]	**104**	Plume Temp [°C]	**84**

The researchers conducted a sensitivity analysis for the three plume temperature correlations identified above. For practical applications, the three correlations yield very similar results, as shown in Figures 5-3 through 5-5. However, Figure 5-4 demonstrates a distinct feature of the McCaffrey temperature correlation, which predicts lower temperatures near the flames

(the combusting region of the plume). That is expected because the correlation actually consists of three equations, including one for each distinct region of the fire plume.

The sensitivity analysis also demonstrated the relatively high level of hazard for targets located in fire plumes. Notice that temperatures up to 250 $^{\circ}$C (482 ^{o}F) are calculated around 7 m (23 ft) above the fire.

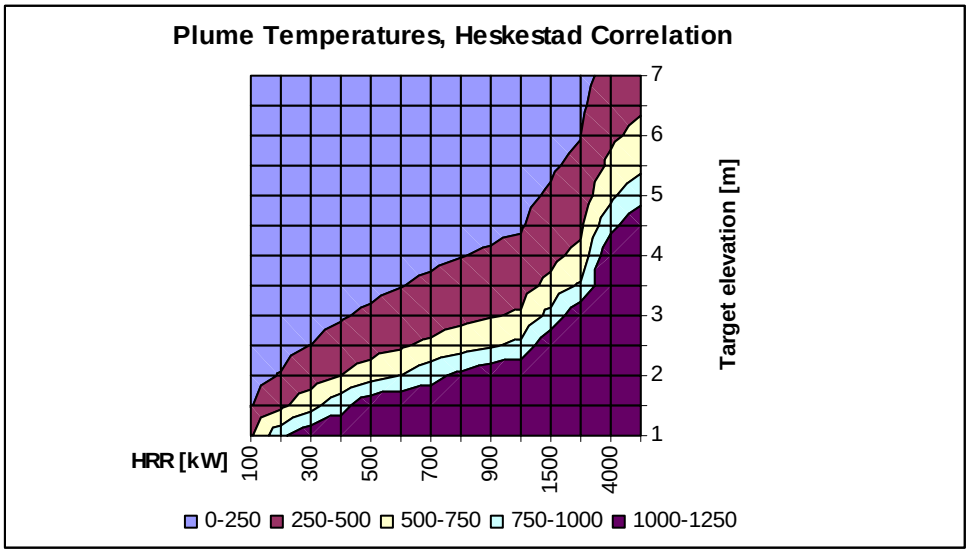

Figure 5-3: Sensitivity Analysis for Heskestad's Plume Temperature Correlation

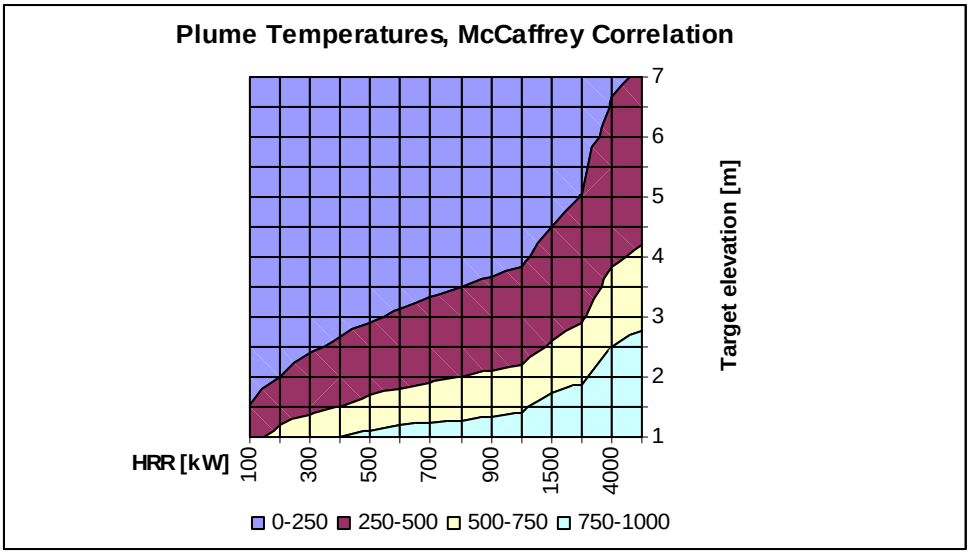

Figure 5-4: Sensitivity Analysis for McCaffrey's Plume Temperature Correlation

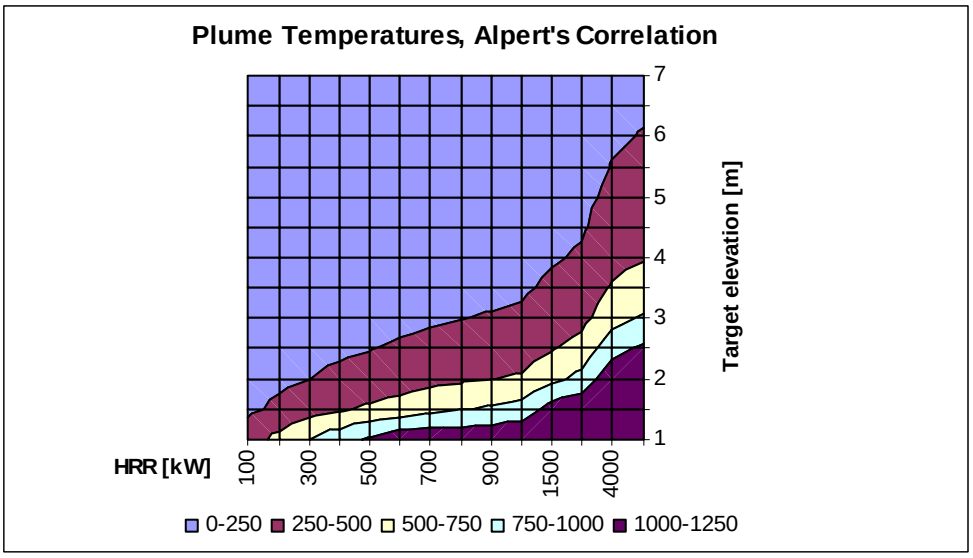

Figure 5-5: Sensitivity Analysis for Alperts's Plume Temperature Correlation

5.2.4 Fire Plume Heat Flux

The following table summarizes the estimated plume heat fluxes at various heights above the fire using base case scenario conditions:

Table 5-3: Plume Heat Flux Results for the Base Case Scenario

EPRI's FIVE-Rev1 Analysis	
Convective heat flux in the fire plume	
Inputs	
Fire heat release rate [kW]	350
Location factor	1
Fire elevation [m]	0
Target elevation [m]	Heat flux [kW/m^2]
1	105.0
2	26.3
3	11.7
4	6.6
4.6	5.0

Note that at low elevations above the fire, the model suggests heat fluxes that are comparable to those generated inside the flames. It is interesting to note that at 2 m (6.6 ft) above the fire, the heat flux significantly decreases, consistent with the flame height estimate (in Section 5.2.2) of just under 2 m (6.6 ft).

The model for estimating incident heat flux inside the fire plume has a mathematical form similar to the point source model for estimating flame radiation. That is, 30 percent of the total heat release rate contributes to the incident heat flux. Such heat flux decreases as the square of the distance between the fire and the target increases. The sensitivity analysis illustrated in Figure 5-6 suggests that at relatively small elevations above the fire source, the model predicts heat fluxes associated with flame heating (above 80 kW/m^2). Another important insight is the fact that a wide range of combinations of elevations above the target and heat release rates would generate heat fluxes that can be associated with damage to typical targets in commercial nuclear power plant fire scenarios. As a result, scenarios involving targets located inside the fire plume deserve particular attention from fire modeling analysts because such targets can be subjected to damaging heat flux in a wide range of conditions.

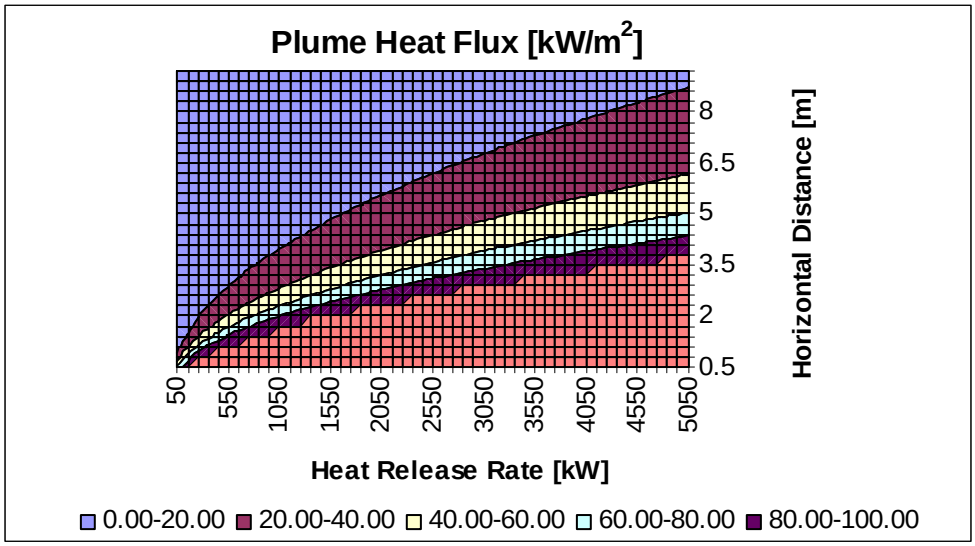

Figure 5-6: Sensitivity Analysis for the Model Used To Predict

5.2.5 Room Temperature (MQH Model)

Table 5-4 summarizes the hot gas layer temperature estimated using the MQH model.

Table 5-4: Hot Gas Layer Results for the Base Case Scenario

EPRI's FIVE-Rev1 Analysis	
MQH Temperature Correlation	
Inputs	
Ambient temperature [°C]	27
Duration [sec]	600
Opening area [m2]	5.76
Height of opening [m]	2.4
Room length [m]	15.2
Room width [m]	9.1
Room height [m]	4.6
Thermal conductivity [kW/mK]	0.00175
Density [kg/m3]	2200
Specific heat [kJ/kg]	1
Wall thickness [m]	0.15
HRR [kW]	350
Results	
Room Temp [°C]	**74**

Notice that the base case scenario is in the lower end of the sensitivity analysis conducted. The sensitivity analysis presented in Figure 5-7 is based on the room geometry described for the base case scenario in Section 5.1. Only heat release rate and fire duration variables were considered for this sensitivity analysis. Heat release rates were varied from 100 to 6,000 kW, while fire durations were varied from 100 to 3,600 seconds.

The MQH model has some specific assumptions that limit its use. In particular, (1) a hot gas layer is formed, and (2) heat is carried out of the enclosure by hot gases moving through openings. These assumptions may limit the use of this correlation in nuclear power plant applications because typical rooms of interest are closed and have no openings other than the access door. However, if used correctly, the MQH model is very useful in determining the level of fire exposure affecting targets.

This particular sensitivity analysis indicates that for the selected room size and ventilation conditions, only a small range of relatively high heat release rates combined with relatively long fire durations may result in flashover conditions (room temperatures above 500 $^{\circ}$C, 930 ^{o}F).

Typical cable damage temperatures used in nuclear power plant fire scenarios are in the range of 220 $^{\circ}$C to 330 $^{\circ}$C (425 to 625 ^{o}F)[Ref. 17]. In this particular analysis, such temperatures would be achieved with heat release rates in the order of 1.6 MW or higher for the selected range of fire durations.

The average gas temperature in the enclosure in post-flashover conditions is often very high (in the range of 700 to 1200 °C, above 1300 °F) [Ref. 9]. Therefore, MQH model results exceeding these limiting temperatures indicate that the model is not being used within its limits of applicability.

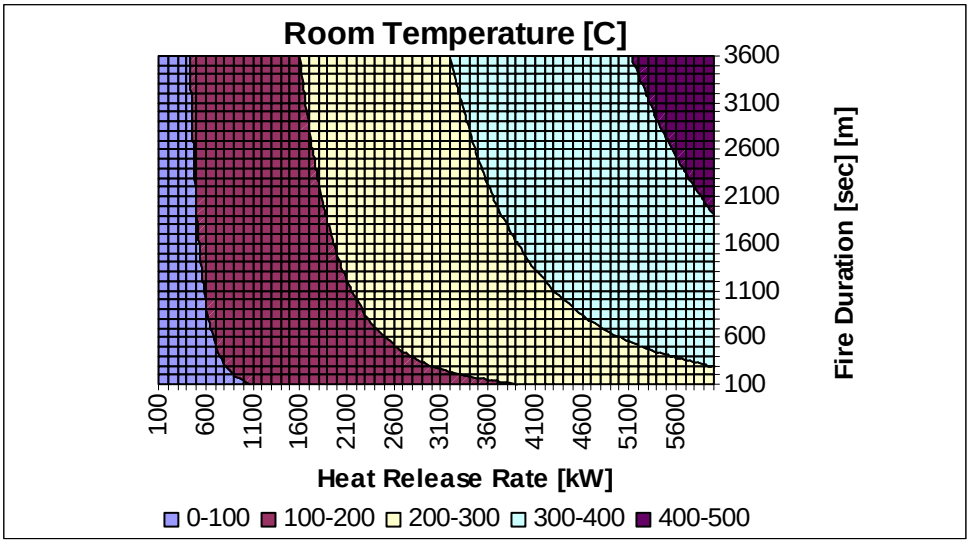

Figure 5-7: Sensitivity Analysis for the MQH Model for Room Temperature Assuming Concrete Walls

The researchers also conducted an analysis identical to that illustrated in Figure 5-7 (above), with the assumption that this analysis assumed steel walls instead of concrete. (The assumed steel properties are C_p = 0.46 kJ/kg-k, ρ = 7850 kg/m^3, and k = 0.046 kW/m-K.) The purpose of this modified analysis was to explore how sensitive the MQH model might be to changes in the boundary properties. Figure 5-8 illustrates the results of this modified analysis.

Notice that changing only the boundary materials decreased the temperatures by a factor of 2. Notice also that in the analysis with concrete walls, the boundaries did not reach uniform temperatures in a fire duration up to 1 hour (3,600 sec). In fact, the thermal penetration time (the variable t_p in Section 3.1.2.4) is estimated to be 118 minutes. By contrast, the sharp vertical lines separating temperature regions in Figure 5-8 indicate that steel boundaries reached uniform temperature in a fire duration of less than 10 minutes (600 sec). In this case, the thermal penetration time (t_p) is only 7.4 minutes. This is expected, given the high thermal conductivity of thin metal walls.

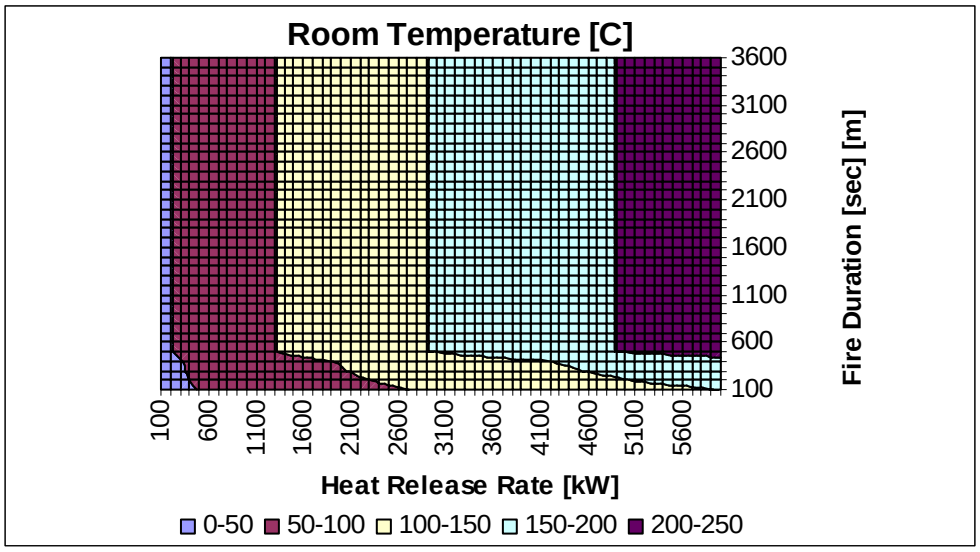

Figure 5-8: Sensitivity Analysis for the MQH Model for Room Temperature Assuming Steel Walls

5.2.6 Room Temperature (FPA Model)

Table 5-5 summarizes the input parameters and results of the calculation using the FPA model, assuming no openings and a ventilation rate of 5 ACPH (375 cfm), in which the base case scenario results in a room temperature of 125 °C (257 °F). This temperature is 50 °C (122 °F) higher than the temperature estimated using the MQH model, which assumes an open door. This result is consistent with the conceptual development of the FPA model, which does not assume heat losses through openings, and replaces the natural ventilation term with mechanical ventilation.

Table 5-5: Room Temperature of the Base Case Scenario Using the FPA Model

EPRI's FIVE-Rev1 Analysis	
FPA Temperature Correlation	
Inputs	
Ambient temperature [°C]	27
Duration [sec]	600
Ventilation rate [cfm]	375
Room length [m]	15.2
Room width [m]	9.1
Room height [m]	4.6
Thermal conductivity [kW/mK]	0.00175
Density [kg/m3]	2200
Specific heat [kJ/kg]	1
Wall thickness [m]	0.15
HRR [kW]	350
Room Temp [°C]	**125**

The FPA model follows the basic correlations of the MQH model, but adds data for forced-ventilation fires [Ref. 11]. Figure 5-9 describes the results of the sensitivity analysis for the base case geometric conditions. Notice that the sensitivity analysis considers heat release rate values that are well above those used to collect experimental data for use in developing the model (150 to 490 kW). As a result, the model predicts temperatures well over the range of 100 °C to 300 °C (212 to 572 °F) observed in the experiments [Ref. 11]. Based on the results, the FPA model does not predict temperatures outside the range of those observed in compartment fires. However, the following considerations are important:

- The FPA model should not be used to calculate temperatures in rooms with flashover conditions (temperatures above the range of 500 °C to 600 °C, above 930 °F).
- The V&V study documented in Chapter 6 indicates that the FPA model yields results that agree with experimental observations for room temperature range of 100 °C to 300 °C (212 to 572 °F). This temperature range is useful for commercial nuclear power plant applications because cable qualified to the standards set forth by the Institute of Electrical and Electronics Engineers (IEEE-qualified cable) is a common target in NPP fire scenarios, and such cable is usually assumed to have damage temperatures on the order of 330 °C (625 °F).

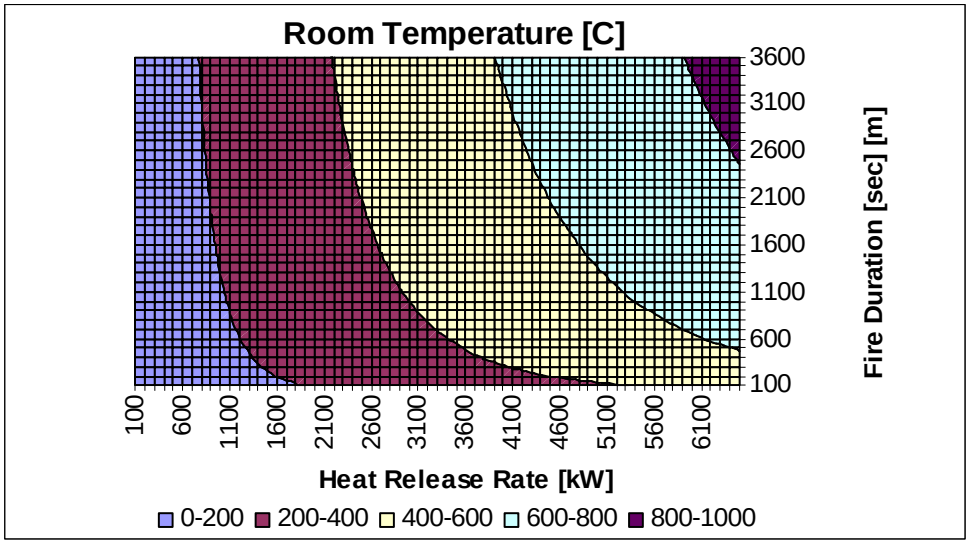

Figure 5-9: Sensitivity Analysis for the FPA Model for Room Temperature

5.2.7 Ceiling Jet Temperature

Table 5-6 summarizes the ceiling jet temperature analysis for the base case scenario using Alpert's correlation with various horizontal distances.

Table 5-6: Ceiling Jet Temperature Calculations for the Base Case Scenario Using Alpert's Correlation

EPRI's FIVE-Rev1 Analysis	
Alpert's Ceiling Jet Correlation	
Inputs	
Ambient temperature [°C]	20
Fire location factor	1
HRR [kW]	350
Fire elevation [m]	0
Room height [m]	4.6
	Results
Horizontal radial distance [m]	Ceiling Jet Temp [°C]
1	**76**
2	**55**
3	**47**
4	**42**

For the ceiling height of the base case scenario, 4.6 m, Alpert's correlation estimates ceiling jet temperatures below 200 °C (392 °F) for horizontal radial distances longer than 2.0 m (6.6 ft) and fire intensities below 5.0 MW. These temperatures are lower than the typical cable damage temperatures used in nuclear power plant fire scenarios. Furthermore, fire intensities higher than 1 MW are necessary to observe temperatures higher than 200 °C (392 °F) for horizontal distances shorter than 2.0 m (6.6 ft). Figure 5-10 illustrates the results of this analysis.

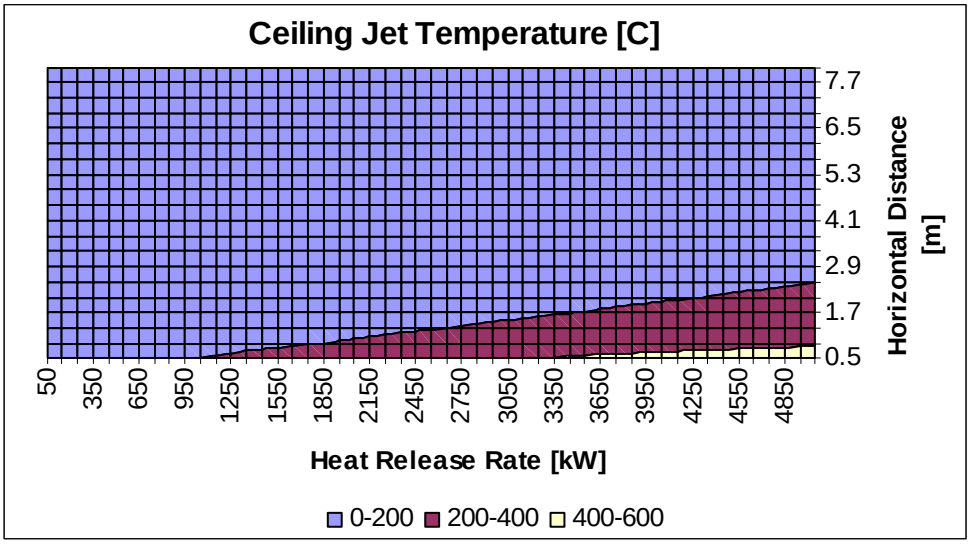

Figure 5-10: Sensitivity Analysis for Alpert's Ceiling Jet Temperature Correlation

It is relevant to stress the importance of the ceiling height in this analysis. That is, variations in the ceiling height can significantly impact the results of Alpert's model. For example, lowering the ceiling height to 3.0 m (9.8 ft) would result in temperatures above 200 $^{\circ}$C (392 ^{o}F) in horizontal distances below 5.0 m (16.4 ft) and heat release rates above 500 kW.

5.2.8 Ceiling Jet Heat Flux

Table 5-7 summarizes the ceiling jet heat flux analysis for the base case scenario with various horizontal distances. Consistent with the discussion of incident heat fluxes inside the fire plume, the ceiling jet also presents a distinct hazard in a fire scenario. Figure 5-11 illustrates the sensitivity analysis results for the model used to predict incident heat flux assuming a 4.6 m (15 ft) high ceiling. Those results clearly indicate that heat fluxes above 5 kW/m^2 can be observed under a wide range of heat release rates and horizontal distances. A value of 5 kW/m2 is commonly used as the damage criterion for certain types of cables in NPP applications [Ref. 17]. In this specific analysis, heat fluxes above 5 kW/m^2 result with fire intensities above 1,200 kW. The vertical distance between the fire and the ceiling is an important term in this model. For example, lowering the ceiling height to 3.0 m (9.8 ft) in the case analyzed in Figure 5-11 would result in heat fluxes above 10 kW/m^2 for heat release rates over 1,200 kW.

Table 5-7: Ceiling Jet Heat Flux Analysis for the Base Case Scenario

EPRI's FIVE-Rev1 Analysis	
Convective heat flux in the ceiling jet	
Inputs	
Fire heat release rate [kW]	350
Fire elevation [m]	0
Room height [m]	4.6
	Results
Horizontal distance [m]	Heat flux [kW/m2]
1	**1.1**
2	**0.9**
3	**0.8**
4	**0.7**

Note, however, that the applications of ceiling jet models are limited in commercial nuclear power plant due to the numerous obstructions just below the ceiling.

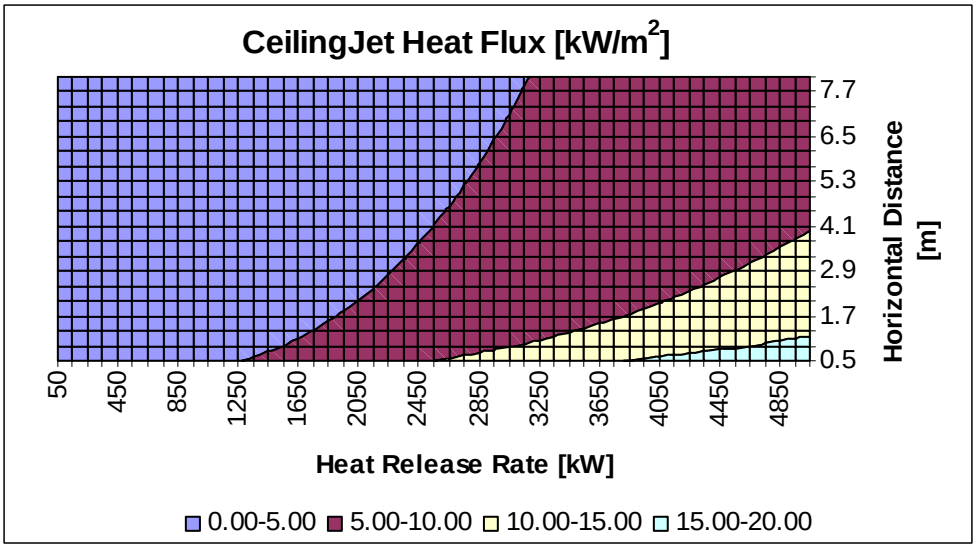

Figure 5-11: Sensitivity Analysis for the Model Used To Predict Incident Heat Flux in the Ceiling Jet

5.2.9 Cable Tray Heat Release Rate

Figure 5-12 illustrates the sensitivity analysis results for the model used to predict the heat release rate from cable tray fires. Notice that the range of bench scale heat release rates to be used with this model [Ref. 7] expands from approximately 100 kW/m^2 to approximately 600 kW/m^2, with a value of 1,071 kW/m^{2}for IEEE cable. This is the range of bench scale values used for the sensitivity analysis. Assuming burning areas up to 4.0 m (13 ft), peak fire intensities are in the range of 2,000 kW.

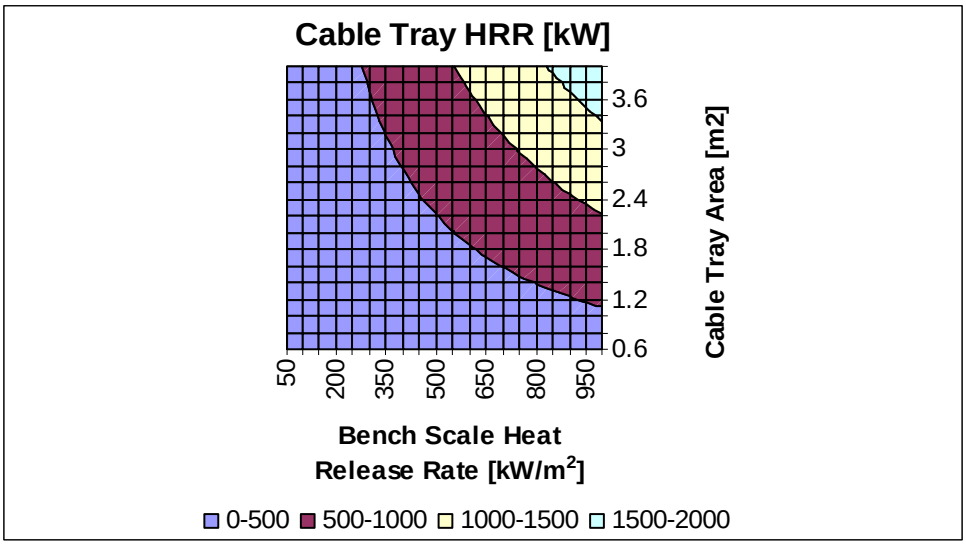

Figure 5-12: Sensitivity Analysis for the Model Used To Predict the Heat Release Rate from Cable Tray Fires

6
MODEL VALIDATION

This chapter summarizes the results of a validation study conducted for engineering calculations in the FIVE-Rev1 library, in which its predictions are compared with measurements collected from six sets of large-scale fire experiments. A brief description of each set of experiments is given here. Further details can be found in Volume 7 and in the individual test reports.

ICFMP BE #2: Benchmark Exercise #2 consists of 8 experiments, representing 3 sets of conditions, to study the movement of smoke in a large hall with a sloped ceiling. The results of the experiments were contributed to the International Collaborative Fire Model Project (ICFMP) for use in evaluating model predictions of fires in larger volumes representative of turbine halls in NPPs. The tests were conducted inside the VTT Fire Test Hall, which has dimensions of 19 m high by 27 m long by 14 m wide (62 ft x 88.5 ft x 46 ft). Each case involved a single heptane pool fire, ranging from 2 MW to 4 MW.

ICFMP BE #3: Benchmark Exercise #3, conducted as part of the International Collaborative Fire Model Project (ICFMP) and sponsored by the US NRC, consists of 15 large-scale tests performed at NIST in June, 2003. The fire sizes range from 350 kW to 2.2 MW in a compartment with dimensions 21.7 m x 7.1 m x 3.8 m (71 ft x 23 ft x 12.5 ft), designed to represent a variety of spaces in a NPP containing power and control cables. The walls and ceiling are covered with two layers of 25 mm thick marinate boards, while the floor is covered with two layers of 25 mm thick gypsum boards. The room has one 2 m x 2 m (6.6 ft x 6.6 ft) door and a mechanical air injection and extraction system. Ventilation conditions and fire size and location are varied, and the numerous experimental measurements include gas and surface temperatures, heat fluxes, and gas velocities.

ICFMP BE #4: Benchmark Exercise #4 consists of kerosene pool fire experiments conducted at the Institut für Baustoffe, Massivbau und Brandschutz (iBMB) of the Braunschweig University of Technology in Germany. The results of two experiments were contributed to the International Collaborative Fire Model Project (ICFMP). These fire experiments involve relatively large fires in a relatively small (3.6 m x 3.6 m x 5.7 m high, 11.8 ft x 11.8 ft x 18.7 ft) concrete enclosure. Only one of the two experiments was selected for the present V&V study (Test 1).

ICFMP BE #5: Benchmark Exercise #5 consists of fire experiments conducted with realistically routed cable trays in the same test compartment as BE #4. Only one test (Test 4) was selected for the present evaluation, and only the first 20 min during which time an ethanol pool fire preheats the compartment.

FM/SNL Series: The Factory Mutual & Sandia National Laboratories (FM/SNL) Test Series is a series of 25 fire tests conducted for the NRC by Factory Mutual Research Corporation (FMRC), under the direction of Sandia National Laboratories (SNL). The primary purpose of these tests was to validate computer models for various types of NPP compartments. The experiments were conducted in an enclosure measuring 60 ft long x 40 ft wide x 20 ft high (18 m x 12 m x 6 m), constructed at the FMRC fire test facility in Rhode Island. All of the tests involved forced

ventilation to simulate typical NPP installation practices. The fires consist of a simple gas burner, a heptane pool, a methanol pool, or a polymethyl-methacrylate (PMMA) solid fire. Four of these tests were conducted with a full-scale control room mockup in place. Parameters varied during testing are the heat release rate, enclosure ventilation rate, and fire location. Only three of these tests have been used in the present evaluation (Tests 4, 5 and 21). Test 21 involves the full-scale mock-up. All are gas burner fires.

NBS Multi-Room Series: The National Bureau of Standards (NBS, now the National Institute of Standards and Technology, NIST) Multi-Compartment Test Series consists of 45 fire tests representing 9 different sets of conditions, with multiple replicates of each set, which were conducted in a three-room suite. The suite consists of two relatively small rooms, connected via a relatively long corridor. The fire source, a gas burner, is located against the rear wall of one of the small compartments. Fire tests of 100, 300 and 500 kW were conducted, but for the current V&V study, only three 100 kW fire experiments have been used (Test 100A, 100O, and 100Z).

This chapter documents the comparison of models in the FIVE-Rev1 library predictions with the experimental measurements for the six test series. Not all models in the FIVE-Rev1 library described in Chapter 3 are subjected to this evaluation. In general, the model was evaluated if the selected tests series included data supporting the evaluation. At the same time, the evaluated models are the ones usually used in the evaluation of nuclear power plant scenarios.

Technical details of the calculations, including output of the model and comparison with experimental data are provided in Appendix A. The results are organized by quantity as follows:

- Section 6.1 discusses the evaluation of hot gas layer temperature correlations in FIVE-Rev1. The MQH model was evaluated using data from compartment fire tests with open doors. The FPA model was evaluated using data from compartment fire tests with closed door and mechanical ventilation.
- Section 6.2 discusses the evaluation of the Alpert ceiling jet temperature correlation.
- Section 6.3 discusses the evaluation of the Heskestad's and McCaffrey plume temperature correlation.
- Section 6.4 discusses the evaluation of Heskestad's flame height correlation.
- Section 6.5 discusses the evaluation of the point source radiation model.

The model predictions are compared to the experimental measurements in terms of the relative difference between the maximum (or where appropriate, minimum) values of each time history:

$$\varepsilon = \frac{\Delta M - \Delta E}{\Delta E} = \frac{\left(M_p - M_o\right) - \left(E_p - E_o\right)}{\left(E_p - E_o\right)}$$

ΔM is the difference between the peak value of the model prediction, M_p, and its original value, M_o. ΔE is the difference between the experimental measurement, E_p, and its original value, E_o.

Each section in this chapter contains a scatter plot that summarizes the relative difference results for all of the predictions and measurements of the quantity under consideration. The details of the calculations, the input assumptions, and the time histories of the predicted and measured output are included in Appendix A. Only a brief discussion of the results is included in this

chapter. At the end of each section, a color rating is assigned to each of the output category, indicating, in a very broad sense, how well the model treats that particular quantity. Colors are assigned based on the following criteria: The following two criteria are used to characterize the model prediction:

Criterion 1 - *Does the physics of the model support the calculation being made?* This criterion reflects examination of the applicability of the model to the physics of the fire scenario. Generally the scope of this V&V is limited to the fire scenarios that are within the stated capability of the selected fire models, e.g., this study does not address the fire scenarios that involve flame spread within single and multiple cable trays.

Criterion 2 - *Are there significant outliers (outside the experimental uncertainty) in the calculated relative differences?* This criterion is used as an indication of how accurate can a model prediction get. As long as we use fire experiments as a way of establishing confidence on model prediction, our confidence can only become as god as our experiments. In other words, if model predictions are within the ranges of experimental uncertainties, they are as reliable as they are going to get. However, one should recognize that the experimental uncertainties vary with the experiment and the attribute being measured (see volume 7 of this report). These ranges could be as much as $\pm$50% or more for the experiments and attributes we used in this V&V study.

The predictive capability of the model is then characterized as follows based on these criteria.

GREEN: If both criteria are satisfied, i.e., the model physics fully supports the calculation being made and the calculated relative differences are close to experimental uncertainty, then the V&V team concludes that the fire model prediction is within the experimental uncertainty and may be used for the recommended range of fire scenarios described in Volume 1. The user should recognize, however, that the model prediction may be off by as much as the experimental uncertainty and for some attributes such as smoke concentration and room pressure these uncertainties may be rather large.

YELLOW+: If the first criterion is satisfied and the calculated relative differences are outside the experimental uncertainty but indicate a consistent pattern of model over-prediction the model predictive capability is characterized as YELLOW+. If desired the model prediction may be used for the recommended range of fire scenarios described in Volume 1, only when it is ensured that model over-prediction reflects conservatism.

YELLOW: If the first criterion is satisfied and the calculated relative differences are outside experimental uncertainty with no clear pattern of over- or under-prediction (or clear pattern of under-prediction), the model predictive capability is characterized as YELLOW. Caution should be exercised in use of the fire model capability. In this case the user is referred to the details related to the experimental condition documented in volumes 2 through 6. The user is advised to review and understand those conditions and determine/justify applicability of the model prediction to the fire scenario for which it is being used.

The measure of model "accuracy" used throughout this study is related to experimental uncertainty. Volume 7 discusses this issue in detail. In brief, the accuracy of a measurement, *e.g.* a gas temperature, is related to the measurement device, *e.g.* a thermocouple. In addition, the accuracy of the numerical prediction of the gas temperature is related to the simplified physical description of the fire and to the accuracy of the input parameters, *e.g.* the specified heat release

rate. Ideally, the purpose of a validation study is to determine the accuracy of the model in the absence of any errors related to the measurement of both its inputs and outputs. Because it is impossible to eliminate experimental uncertainty, at the very least a combination of the uncertainty in the measurement of model inputs and output can be used to determine accuracy. If the numerical prediction falls within the range of uncertainty due to both the measurement of the input parameters and the output quantities, it is not possible to quantify its accuracy further. At this stage, it is said that the prediction is *within experimental uncertainty.*

6.1 Hot Gas Layer (HGL) Temperature

The single most important prediction a fire model can make is the temperature of the hot gas layer (HGL). After all, the impact of the fire is often assessed not only a function of the heat release rate, but also as a function of the compartment temperature. A good prediction of the height of the HGL is largely a consequence of a good prediction of its temperature because smoke and heat are largely transported together and most numerical models describe the transport of both with the same type of algorithm. Following is a summary of the accuracy assessment for the HGL predictions of the six test series:

Hot gas layer temperatures were predicted using the MQH or FPA temperature models depending on the ventilation characteristics of the tests.

ICFMP BE #2: The MQH over-predicts the HGL temperature by over 600% for all three cases. The experimental description suggests wall boundaries as having a 1 mm thick layer of steel and an outside layer of mineral wool. If the hot gas layer temperature is calculated assuming steel only, results are under-predictions of approximately 75%. If the analysis is conducted assuming walls with wool properties, the results are the over-predictions mentioned above. A graphical comparison of the MQH predictions and the experimental observations for these three cases is presented in Figure A-2 in Appendix A. The scatter plot in Figure 6-1 illustrates the relative differences between the measured and predicted peak hot gas layer temperatures and heights.

ICFMP BE #3: The MQH (open door tests) and FPA (closed door with mechanical ventilation tests) models over predict the HGL temperature for all 9 tests for which calculations were made. Both models over-predicted temperatures by approximately 50%. This analysis does not include tests 1, 2, 7, 8, 13, and 17 since no model was available in the FIVE-Rev1 library for the corresponding experimental conditions (closed door and no mechanical ventilation).

The collection of graphical comparisons between MAGIC predictions for hot gas layer temperatures and heights for ICFMP BE #3 is presented in Figures A-3 to A-4. The relative differences calculated for peak values are summarized in Table A-4 and Figure 6-1.

ICFMP BE #4: The MQH model under predicts the temperature for this test. However, the under prediction is within the experimental uncertainty of " 15%. Furthermore, both the experimental measurement and MQH predictions are above 500 ^{o}C (932 ^{o}F), which are well above typical target damage values for targets in the commercial nuclear industry. Figure A-6 illustrates both the experimental and predicted temperature profiles.

ICFMP BE #5: The MQH model predicts the room temperature within experimental uncertainty in this test. The graphical comparison between experimental measurements and model predictions, illustrated in Figure A-8 suggests very good agreement between the profiles. The calculated relative differences for peak HGL temperature and height are listed in Table A-8.

FM/SNL: The FPA model over predicts considerably the HGL temperature for Tests 4, 5 and 21. Graphical comparisons are provided in Figure A-10.

NBS Multi-Room: MQH predictions in this test series are within the experimental uncertainty for the fire room. These under predictions are depicted in Figure A-11. It should be noted that the ceramic fiber insulating material covering the fire-brick was selected for the room boundaries. Selecting the fire brick as the room material resulted in significant under predictions.

Summary: **HGL Temperature**

- Evaluation results suggest that the MQH and FPA models over-predicts room temperatures by 50 % or more. It should be stressed that in the case of rooms with different layers of wall boundaries (ICFMP BE#2, and NBS), the most insulating one was selected. Under predictions would have resulted if steel properties.
- The scatter plots in Figure 6-1 summarize the relative differences calculated for hot gas layer temperatures.
- Since most of the validation results are above the experimental uncertainty, a color assignment of Yellow+ is recommended for the room of fire origin. Analysts should consider that these are correlations developed for specific scenario conditions. Furthermore, models should be used with caution if wall materials are good heat conductors since results can be under-predictions.

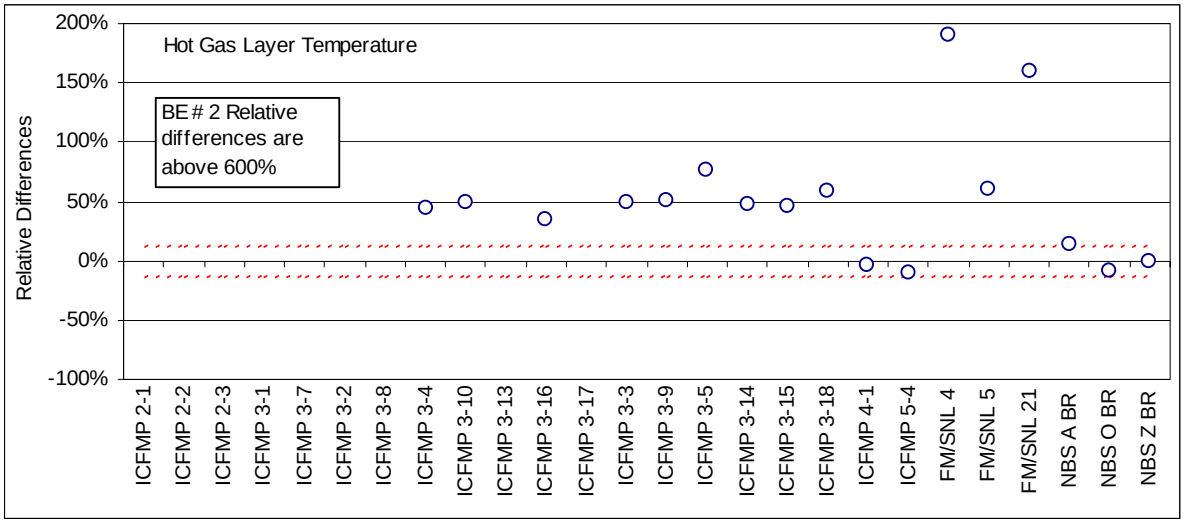

Figure 6-1: Scatter plot of relative differences for hot gas layer temperature for ICFMP BE #2, 3, 4, 5, and the selected FM/SNL and NBS Tests

6.2 Ceiling Jet Temperature

The FIVE-Rev1 library includes the Alpert correlation for ceiling jet temperature. The correlation applies to the flow of hot gases under flat unobstructed ceilings, which usually limits its applications in nuclear power plant scenarios. Furthermore, the correlation is not intended to model the ceiling jet temperature in compartments with a well-developed hot gas layer.

Only two of the six test series (ICFMP BE #3 and FM/SNL) involve a ceiling jet formed over a relatively wide, flat ceiling.

ICFMP BE #3: Alpert correlation consistently under-predicts the ceiling jet temperature by approximately 80%. Figure 6-2 illustrates this consistent pattern of under-predictions. As mentioned earlier in the report, FIVE studies in the early 1990's conservatively added the ceiling jet and layer temperatures in order to obtain an upper bound of the expected gas temperature in the ceiling jet. That practice appears to result in over predictions of the ceiling jet temperature. The over predictions range accordingly with the over predictions of the hot gas layer temperature calculated with the MQH and FPA models. Notice that Figure 6-1 does not include markers for ICFMP BE #3 tests with closed doors and no mechanical ventilation because no hot gas layer temperature was calculated for them.

The graphical comparisons between experimental measurements and MAGIC predictions for ceiling jet temperature are grouped in Figures A-12 and A-13. Table A-14 lists the calculated relative differences.

FM/SNL: The Alpert correlation again under predicts the ceiling jet temperature by approximately 80%. If the hot gas layer temperature is considered, over predictions of more than 50 % were observed. The graphical comparisons are provided in Figure A-14. The calculated relative differences are listed in Table A-16, and plotted in Figure 6-2.

Summary: Ceiling Jet Temperature

- The Alpert correlation under predicts ceiling jet temperatures in compartment fires with an established hot gas layer. For these cases, the results from the Alpert correlation should be corrected. The original version of FIVE made this correction by adding the ceiling jet and hot gas layer temperature. This practice results in consistent over predictions of the ceiling jet temperature.
- Based on the above discussion, a classification of yellow + is recommended if hot gas layer effects on the ceiling jet temperature are considered. The Alpert correlation is not intended to be used in rooms with an established hot gas layer.

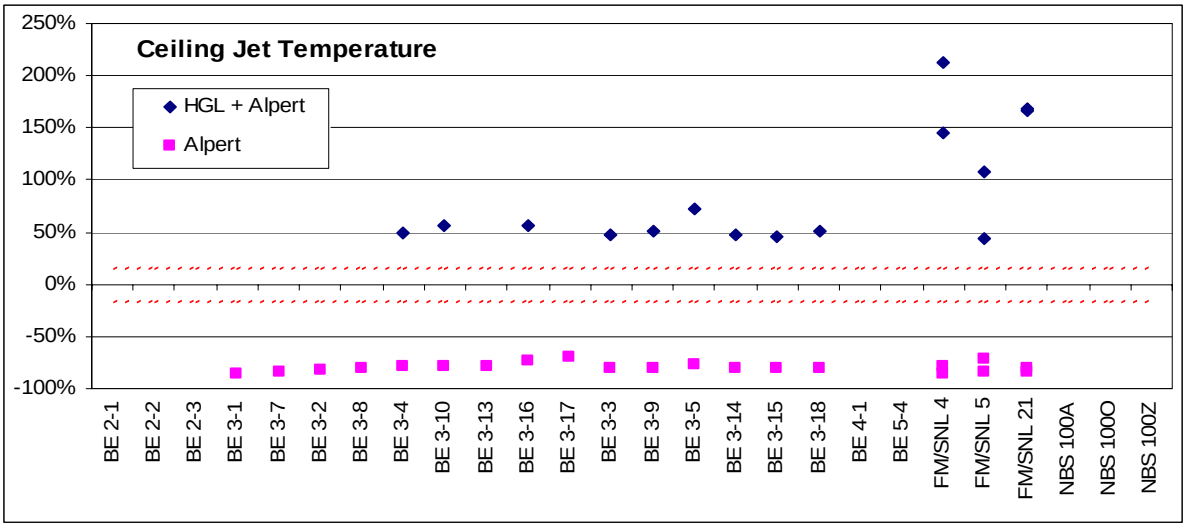

Figure 6-2. Scatter plot of relative differences for ceiling jet temperatures in ICFMP BE #3, and the selected FM/SNL Tests

6.3 Plume Temperature

This evaluation includes the McCaffrey and Heskestad's plume temperature correlations included in the FIVE-Rev1 library. These correlations were developed considering unobstructed plumes in rooms with no hot gas layer. Data from ICFMP BE #2 and the FM/SNL test series have been used to assess the accuracy of plume temperature predictions.

ICFMP BE #2: McCaffrey and Heskestad's correlations suggested under-predictions of the plume temperature. It is interesting to note however that predictions for TG1 are close or within experimental uncertainty and the ones for TG2 are not. Thermocouple TG1 is closer to the fire where hot gas layer effects may not influence as much the plume temperature. Both under and over predictions were observed. Figure A-16 provides the graphical comparisons between model predictions and experimental measurements. The calculated relative differences are listed in Table A-18 and plotted in Figure 6-3. If the hot gas layer temperature (calculated with the MQH model) is added to the plume temperature, the results are over predictions of up to 100%.

FM/SNL: McCaffrey and Heskestads correlation under predicted plume temperatures in Test 4 and 5. See Figure A-14 and Table A-16 for the graphical comparisons and the calculated relative differences. No comparison was made in Test 21 since the fire was inside a cabinet and is not clear how this configuration affected the plume flow. As illustrated in Figure 6-3, summing the hot gas layer temperature and plume temperature results in over predictions of more than 50%.

Summary: **Plume Temperature**

- McCaffrey and Heskestad's correlations under predicts ceiling jet temperatures in compartment fires with an established hot gas layer. For these cases, correlation results should be corrected. The original version of FIVE made this correction by adding the plume and hot gas layer temperature. This practice results in consistent over predictions of the ceiling jet temperature. In the case of BE 2, the over predictions are significant due to over predictions in the hot gas layer discussed in Section 6.1.
- Based on the above discussion, a classification of yellow + is recommended if hot gas layer effects on the plume temperature are considered. The McCaffrey and Heskestad's correlations are not intended to be used in rooms with an established hot gas layer.

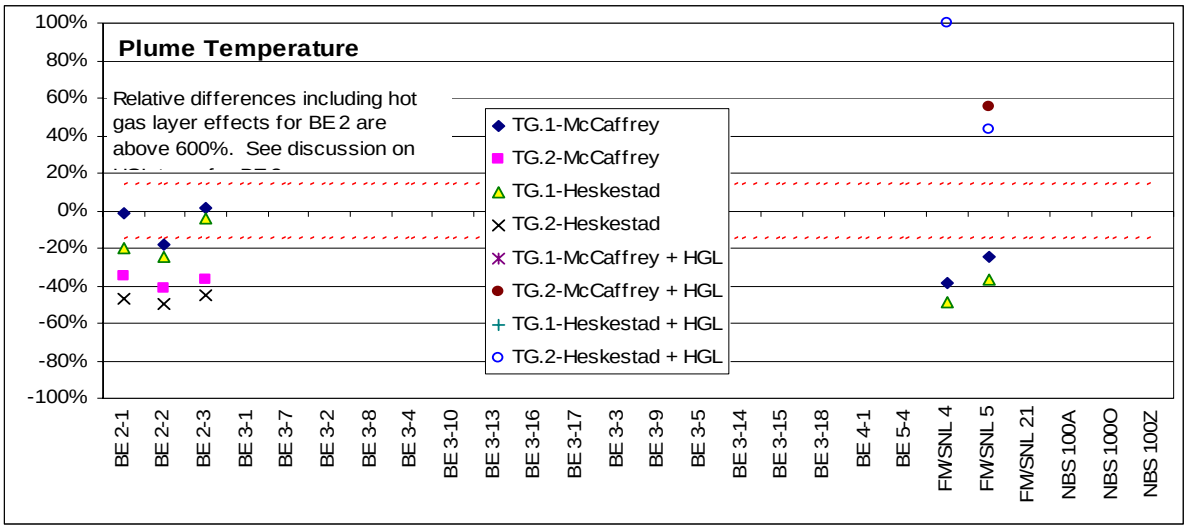

Figure 6-3: Scatter plot of relative differences for plume temperatures in ICFMP BE #2, and the selected FM/SNL Tests

6.4 Flame Height

Flame height is recorded by visual observations, photographs or video footage. Videos from the ICFMP BE # 3 test series and photographs from BE #2 are available. It is difficult to precisely measure the flame height, but the photos and videos allow one to make estimates accurate to within a pan diameter. In FIVE-Rev1, flames heights are calculated using Heskestad's correlation.

ICFMP BE #2: The height of the visible flame in the photographs of BE #2 has been estimated to be between 2.4 and 3 pan diameters (3.8 m to 4.8 m, 12.5 ft to 15.7 ft). From Figure A-19, which reports flame height predictions, flame heights are 3 to 5 m (9.8 ft to 16.4 ft) high. Those predictions are consistent with the experimental observations.

ICFMP BE #3: The Heskestad correlation appears to predicts the flame height accurately in this test series, at least to the accuracy of visual observations and a few photographs taken before the HGL obscures the upper part of the fire. The experiments were not designed to measure the flame height other than through visual observation. Flame height pictures and model predictions can be found in Figures A-21 to A-23.

Summary: Flame Height

- Based on a comparison between visual observations and Heskestad's correlation predictions, the correlation is appropriate to calculate flame height for scenarios similar to the ones evaluated in this study.
- Visual observations of flames compared with Heskestad's predictions suggest good agreement. It is not possible to provide a quantitative assessment of the comparison given that no flame height data was collected during the experiments. However, this evaluation does not suggest that the Heskestad correlation is consistently under-predicting or over predicting flame height. A green classification is recommended for applications involving flames away from walls.

6.5 Radiation and Total Heat Flux and Target Temperature

Radiant heat flux data is available from ICFMP BE #3 only. This evaluation compares point source model results with experimental measurements using radiation gauges. Graphical comparisons of experimental measurements and model results are included in Figures A-24 to A-31. Relative differences are listed in Table A-22.

- **ICFMP BE #3**: Four radiation gauges were selected for comparison, Gauges 1, 3, 7, and 10. The experimental uncertainty is about 20 % for both heat flux and surface temperature. Figure 6-4 shows the relative differences. The following observations are relevant:
  - Experimental measurements for Gauge 10 are consistently under predicted by about 50%.
  - Gauges 1, 3, and 7 show similar patterns per test of over and under predictions. Closed door tests are over predicted, and opened door tests are either within experimental uncertainty or under predicted.
  - The point source model is intended for predicting radiation from flames in an unobstructed and smoke-clear path between flames and targets. That is not the case in most of these comparisons. Gauge 10 has the lowest elevation from the floor, but its location alone does not explain a consistent under-prediction in open and close door tests. Gauges 1, 3, and 7 were located 2, 2.5, and 3 m (6.6 ft, 8 ft, and 9.8 ft) respectively above the floor. The hot gas layer in opened door tests descended to 1 m (3.3. ft) above the floor. Therefore, these three gauges were immersed in smoke during all tests by the time were the radiation measurements were selected for comparison. Given that the point source inputs are the same for all tests with the exception of the heat release rate, the difference between the over predictions in closed door tests and under predictions is open door tests is due to the effect experimental measurements. That is, experimental measurements are lower in open door tests than in close door tests. This observation is difficult to generalize for practical purposes since conditions like location of the hot gas layer, soot concentration and location of the target relative to the fire will need to be considered on a case by case basis.
  - Based on the above discussion, a yellow classification is recommended. Analysts should consider that the point source model is intended for predicting radiation from flames in an unobstructed and smoke-clear path between flames and targets. No data was available in this study from a scenario with such conditions.

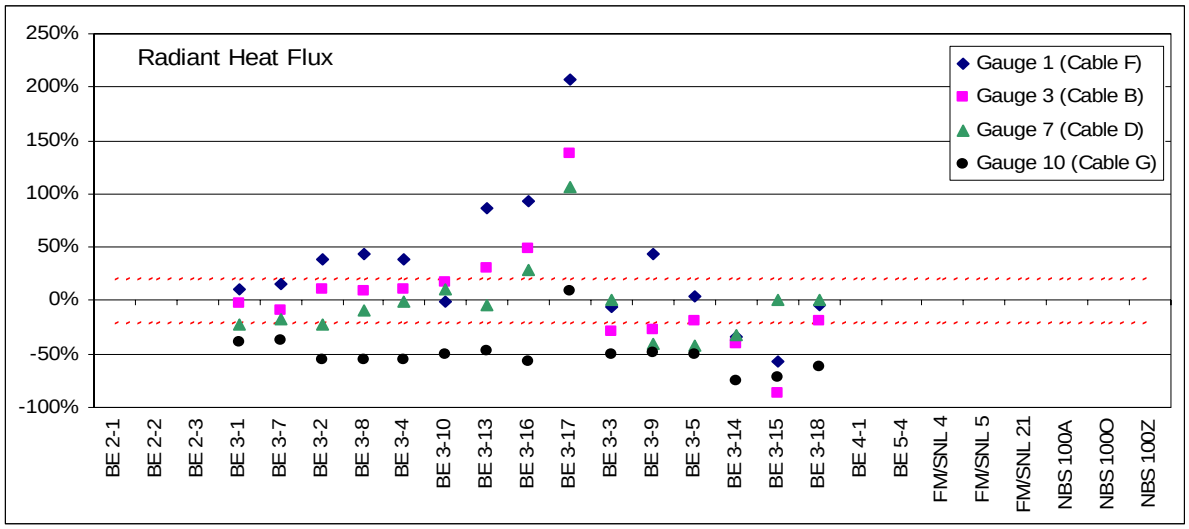

Figure 6-4. Scatter plot of relative differences for target temperature and heat flux in ICFMP BE#4 and 5.

7
REFERENCES

1. EPRI TR-1002981, "Fire Modeling Guide for Nuclear Power Plant Applications," August 2001.
2. ASTM E1355, "*Standard Guide for Evaluating the Predictive Capability of Deterministic Fire Models*."
3. EPRI TR-100443, "*Methods for Quantitative Fire Hazard Analysis*," May 1992.
4. *SFPE Handbook of Fire Protection Engineering, 3rd. Edition*, 2002.
5. Karlsson, B. and J. Quintiere. *Enclosure Fire Dynamics*. CRC Press, Boca Raton, FL, 2000.
6. Drysdale, D. *An Introduction to Fire Dynamics*, John Wiley and Sons, Inc., Chichester, 1996.
7. Lee, B. T. "Heat Release Rate Characteristics of Some Combustible Fuel Sources in Nuclear Power Plants" National Bureau of Standards NBS 85-3195. July 1985.
8. Heskestad, G. "Fire Plumes, Flame Height, and Air Entrainment" *SFPE Handbook of Fire Protection Engineering*, 3rd Edition. Chapter 2-1.
9. Beyler, C. "Fire Plumes and Ceiling Jets". *Fire Safety Journal* 11 (1986) pp 53–75.
10. Alpert, R. "Ceiling Jet Flows" *SFPE Handbook of Fire Protection Engineering*, 3rd Edition. Chapter 2-2.
11. Thomas, P., and D. Walton. "Estimating Temperatures in Compartment Fires," *SFPE Handbook of Fire Protection Engineering, 3rd. Edition*, 2002. Chapter 3–6.
12. Cooper, L. "Fire Plume Generated Ceiling Jet Characteristics and Convective Heat Transfer to Ceiling and Wall Surfaces in a Two-Layer Fire Environment: Uniform Temperature, Ceiling and Walls" *Fire Science & Technology,* Vol. 13, No. 1 & No. 2 (1–17), 1993.
13. Mulholland, G. "Smoke Production and Properties" *SFPE Handbook of Fire Protection Engineering*, 3rd Edition. Chapter 2–13.
14. Alpert, R. "Evaluation of Unsprinklered Fire Hazards" *Fire Safety Journal*, 7 (1984) p 127–143.
15. SFPE – DETACT
16. NUREG-1758, "Evaluation of Fire Models for Nuclear Power Plant Applications: Cable Tray Fires"
17. U.S. NRC, Inspection Manual Chapter 06.09, Appendix F, "Fire Protection Significance Determination Process," May 28, 2004.

A
TECHNICAL DETAILS OF FIVE-REV1 VALIDATION STUDY

This appendix provides technical basis for the relative difference values listed in Chapter 6 of Volume 3 for the output parameters in the FIVE-Rev1 library of fire modeling engineering calculations. This appendix is organized into sections for the parameters that have been verified and validated in this study for this specific tool. Not all of the models in FIVE-Rev2 have been subjected to verification and validation due to a lack of experimental data or model applicability. Each section presents a graph of the experimental data and the model output and a table of relative differences at the peaks between experimental data and the model output. The sections also list the values selected for input to the model. Within each section, the graphs are grouped by experimental test series. Discussion and analysis of the relative differences can found in Chapter 6 of Volume 3. The Appendix is organized into the following sections:

A.1 Hot Gas Layer Temperature

A.2 Ceiling Jet Temperature

A.3 Plume Temperature

A.4 Flame Height

A.5 Radiant Heat Flux

Volume 7 includes detailed discussion of the uncertainties associated with both the experimental data and model predictions presented in this Appendix.

The model predictions are compared to the experimental measurements in terms of the relative difference between the maximum (or where appropriate, minimum) values of each time history:

$$\varepsilon = \frac{\Delta M - \Delta E}{\Delta E} = \frac{\left(M_p - M_o\right) - \left(E_p - E_o\right)}{\left(E_p - E_o\right)}$$

ΔM is the difference between the peak value of the model prediction, M_p, and its original value, M_o. ΔE is the difference between the experimental measurement, E_p, and its original value, E_o. A positive value of the relative difference indicates that the model has over-predicted the severity of the fire; for example, a higher temperature, lower oxygen concentration, higher smoke concentration, *etc*.

Finally, all of the calculations performed in the evaluation were *open*; that is, the heat release rate of the fire was a *specified* model input, and the results of the experiments were provided to the analysts.

A.1 Hot Gas Layer Temperature

Relative differences for hot gas layer temperature were calculated using experimental data from ICFMP benchmark exercises 2, 3, 4, and 5, the FM/SNL test series, and the NBS multi-compartment fire test series. In the case of hot gas layer temperature, positive relative differences are an indication that the temperature predictions are higher than the experimental observations.

As described in Chapter 3, the hot gas layer temperature in the FIVE-Rev1 library can be calculated using the FPA for closed mechanically ventilated rooms or MQH model for naturally ventilated enclosures.

A.1.1 ICFMP BE #2

The HGL temperature for the ICFMP BE #2 experiments was calculated using the MQH model. The experimental description suggests that although the structure was closed in the first two experiments, leakages up to 2 m^2 may exist. The third experiment had an exhaust system ($11 m^3/s$). However, considering that the system was not supplying any air into the enclosure, and that there were two opened doors, the MQH model may be more appropriate for temperature calculations since fresh air only moves in through the openings.

The input parameters to the MQH model are listed in Table A-1 and Figure A-1. The comparison between measured hot gas layer temperatures for ICFMP BE #2 Cases 1, 3 and 3 are presented in Figure A-2.

Table A-1: Inputs to MQH model in ICFMA BE # 2

Ambient temp [C]	20
Room Size	
Room length [m]	27
Room width [m]	13.8
Room height [m]	15.8
Wall Properties	
Wall k [kW/m-K]	0.0002
Wall Cp [kJ/Kg-K]	0.15
Wall ρ [kg/m^3]	500
Thickness [m]	0.05
Nat & Mech Vent	
Opening height Ho [m]	0.7
Opening area Ao [m^2]	2

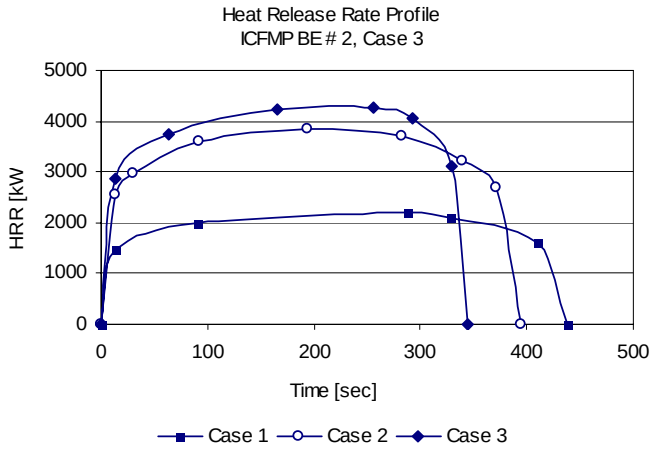

Figure A-1: Heat release rate profile for ICFMP BE #2

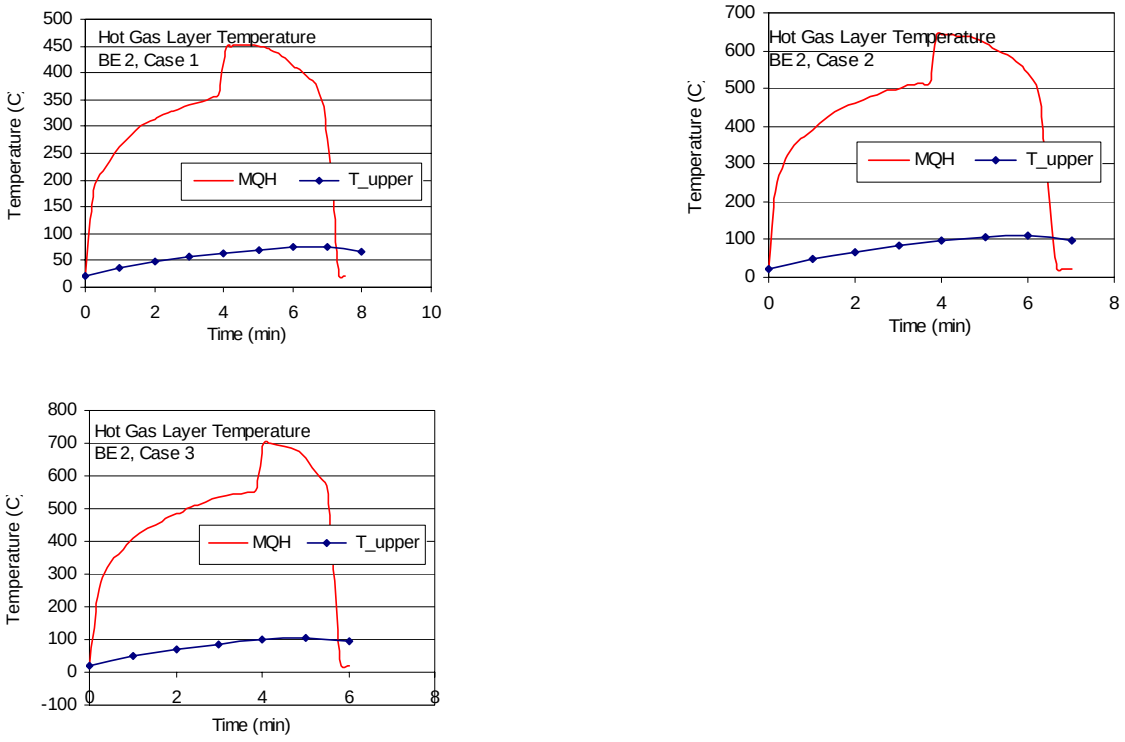

Figure A-2: Hot Gas Layer (HGL) Temperature and Height, ICFMP BE #2.

Table A-2 summarizes the relative differences calculated for the hot gas layer temperature. MAGIC under predicts the measured temperature.

Table A-2: Relative differences of hot gas layer temperature in ICFMP BE# 2

	Hot Gas Layer Temperature		
Test	ΔE (°C)	ΔM (°C)	Relative Difference
ICFMP 2-1	54.8	432.6	690%
ICFMP 2-2	86.3	624.1	623%
ICFMP 2-3	82.6	678.4	722%

A.1.2 ICFMP BE # 3

BE #3 consists of 15 liquid spray fire tests with different heat release rate, pan locations, and ventilation conditions. Gas temperatures were measured using seven floor-to-ceiling thermocouple arrays (or "trees") distributed throughout the compartment. The average hot gas layer temperature was calculated using thermocouple Trees 1, 2, 3, 5, 6 and 7. Tree 4 was not used because one of its thermocouples (4-9) malfunctioned during most of the experiments.

It is important to indicate also that the HGL reduction method produces spurious results in the first few minutes of each test because no clear layer has yet formed.

The comparison between MAGIC simulations and measured hot gas layer temperatures are compiled in Figure A-3 to Figure A-4. Notice that comparisons are only available for tests with opened doors with or without mechanical ventilation, and closed doors with mechanical ventilation. The temperature for the former group was calculated using the MQH model. The temperature for the later group was calculated with the FPA model. No comparisons are provided for tests with closed door and no mechanical ventilation because the FIVE-Rev1 library does not include a model for such conditions. The inputs for the MQH and FPA models are listed in Table A-3 The heat release rate profiles are identical to the ones used in the MAGIC simulations, and are described in Volume 7 of this report.

Table A-3: Inputs to the MQH and FPA model in ICFMP BE #3

Ambient temp [C]	22
Room Size	
Room length [m]	21.7
Room width [m]	7.04
Room height [m]	3.82
Wall Properties	
Wall k [kW/m-K]	0.00013
Wall Cp [kJ/Kg-K]	1.17
Wall ρ [kg/m^3]	737
Thickness [m]	0.025
Nat & Mech Vent	
Opening height Ho [m]	2
Opening area Ao [m^2]	4
CFM	1907

No plot for BE #3, Test 1. This is a closed door test with no mechanical ventilation.

No plot for BE #3, Test 2. This is a closed door test with no mechanical ventilation.

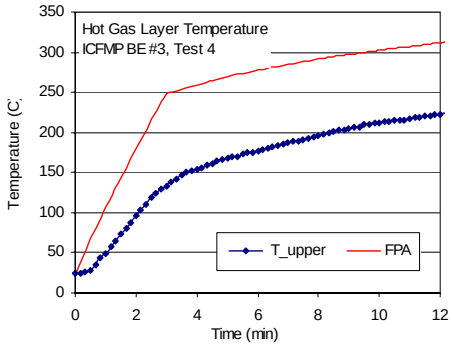

No plot for BE #3, Test 13. This is a closed door test with no mechanical ventilation.

No plot for BE #3, Test 7. This is a closed door test with no mechanical ventilation.

No plot for BE #3, Test 8. This is a closed door test with no mechanical ventilation.

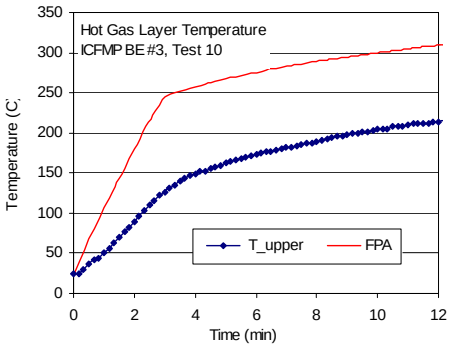

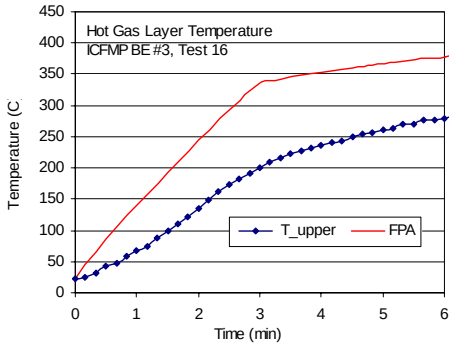

Figure A-3. Hot Gas Layer (HGL) temperature, ICFMP BE #3, closed door tests with mechanical ventilation.

No plot for BE #3, Test 17. This is a closed door test with no mechanical ventilation.

Open Door Tests

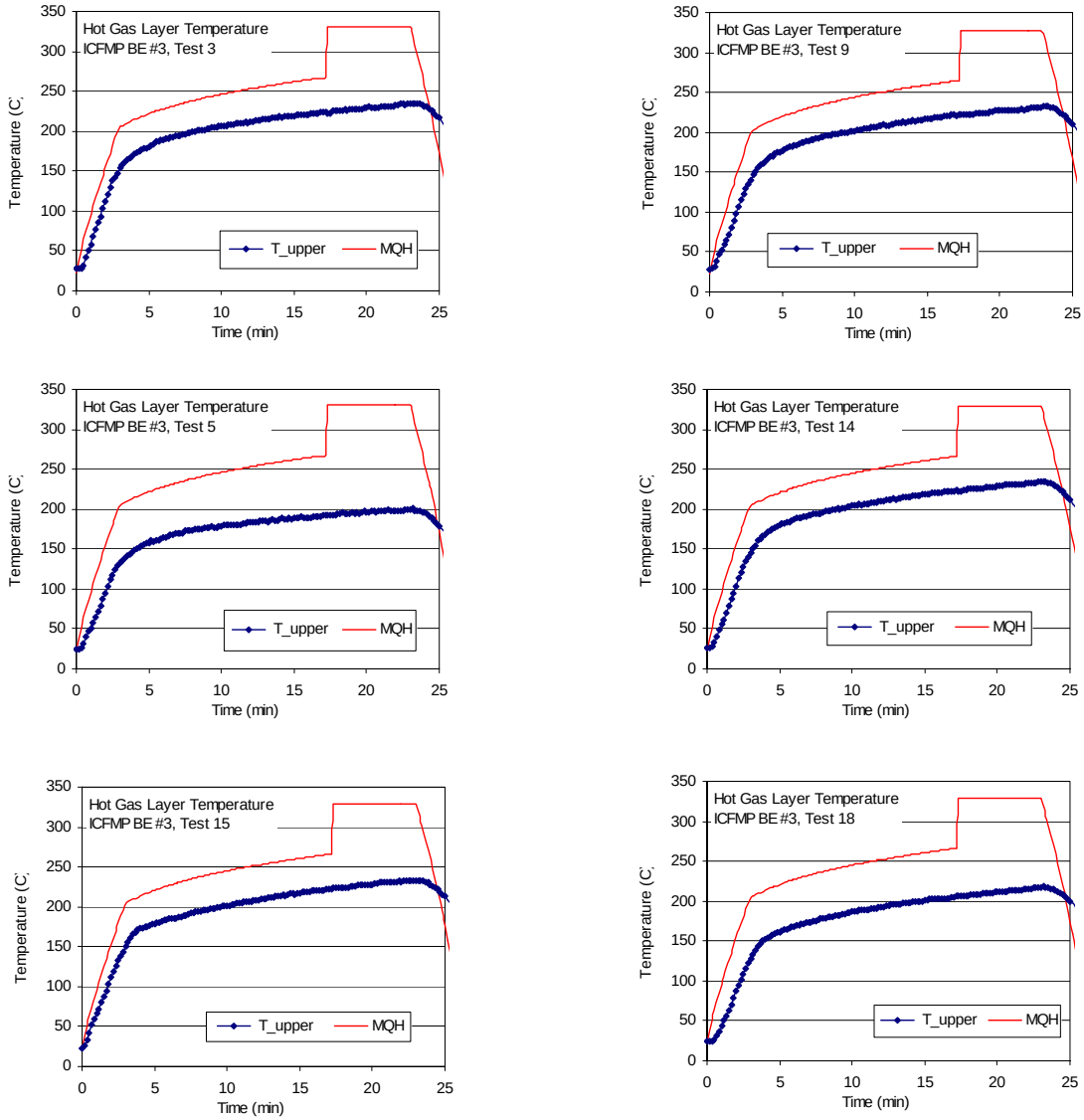

Figure A-4: Hot Gas Layer (HGL) temperature ICFMP BE #3, open door tests.

Table A-4: Relative differences of hot gas layer temperature and height in ICFMP BE# 3

	Hot Gas Layer Temperature		
Test	ΔE (^{o}C)	ΔM (^{o}C)	Relative Difference
ICFMP 3-1			N/A[1]
ICFMP 3-7			N/A[1]
ICFMP 3-2			N/A[1]
ICFMP 3-8			N/A[1]
ICFMP 3-4	204.3	295.5	45%
ICFMP 3-10	197.8	293.8	49%
ICFMP 3-13			N/A[1]
ICFMP 3-16	268.4	359.8	34%
ICFMP 3-17			N/A[1]
ICFMP 3-3	207.3	309.2	49%
ICFMP 3-9	204.0	306.1	50%
ICFMP 3-5	175.5	309.2	76%
ICFMP 3-14	208.2	307.6	48%
ICFMP 3-15	210.6	307.6	46%
ICFMP 3-18	193.4	307.6	59%

1. No relative differences calculated for closed-door rooms with no mechanical ventilation. There is no model applicable to this case in the FIVE-Rev1 library.

A.1.3 ICFMP BE #4

ICFMP BE # 4 consisted of two experiments, of which one was chosen for validation, Test 1. Compared to the other experiments, this fire was relatively large in a relatively small compartment. Thus, its HGL temperature is considerably higher than the other fire tests under study. The hot gas layer temperature was calculated with using the MQH model. Table A-5 lists the input parameters. The heat release rate profile is presented in Figure A-5.

Table A-5: Inputs to the MQH model in ICFMP BE #4

Ambient temp [C]	20
Room Size	
Room length [m]	3.6
Room width [m]	3.6
Room height [m]	5.7
Wall Properties	
Wall k [kW/m-K]	0.00075
Wall Cp [kJ/Kg-K]	0.84
Wall ρ [kg/m^3]	1500
Thickness [m]	0.025
Nat & Mech Vent	
Opening height Ho [m]	3.6
Opening area Ao [m^2]	2.1

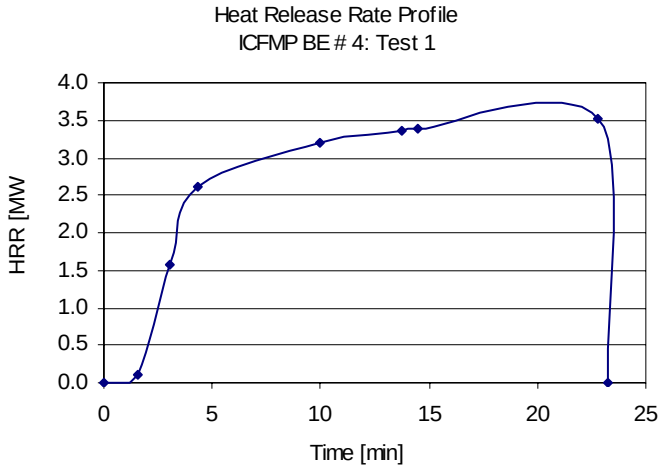

Figure A-5: Heat release rate profile for ICFMP BE #4.

Figure A-6 includes the comparison between experimental and predicted hot gas layer temperature and height. The relative differences calculated for this experiment are listed in Table A-6.

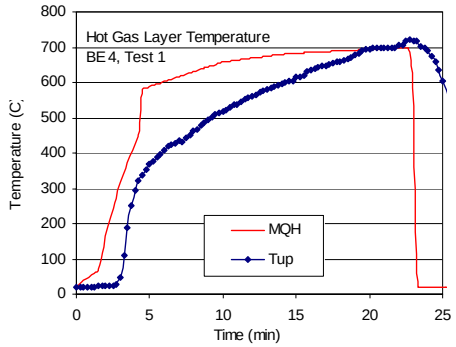

Figure A-6: Hot Gas Layer (HGL) Temperature and Height, ICFMP BE #4, Test 1.

Table A-6: Relative differences of hot gas layer temperature in ICFMP BE# 4

	Hot Gas Layer Temperature		
Test	ΔE (^{o}C)	ΔM (^{o}C)	Relative Difference
ICFMP 4-1	700.1	589.0	-16%

A.1.4: ICFMP BE #5

BE #5 was performed in the same fire test facility as BE #4. Only one of the experiments from this test series was used in the evaluation, Test 4, and only the first 20 min of the test, during the "pre-heating" stage when only the ethanol pool fire was active. The burner was lit after that point, and the cables began to burn. Figure A-7 presents the heat release rate profile measured during the test. The inputs for the MQH equation are listed in Table A-7.

Table A-7: Inputs to the MQH model in ICFMP BE #5

Ambient temp [C]	20
Room Size	
Room length [m]	3.6
Room width [m]	3.6
Room height [m]	5.7
Wall Properties	
Wall k [kW/m-K]	0.0016
Wall Cp [kJ/Kg-K]	0.75
Wall ρ [kg/m^3]	2400
Thickness [m]	0.3
Nat & Mech Vent	
Opening height Ho [m]	2.2
Opening area Ao [m^2]	1.54

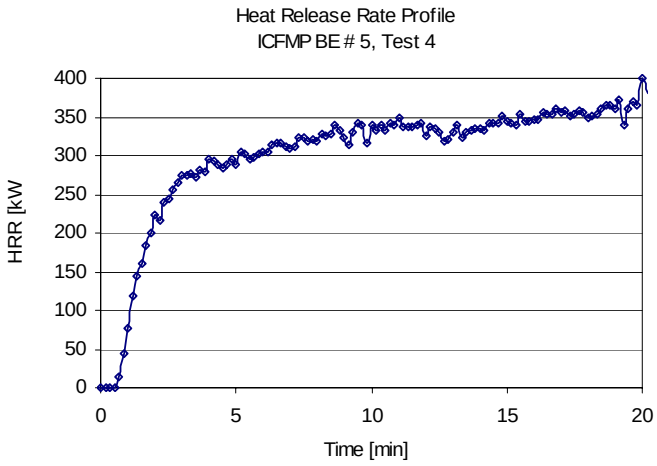

Figure A-7: Heat release rate profile for ICFMP BE #5.

Figure A-8 summarizes the comparison between the experimental and predicted hot gas layer and height during the first 20 minutes of simulation. The corresponding relative differences are listed in Table A-8.

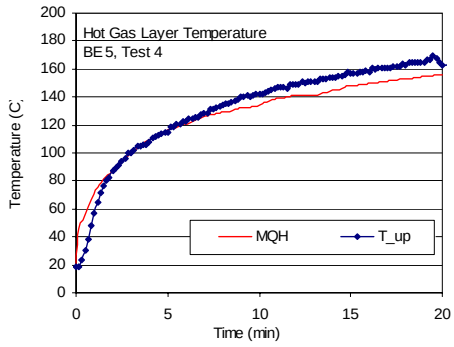

Figure A-8: Hot Gas Layer (HGL) Temperature and Height, ICFMP BE #5, Test 4.

Table A-8: Relative differences of hot gas layer temperature in ICFMP BE# 5

	Hot Gas Layer Temperature		
Test	ΔE (^oC)	ΔM (^oC)	Relative Difference
ICFMP 5-4	150.3	136.0	-10%

A.1.5 FM/SNL Test Series

Tests 4, 5, and 21 from the FM-SNL test series were selected for comparison. Hot gas layer temperatures were calculated using the FPA model. Figure A-9 and Table A-9 provide the input parameters for the FPA model. The experimental hot gas layer temperature and height were calculated using the standard method. The thermocouple arrays that are referred to as Sectors 1, 2 and 3 were averaged (with an equal weighting for each) for Tests 4 and 5. For Test 21, only Sectors 1 and 3 were used, as Sector 2 fell within the smoke plume.

Table A-9: Input parameters for the FPA model in FM/SNL tests

	Test 5	Test 4 & 21
Ambient temp [C]	20	20
Room Size		
Room length [m]	18.3	18.3
Room width [m]	12.2	12.2
Room height [m]	6.1	6.1
Wall Properties		
Wall k [kW/m-K]	0.00012	0.00012
Wall Cp [kJ/Kg-K]	1.25	1.25
Wall ρ [kg/m^3]	720	720
Thickness [m]	0.0125	0.0125
Mech Vent		
CFM	8000	800

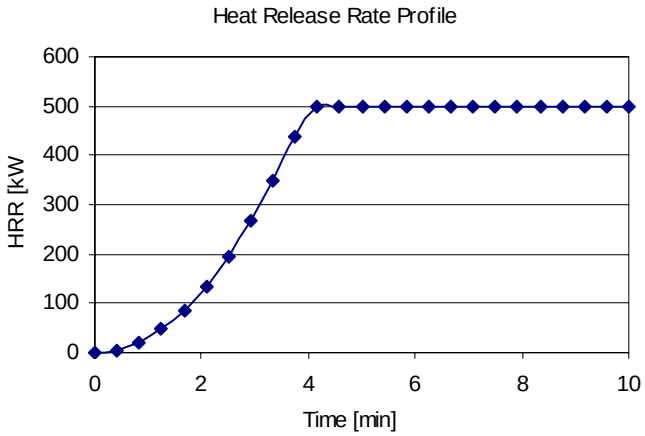

Figure A-9: Heat release rate profiles for the selected FM.SNL tests.

Figure A-10 summarizes the graphical comparison of hot gas layer temperatures and heights for Tests 4, 5, and 21. The relative differences are included in Table A-10.

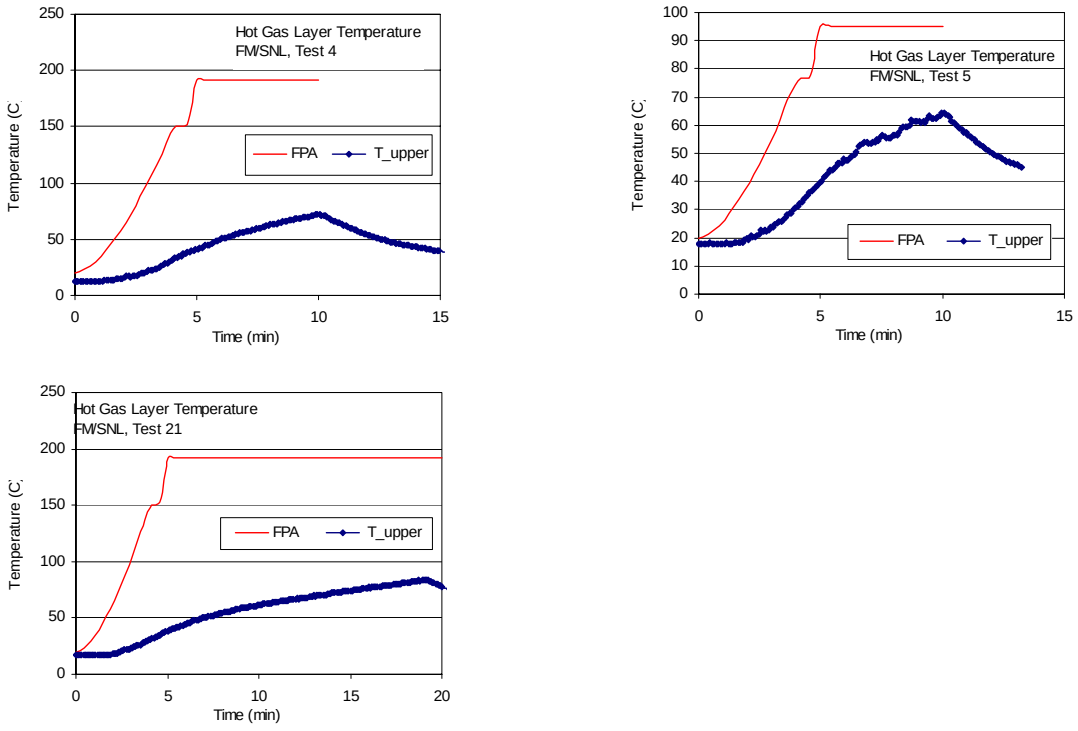

Figure A-10: Hot Gas Layer (HGL) Temperature and Height, FM/SNL Series.

Table A-10: Relative differences of hot gas layer temperature and height in FM/SNL

	Hot Gas Layer Temperature		
Test	ΔE (^{o}C)	ΔM (^{o}C)	Relative Difference
FM/SNL 4	59.2	171.5	190%
FM/SNL 5	46.6	74.9	61%
FM/SNL 21	66.0	171.5	160%

A.1.6 The NBS Multi-Room Test Series

This series of experiments consisted of two relatively small rooms connected by a long corridor. The fire was located in one of the rooms. Eight vertical arrays of thermocouples were positioned throughout the test space: one in the burn room, one near the door of the burn room, three in the corridor, one in the exit to the outside at the far end of the corridor, one near the door of the other or "target" room, and one inside the target room. Four of the eight arrays were selected for comparison with model prediction: the array in the burn room, the array in the middle of the corridor, the array at the far end of the corridor, and the array in the target room. In Tests 100A and 100O, the target room was closed, in which case the array in the exit doorway was used.

The standard reduction method was not used to compute the experimental HGL temperature for this test series. Rather, the test director reduced the layer information individually for the eight thermocouple arrays using an alternative method (Peacock 1991).

This evaluation is limited to the room of fire origin only. The MQH model was selected for the evaluation since the room has an open door and no mechanical ventilation. Table A-11 lists the input parameters for the MQH model.

Table A-11: Input parameters for the MQH model in the NBS tests

Ambient temp [C]	20
Room Size	
Room length [m]	2.3
Room width [m]	2.3
Room height [m]	2.16
Wall Properties	
Wall k [kW/m-K]	0.00009
Wall Cp [kJ/Kg-K]	128
Wall ρ [kg/m^3]	1.04
Thickness [m]	0.05
Nat & Mech Vent	
Opening height Ho [m]	1.6
Opening area Ao [m^2]	1.28
Fire	
HRR [kW] -- Constant	110

Figure A-11 compiles the graphical comparison between experimental measurements and modeling results for hot gas layer temperature for the three selected experiments. The corresponding relative differences are listed in Table A-12.

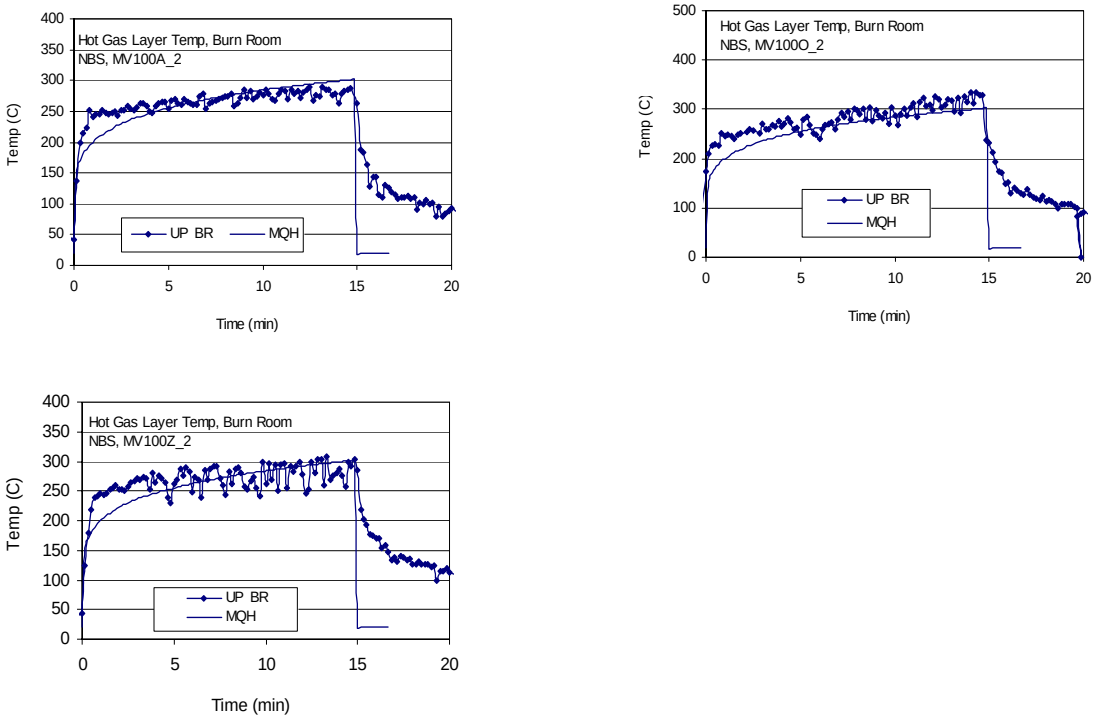

Figure A-11: Hot Gas Layer (HGL) Temperature, NBS Multiroom, Test 100A.

Table A-12: Relative differences of hot gas layer temperature and height in NBS Tests

		Hot Gas Layer Temperature		
		ΔE (^oC)	ΔM (^oC)	Relative Difference
NBS A	Burn Room	247.8	166.0	-33%
NBS O	Burn Room	310.3	166.0	-47%
NBS Z	Burn Room	283.9	166.0	-42%

A.2 Ceiling Jet Temperature

The FIVE-Rev1 library includes the Alpert correlation for ceiling jet temperature. Experimental measurements for the ceiling are available from ICFMP BE #3 and the FM/SNL series only.

Positive relative differences are an indication that the MAGIC prediction is higher than the experimental observation.

The ceiling jet temperature correlation using experimental data collected from controlled environments with no hot gas layer effects. If such correlations are used for analyzing fire scenarios involving a hot gas layer, a correction is recommended to account for the thermal effects of the hot gas layer in the ceiling jet temperature. In the case of the ceiling jet, hot gas layer effects may not be important in the following two situations: 1) in the early phases of the fire event, when a hot gas layer has not been established, and 2) in relatively large rooms with relatively small fires, where the hot gas layer temperature is close to ambient.

In the first version of FIVE, the hot gas layer effects were included in the analysis by adding (superimposing) the calculated temperature rise in the ceiling jet to the hot gas layer temperature. In some cases, this simplification produce over predictions in the ceiling jet temperature. The equation is: $T_{P-HGL} = T_{HGL} + \Delta T_P = T_{HGL} + T_P - T_{amb}$

This section presents both comparisons: with and without considerations for the hot gas layer effects. The hot gas layer temperature added to the ceiling jet was reported earlier in section A.1.

A.2.1 ICFMP BE # 3

The thermocouple nearest the ceiling in Tree 7, located towards the back of the compartment, was chosen as a surrogate for the ceiling jet temperature. The 15 graphical comparisons of experimental measurements and model results are grouped in Figure A-12 and Figure A-13. The corresponding relative differences are listed in Table A-14.

Table A-13 lists specific location parameters required for the plume temperature correlation. The heat release rate values are listed in Volume 7.

Table A-13: Target location information for ceiling jet correlation

Ceiling Jet				
Target height [m]	3.5			
Fire elevation [m]	0			
Instrument	All Others	Test 14	Test 15	Test 18
Radial dist [m]	5.9	6.1	6.3	4.8

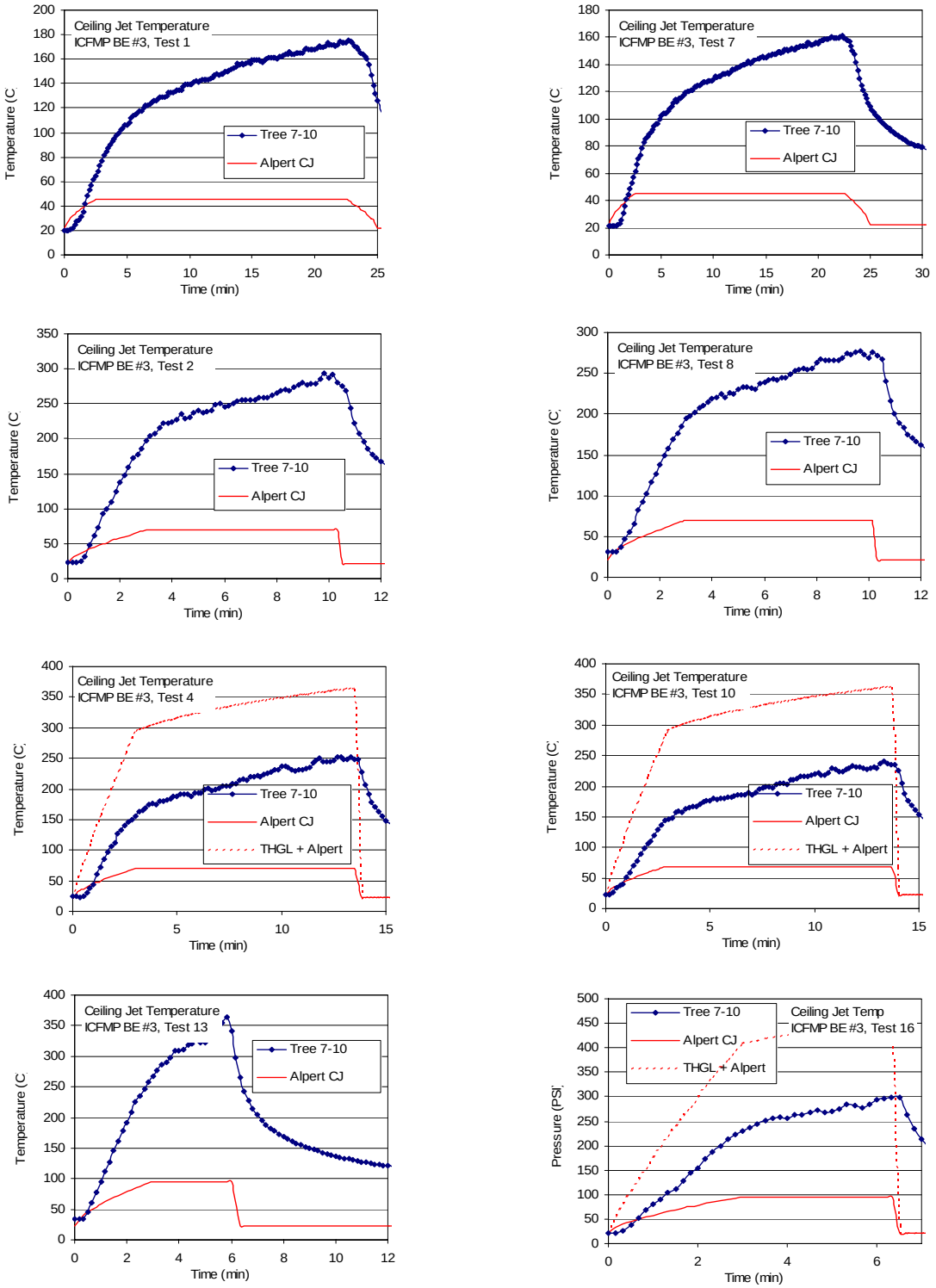

Figure A-12: Near-ceiling gas (ceiling jet) temperatures, ICFMP BE #3, closed door tests.

Open Door Tests

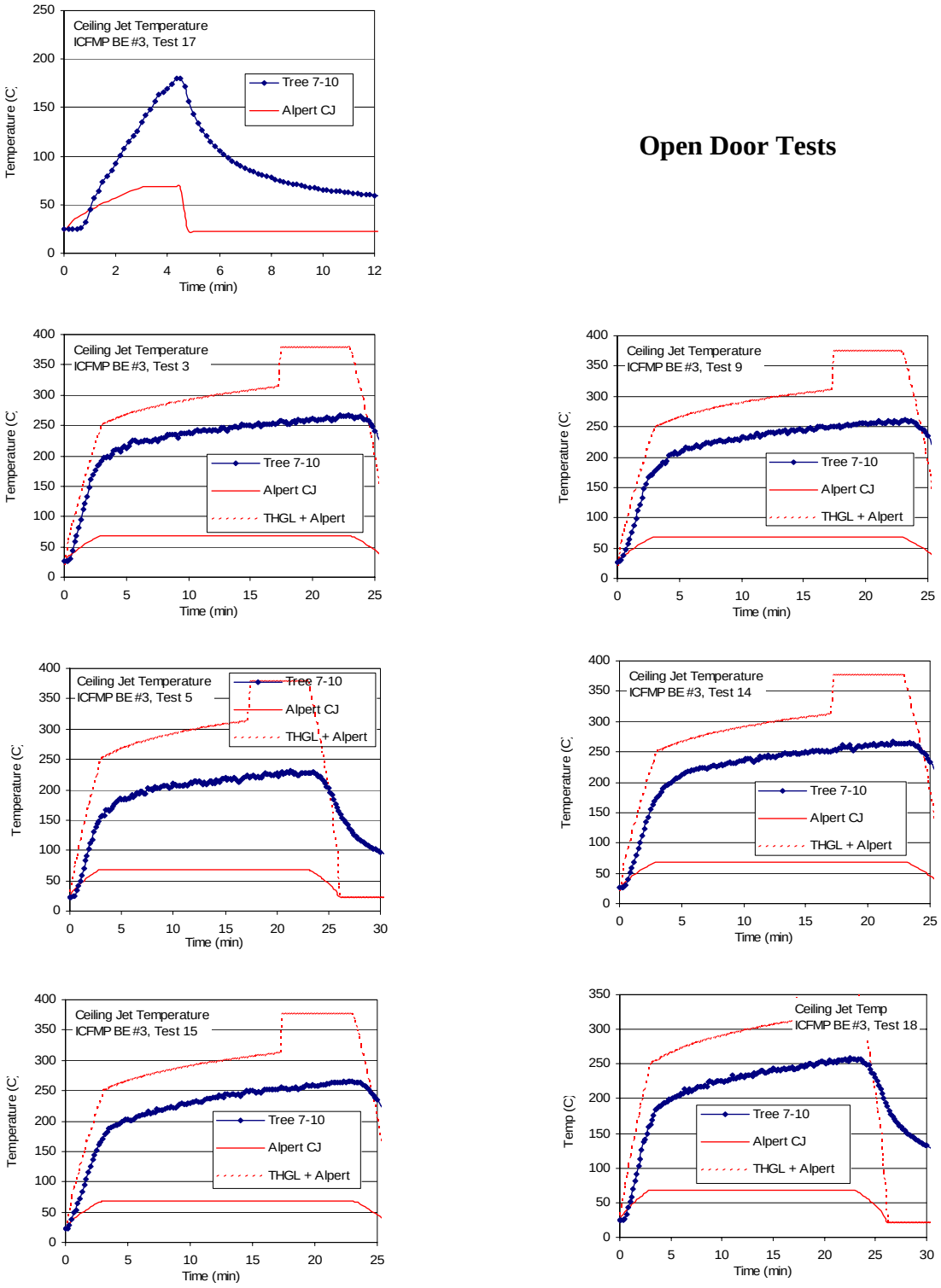

Figure A-13: Near-ceiling gas (ceiling jet) temperatures, ICFMP BE #3, open door tests

Table A-14: Relative differences for ceiling jet temperature in ICFMP BE #3

		No Hot Gas Layer Effects			Hot Gas Layer Effects		
		ΔE (^oC)	ΔM (^oC)	Relative Difference	ΔE (^oC)	ΔM (^oC)	Relative Difference
ICFMP 3-1	Tree 7-10	154.90	23.29	-85%	154.9	175.3	13%
ICFMP 3-7	Tree 7-10	139.32	23.29	-83%	139.3	175.3	26%
ICFMP 3-2	Tree 7-10	270.60	47.03	-83%	270.6	272.3	1%
ICFMP 3-8	Tree 7-10	246.93	47.03	-81%	246.9	271.5	10%
ICFMP 3-4	Tree 7-10	228.86	47.39	-79%	228.9	342.8	50%
ICFMP 3-10	Tree 7-10	217.55	47.03	-78%	217.5	340.9	57%
ICFMP 3-13	Tree 7-10	330.51	73.38	-78%	330.5	395.7	20%
ICFMP 3-16	Tree 7-10	277.66	72.73	-74%	277.7	432.6	56%
ICFMP 3-17	Tree 7-10	155.86	46.32	-70%	155.9	239.2	53%
ICFMP 3-3	Tree 7-10	240.67	47.03	-80%	240.7	356.2	48%
ICFMP 3-9	Tree 7-10	234.60	46.56	-80%	234.6	352.6	50%
ICFMP 3-5	Tree 7-10	207.74	47.03	-77%	207.7	356.2	71%
ICFMP 3-14	Tree 7-10	240.80	46.80	-81%	240.8	354.4	47%
ICFMP 3-15	Tree 7-10	243.66	46.80	-81%	243.7	354.4	45%
ICFMP 3-18	Tree 7-10	235.13	46.80	-80%	235.1	354.4	51%

A.2.2 The FM/SNL Test Series

The near-ceiling thermocouples in Sectors 1 and 3 were chosen as surrogates for the ceiling jet temperature. The results are shown below.

Table A-15 lists specific location parameters required for the plume temperature correlation. The heat release rate values are listed in Volume 7.

Figure A-14 compiles the graphical comparisons between experimental measurements for ceiling jet temperature and the correlation predictions. The corresponding relative differences are listed in Table A-16.

Table A-15: Target location information for ceiling jet correlation

Ceiling Jet				
Target height [m]	5.9			
Fire elevation [m]	0			
Instrument	X	Y	Z	
Fire	12.0	6.1	0.3	Radial dist [m]
3-98	3.04	2.032	5.97	9.8
1-98	15.24	6.09	5.97	7.1

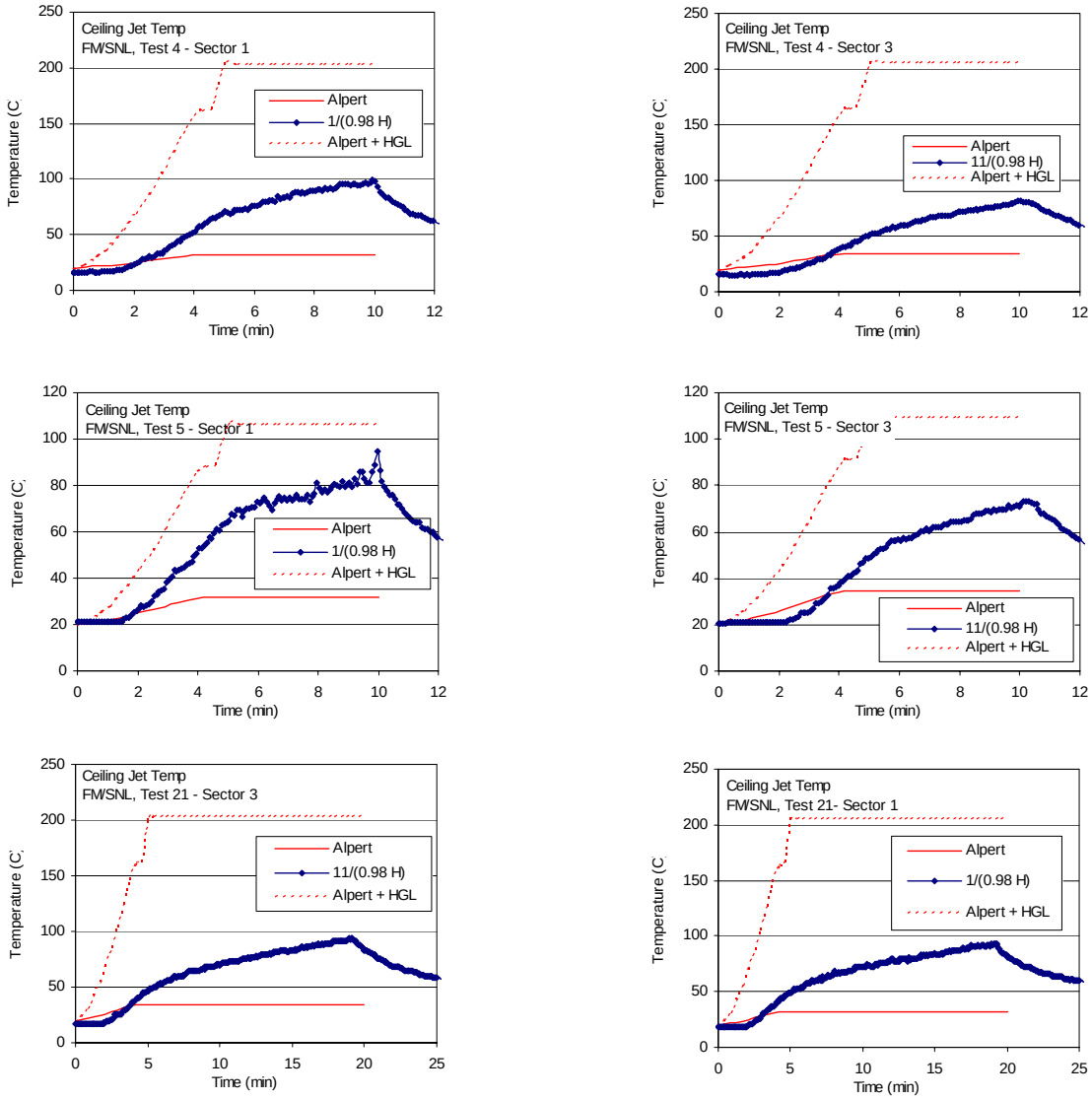

Figure A-14: Near-ceiling gas (ceiling jet) temperatures, FM/SNL Series, Sectors 1 and 3.

Table A-16: Relative differences for ceiling jet temperatures in FM/SNL Tests

		No Hot Gas Layer Effects			Hot Gas Layer Effects		
		ΔE (°C)	ΔM (°C)	Relative Difference	ΔE (°C)	ΔM (°C)	Relative Difference
FM/SNL 4	1/98H	82.8	11.8	-86%	82.8	183.3	121%
	11/98H	66.1	14.7	-78%	66.1	186.2	182%
FM/SNL 5	1/98H	73.7	11.8	-84%	73.7	86.7	18%
	11/98H	52.6	14.7	-72%	52.6	89.5	70%
FM/SNL 21	1/98H	75.9	11.8	-84%	75.9	86.7	14%
	11/98H	77.2	14.7	-81%	77.2	89.5	16%

A.3 Plume Temperature

Plume temperature measurements are available from ICFMP BE #2 and the FM/SNL series. For all the other series of experiments, the temperature was not measured above the fire, the fire plume leaned because of the flow pattern within the compartment, or the fire was set up against a wall. Only for BE #2 and the FM/SNL series were the plumes relatively free from perturbations.

The Heskestad's and McCaffrey's plume temperature correlations are considered in this evaluation.

The plume temperature correlations using experimental data collected from controlled environments with no hot gas layer effects. If such correlations are used for analyzing fire scenarios involving a hot gas layer, a correction is recommended to account for the thermal effects of the hot gas layer in the ceiling jet temperature. In the case of the plume, hot gas layer effects may not be important in the following two situations: 1) in the early phases of the fire event, when a hot gas layer has not been established, and 2) in relatively large rooms with relatively small fires, where the hot gas layer temperature is close to ambient.

In the first version of FIVE, the hot gas layer effects were included in the analysis by adding (superimposing) the calculated temperature rise in the ceiling jet to the hot gas layer temperature. In some cases, this simplification produces over predictions in the ceiling jet temperature. The equation is: $T_{P-HGL} = T_{HGL} + \Delta T_P = T_{HGL} + T_P - T_{amb}$.

This section presents both comparisons: with and without considerations for the hot gas layer effects. The hot gas layer temperature added to the ceiling jet was reported earlier in section A.1.

A.3.1 ICFMP BE # 2

BE #2 consisted of liquid fuel pan fires conducted in the middle of a large fire test hall. Plume temperatures were measured at two heights above the fire, 6 m and 12 m. The flames extended to about 4 m above the fire pan. (Figure A-15). The suspended rectangle contains an array of thermocouples designed to locate the plume centerline. Notice that the smoke plume does not always rise straight up because of air currents within the large test hall.

Figure A-15: Fire plumes in ICFMP BE #2. Courtesy Simo Hostikka, VTT Building and Transport, Espoo, Finland.

Table A-17 lists specific location parameters required for the plume temperature correlation. The heat release rate values are listed in Volume 7. Table A-16 compiles the graphical comparisons between experimental measurements for plume temperature and the correlation predictions. The corresponding relative differences are listed in Table A-18.

Table A-17: Target location information for plume correlations

Plume	TG.1	TG.2
Target height [m]	6	12
Fire elevation [m]	0	
Fire diameter [m]	1.6	
Rad fraction, Xr	0.4	

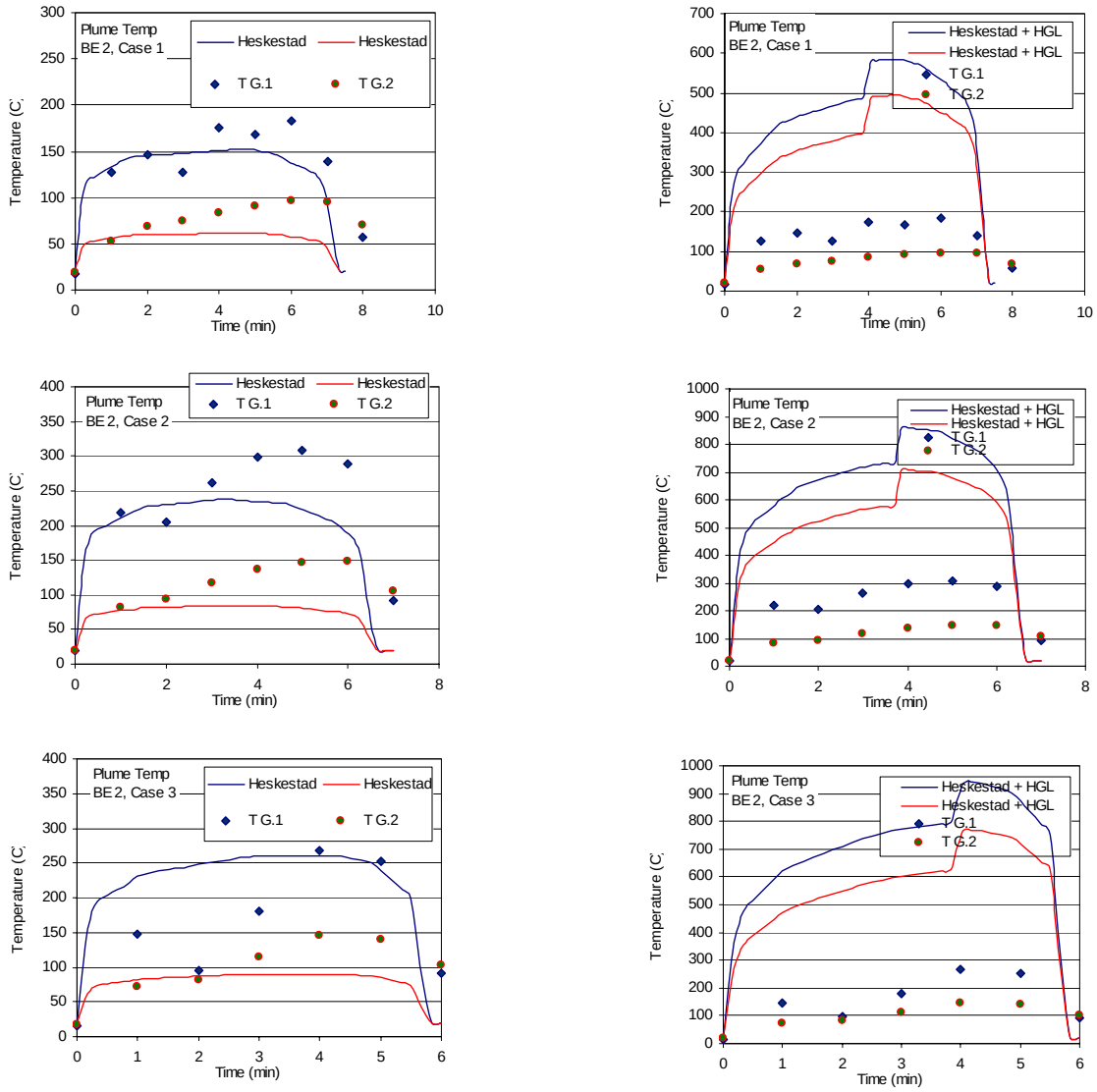

Figure A-16: Near-ceiling gas temperatures, FM/SNL Series, Sectors 1 and 3 compared with Heskestad's plume temperature correlation.

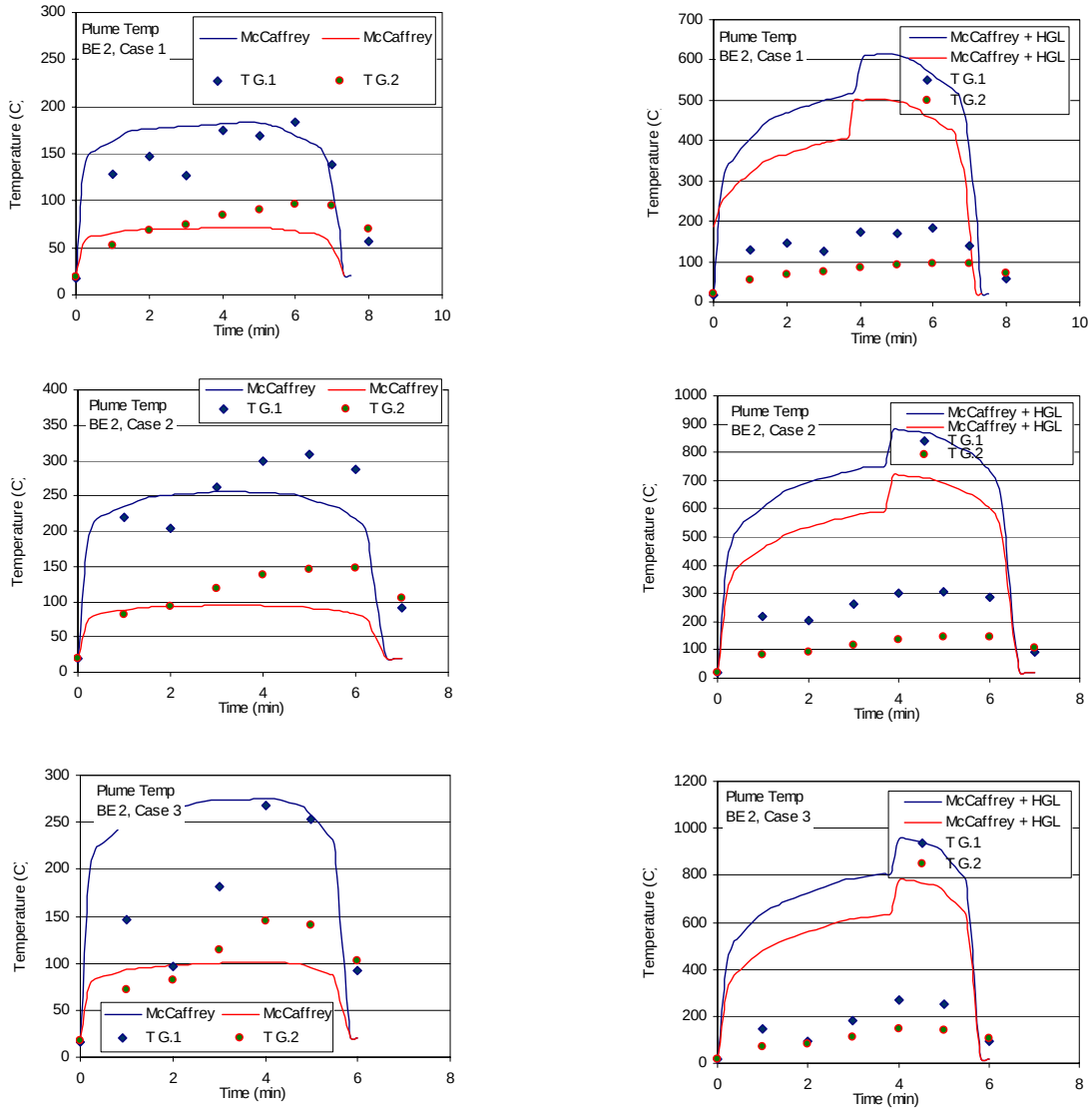

Figure A-17: Near-ceiling gas temperatures, FM/SNL Series, Sectors 1 and 3 compared with McCaffrey plume temperature correlation.

Figure A-16 and Figure A-17 above illustrate the graphical comparison between experimental plume temperatures and MAGIC prediction for the three cases in ICFMP BE #2. The corresponding relative differences are listed in Table A-18.

Table A-18: Relative differences of hot gas layer temperature and height in ICFMP BE #2

			ΔE (°C)	ΔM (°C)	Relative Difference	ΔM (°C)	Relative Difference
Case 1	TG.1	McCaffrey	166.0	163.2	-2%	595.8	259%
	TG.2	McCaffrey	79.0	51.7	-35%	484.3	513%
	TG.1	Heskestad	166.0	132.6	-20%	565.2	240%
	TG.2	Heskestad	79.0	41.7	-47%	474.3	500%
Case 2	TG.1	McCaffrey	288.0	237.1	-18%	858.8	198%
	TG.2	McCaffrey	128.0	75.0	-41%	698.4	446%
	TG.1	Heskestad	288.0	218.0	-24%	839.1	191%
	TG.2	Heskestad	128.0	64.3	-50%	687.7	437%
Case 3	TG.1	McCaffrey	252.0	254.9	1%	933.2	270%
	TG.2	McCaffrey	128.0	80.6	-37%	759.0	493%
	TG.1	Heskestad	252.0	241.1	-4%	919.5	265%
	TG.2	Heskestad	128.0	70.1	-45%	748.4	485%

A.3.2 The FM/SNL Test Series

In Tests 4 and 5, thermocouples were positioned near the ceiling directly (5.9 m) over the fire pan. In Test 21, the fire pan was inside a cabinet. For that reason, no plume temperature comparison has been made. Figure A-18 presents the graphical comparisons and Table A-20 lists the corresponding relative differences. Target location inputs are listed in Table A-19.

Table A-19: Target location information for plume correlations

Plume	TG.1
Target height [m]	5.9
Fire elevation [m]	0
Fire diameter [m]	0.8
Xr	0.4

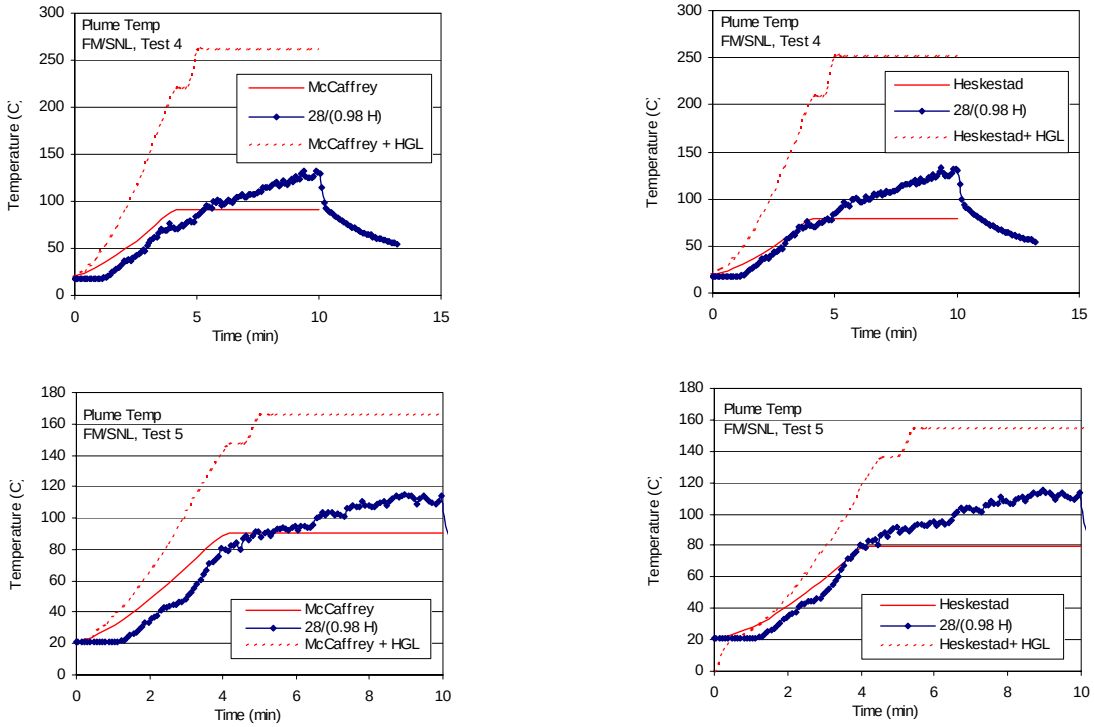

Figure A-18: Near-plume temperatures, FM/SNL Series, Sectors 13.

Table A-20: Relative differences of plume temperature in FM/SNL tests

			No Hot Gas Layer Effects			Hot Gas Layer Effects		
			ΔE (°C)	ΔM (°C)	Relative Difference	ΔE (°C)	ΔM (°C)	Relative Difference
Test 4	McCaffrey	28/98H	115.8	70.7	-39%	115.8	242.2	109%
	Heskestad	28/98H	115.8	59.6	-49%	115.8	231.1	100%
Test 5	McCaffrey	28/98H	93.8	70.7	-25%	93.8	145.5	55%
	Heskestad	28/98H	93.8	59.6	-36%	93.8	134.5	43%

A.4 Flame Height

Flame height is recorded by visual observations, photographs or video footage. Videos from the ICFMP BE # 3 test series and photographs from BE #2 are available. It is difficult to precisely measure the flame height, but the photos and videos allow one to make estimates accurate to within a pan diameter.

A.4.1 ICFMP BE #2

Shown in Figure A-19 are Heskestad's correlation predictions for flame height. Figure A-20 contains photographs of the actual fire. The height of the visible flame in the photographs has been estimated to be between 2.4 and 3 pan diameters (3.8 m to 4.8 m). The height of the simulated fire fluctuates from 5 m to 6 m during the peak heat release rate phase.

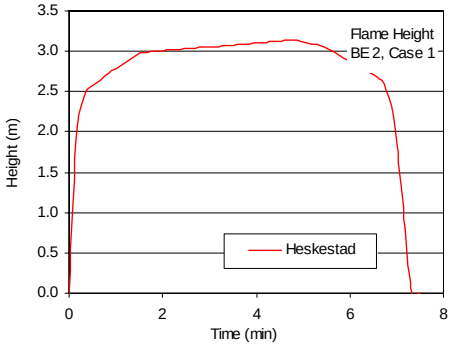

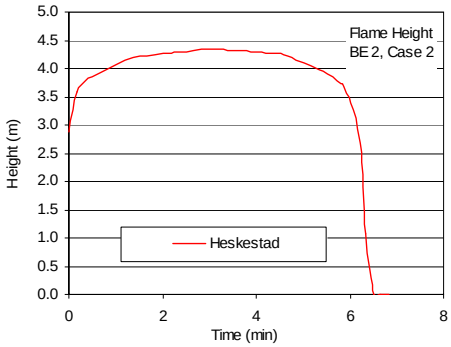

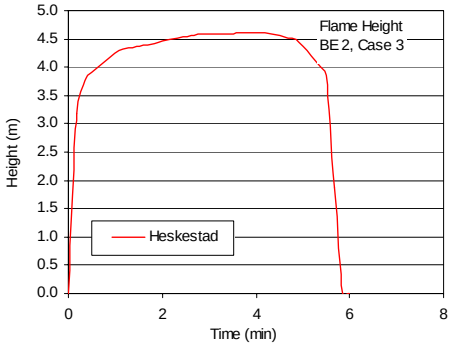

Figure A-19: Flame heights for ICFMP BE # 2

Figure A-20: Photographs of heptane pan fires, ICFMP BE #2, Case 2. Courtesy, Simo Hostikka, VTT Building and Transport, Espoo, Finland.

A.4.2 ICFMP BE #3

No measurements were made of the flame height during BE #3, but numerous photographs were taken. Figure A-21 is one of these photographs. These photographs provide at least a qualitative assessment of the Heskestad flame height prediction. Recall that the size of the door is 2.0 m high. Inspection of the picture suggests that the flame height, at least is some of its oscillations, can be more than 2.0 m high.

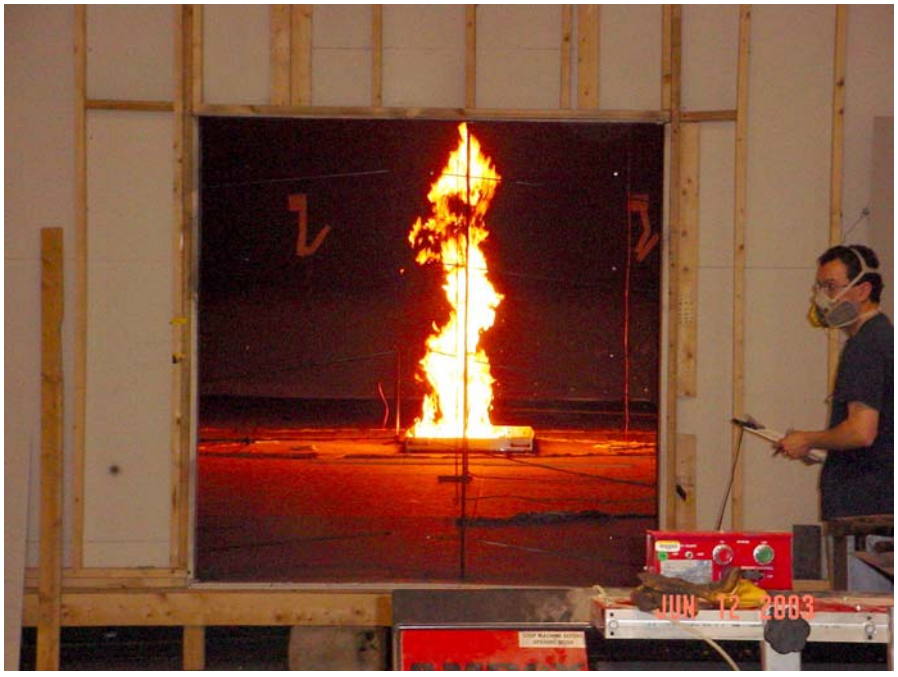

Figure A-21: Photograph and simulation of ICFMP BE #3, Test 3, as seen through the 2 m by 2 m doorway. Photo courtesy of Francisco Joglar, SAIC.

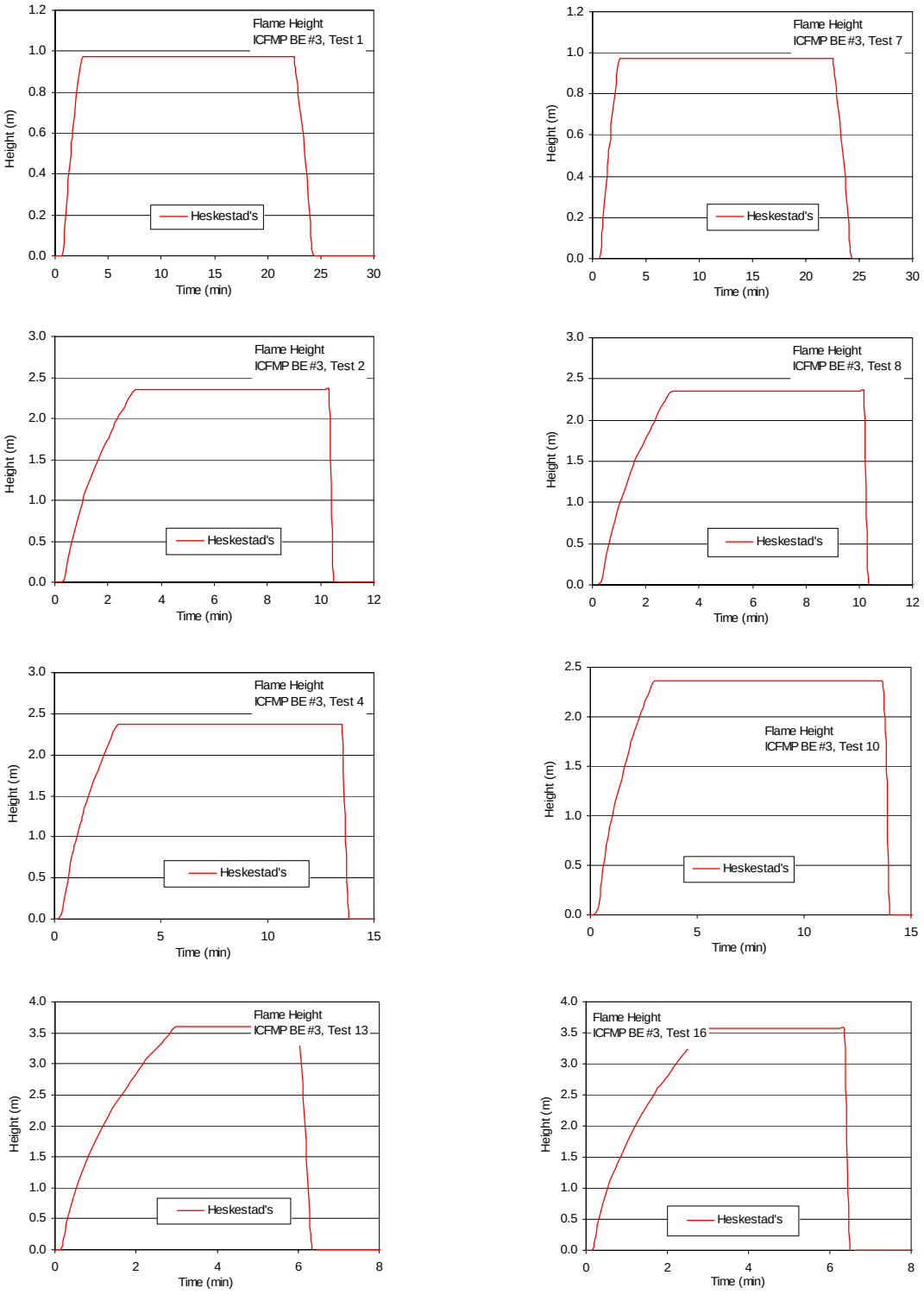

Figure A-22: Near-ceiling gas temperatures, ICFMP BE #3, closed door tests.

Open Door Tests

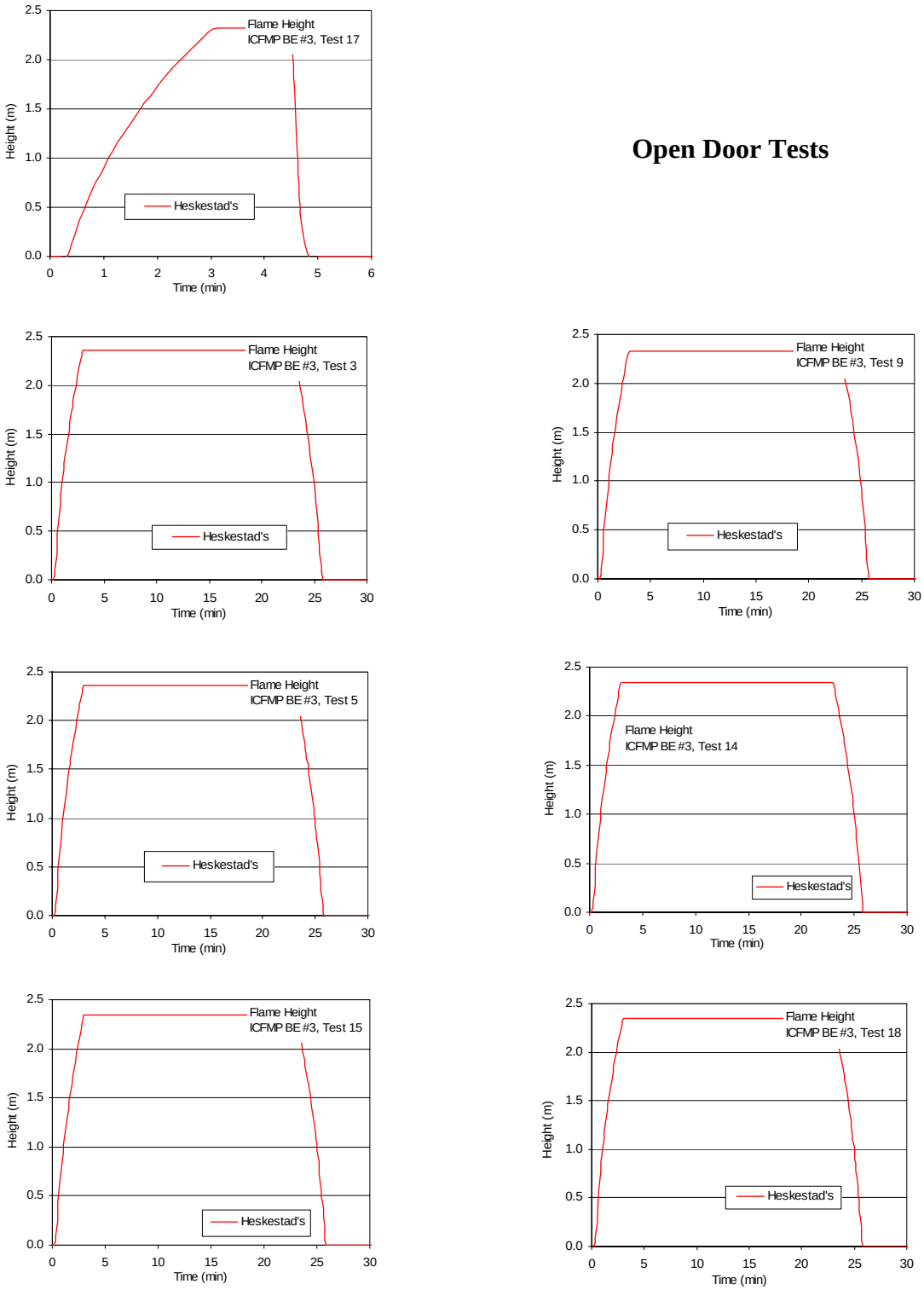

Figure A-23: Flame heights, ICFMP BE #3, open door tests

A.5 Radiant Heat Flux

Radiant heat flux data is available only from ICFMP BE #3. This data is compared with results from the point-source radiant heat flux model available in the FIVE-Rev1 library of equations.

The four radiometers selected for this study are labeled Rad Gauge 1, 3, 7 and 10. Table A-21 lists the effective distance from the gauges to the fire. A radiation fraction of 0.4 was assumed for the analysis. The heat release rate profiles for each of the tests is described in Volume 7 of this report.

Table A-21: Effective horizontal distances from the fire to the rad gauges

Instrument	All Others	Test 14	Test 15	Test 18
R Gauge 1 [m]	3.70	5.16	2.18	2.76
R Gauge 3 [m]	3.45	4.74	2.55	2.98
R Gauge 7 [m]	3.44	4.45	3.14	3.44
R Gauge 10 [m]	3.75	2.41	5.91	5.83

Figures A-24 to A-27 provide the graphical comparisons between the point source radiation predictions and the experimental measurements. When available, the corresponding measured total heat flux was also included in the comparison. Finally, Table A-22 lists the calculated relative differences for this comparison.

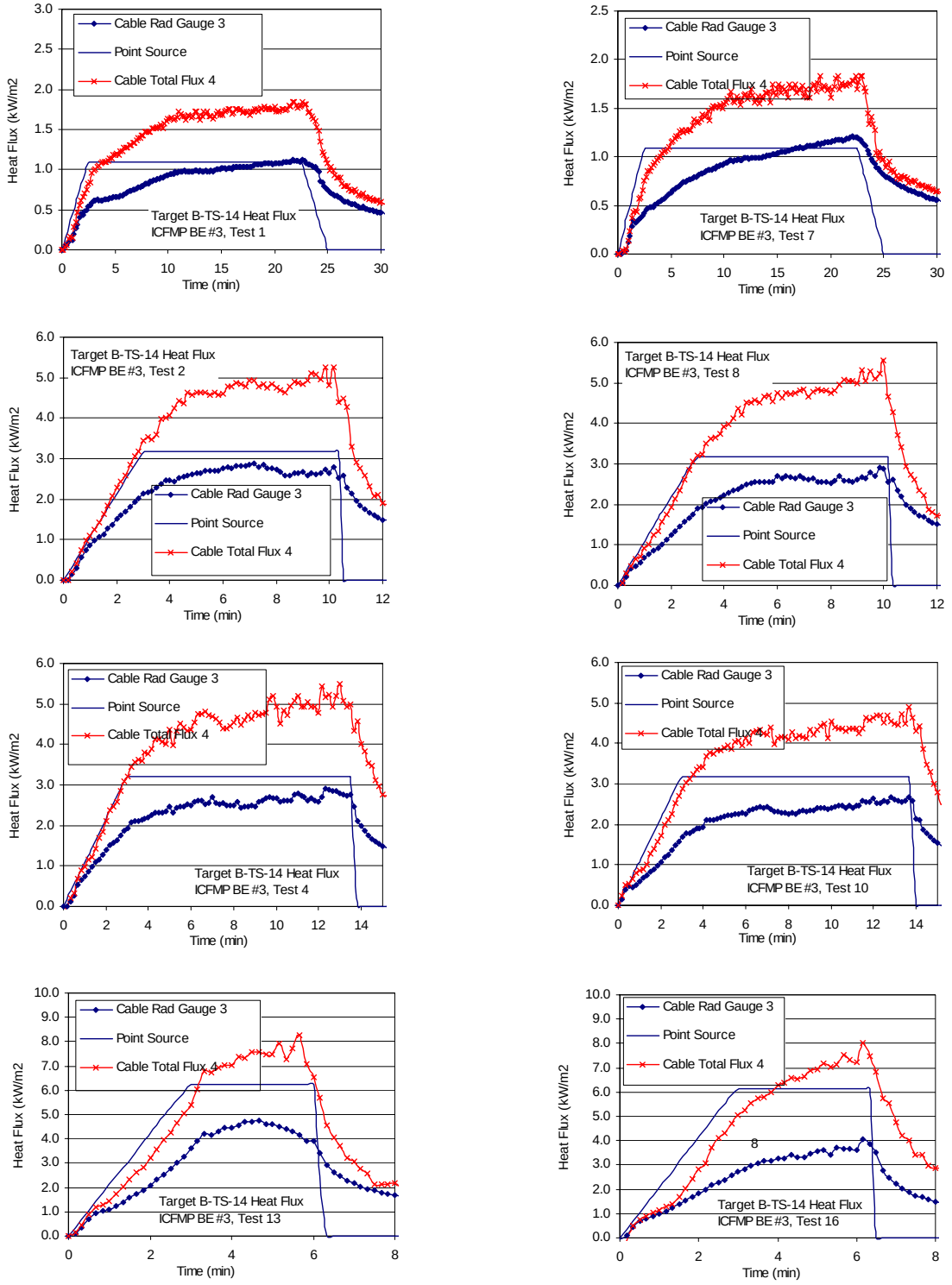

Figure A-24: Radiative heat flux to cable B

Open Door Tests

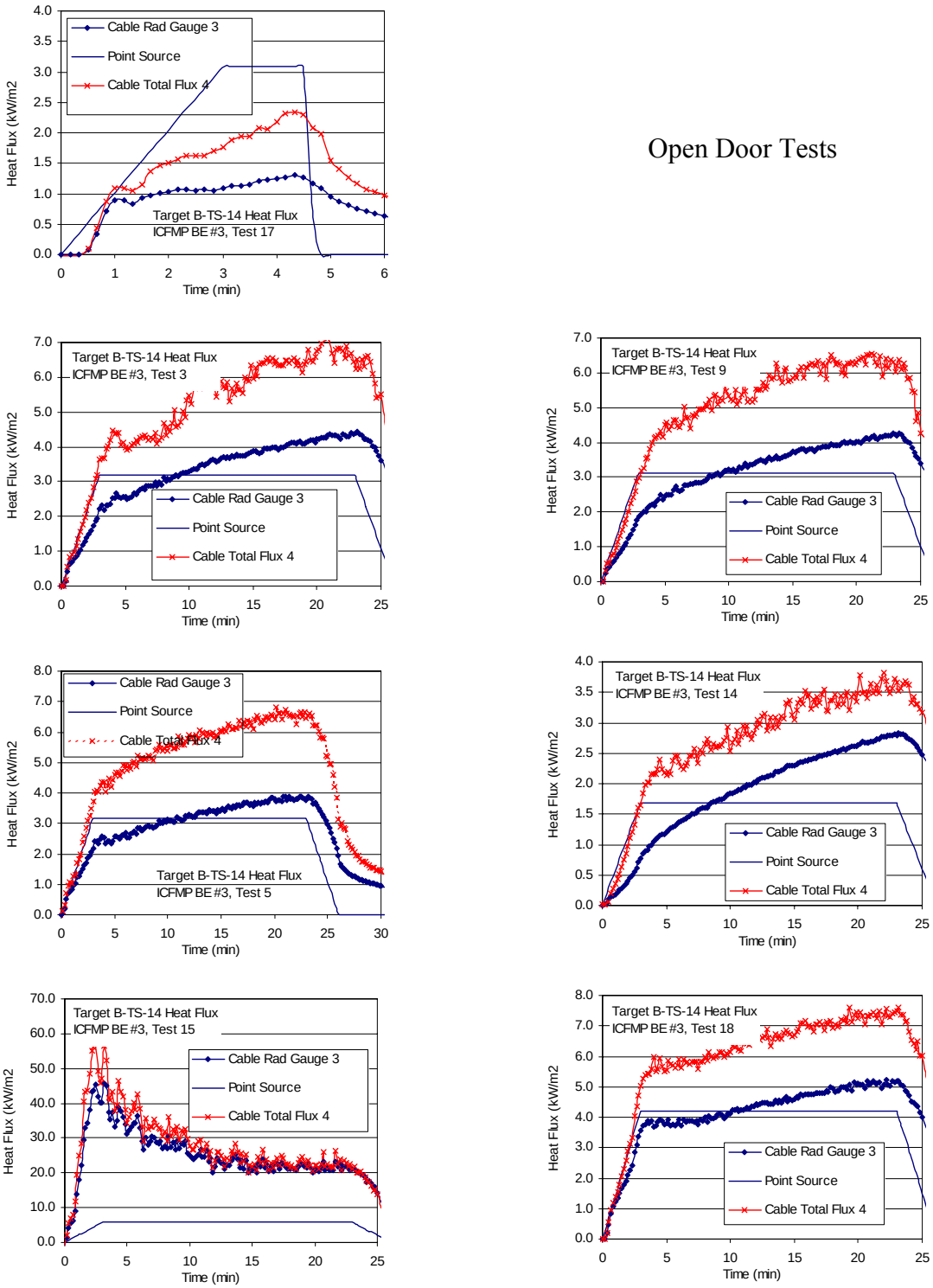

Figure A-25: Radiative heat flux to cable B

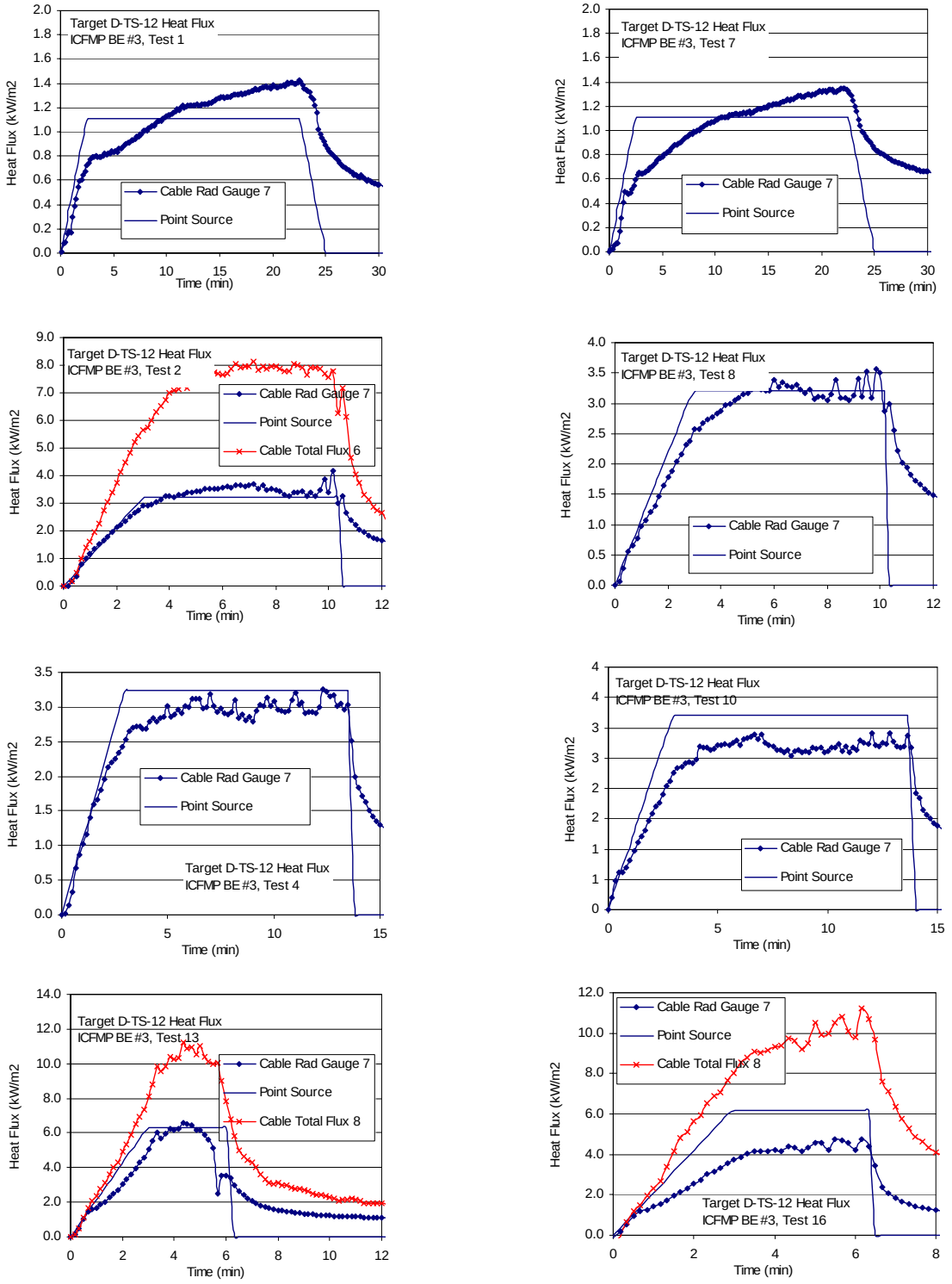

Figure A-26: Radiative heat flux to cable D

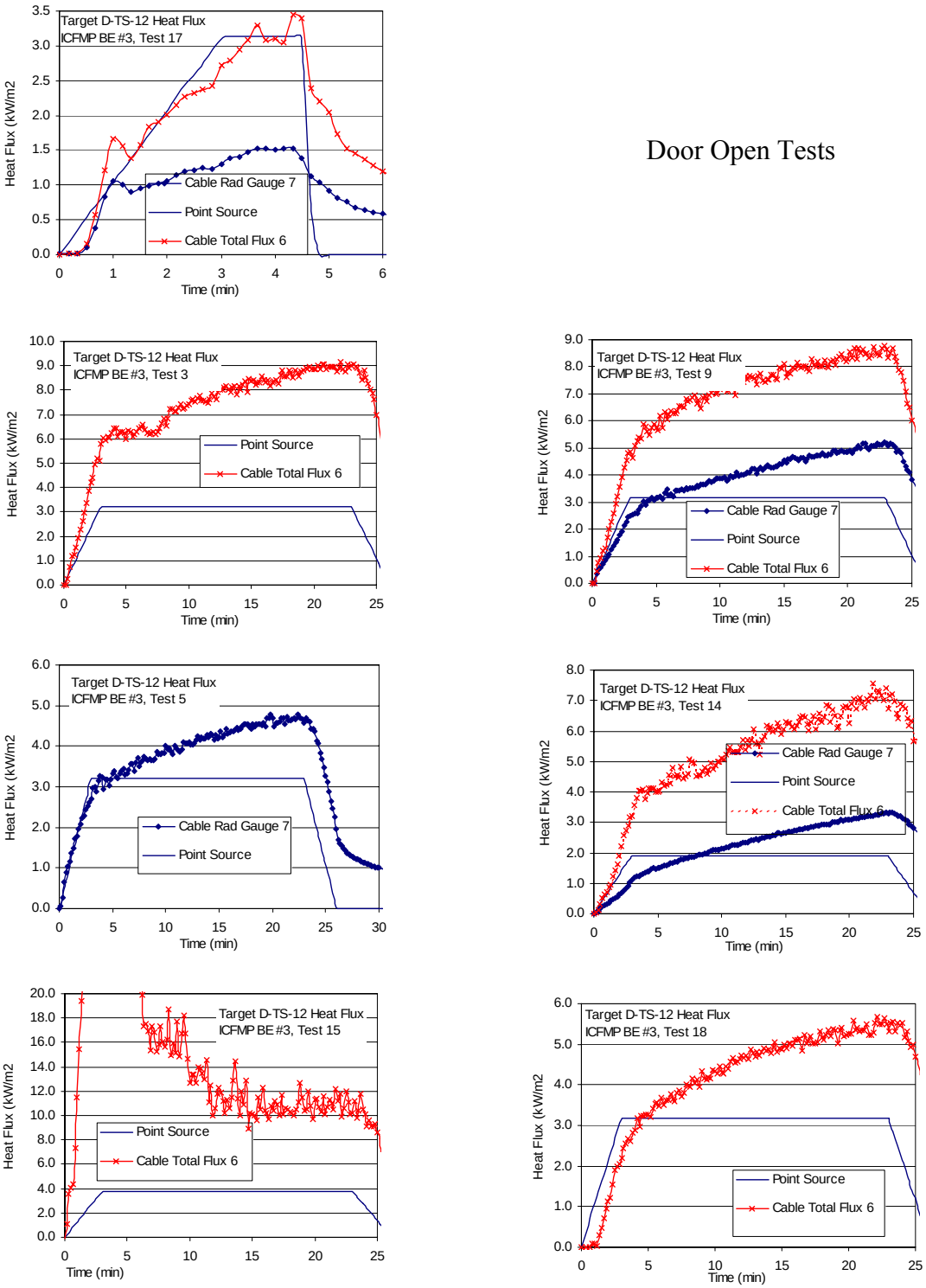

Figure A-27: Radiative heat flux to cable D

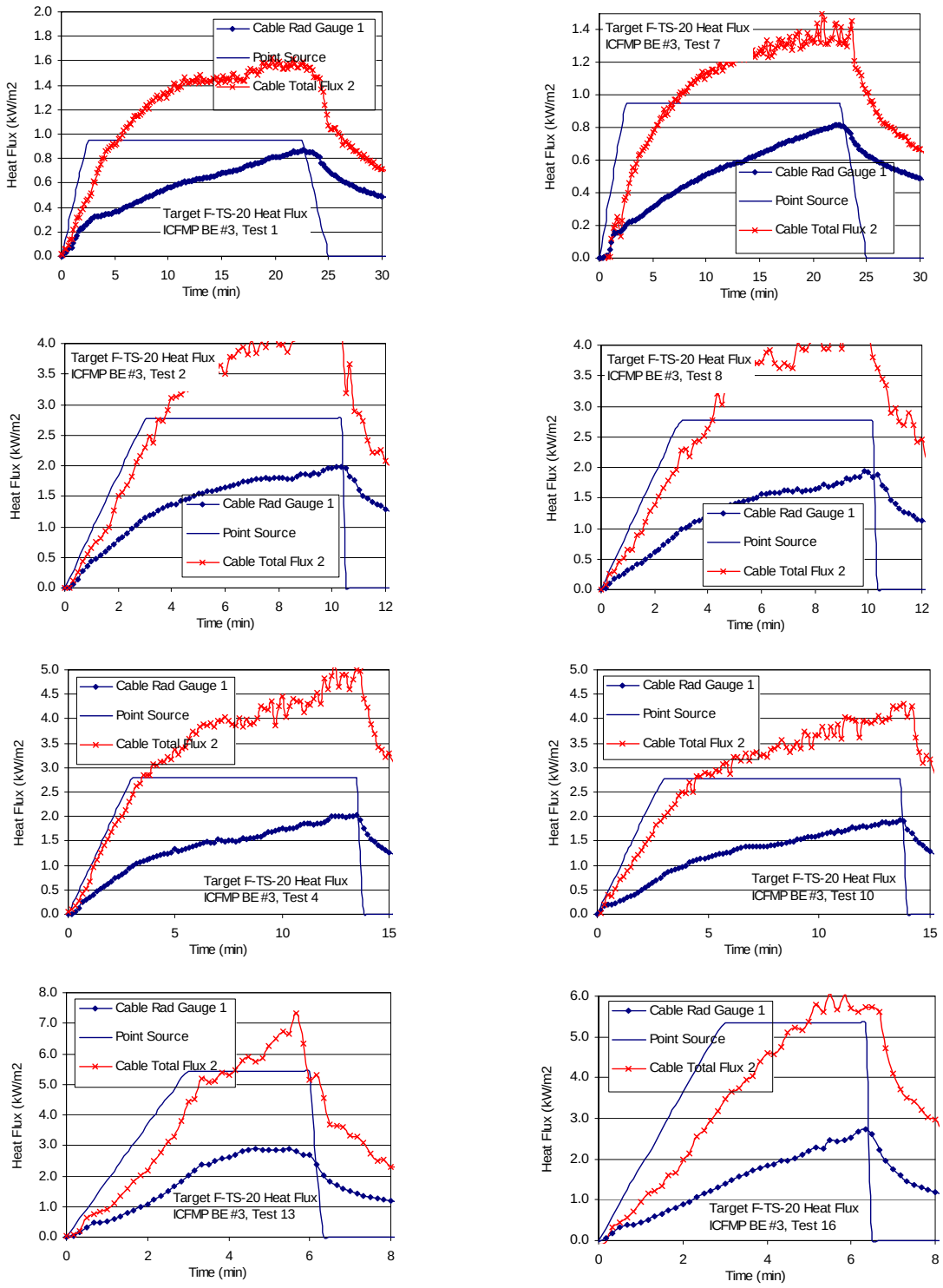

Figure A-28: Radiative heat flux to cable F

Open Door Tests

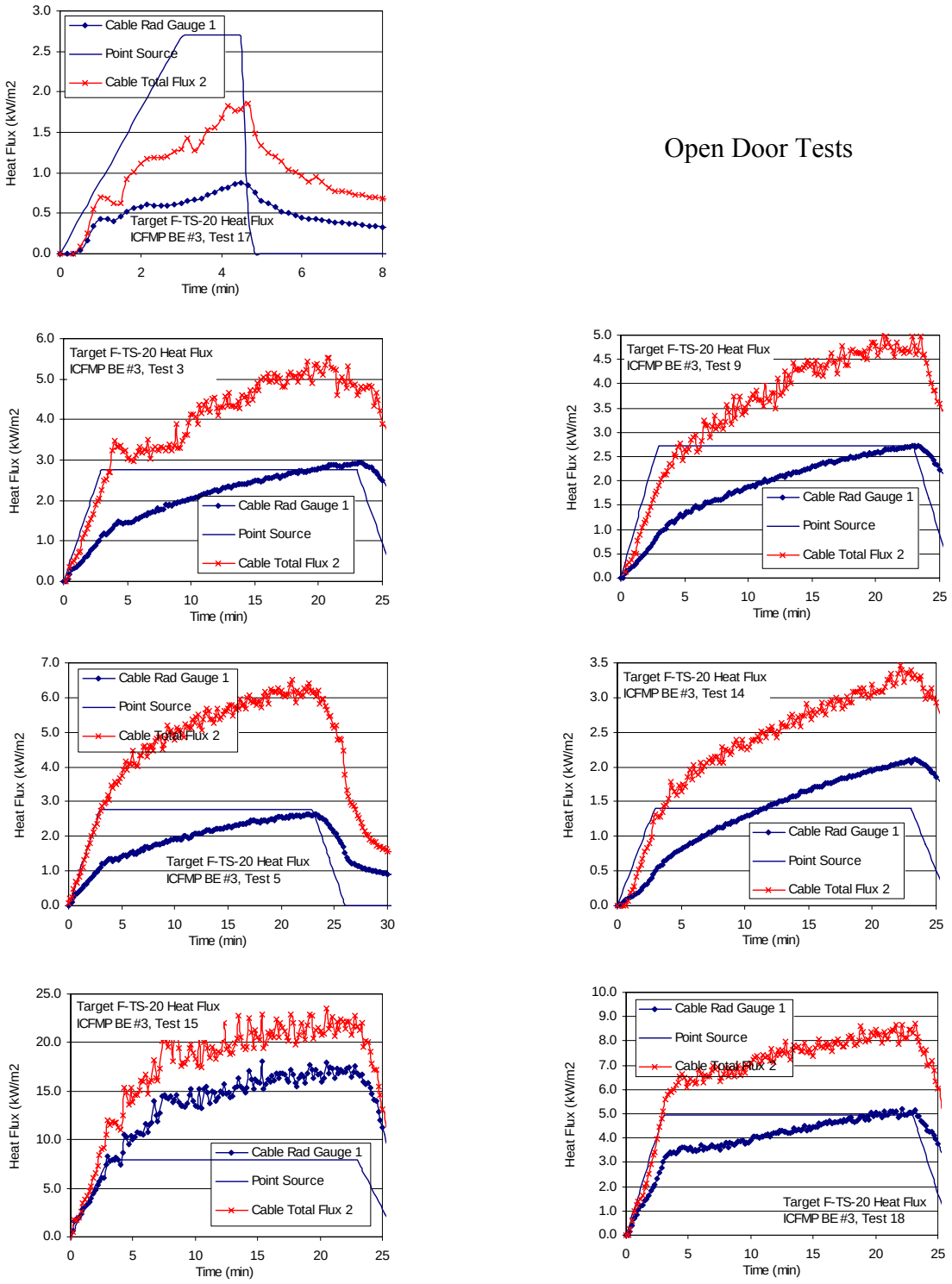

Figure A-29: Radiative heat flux to cable F

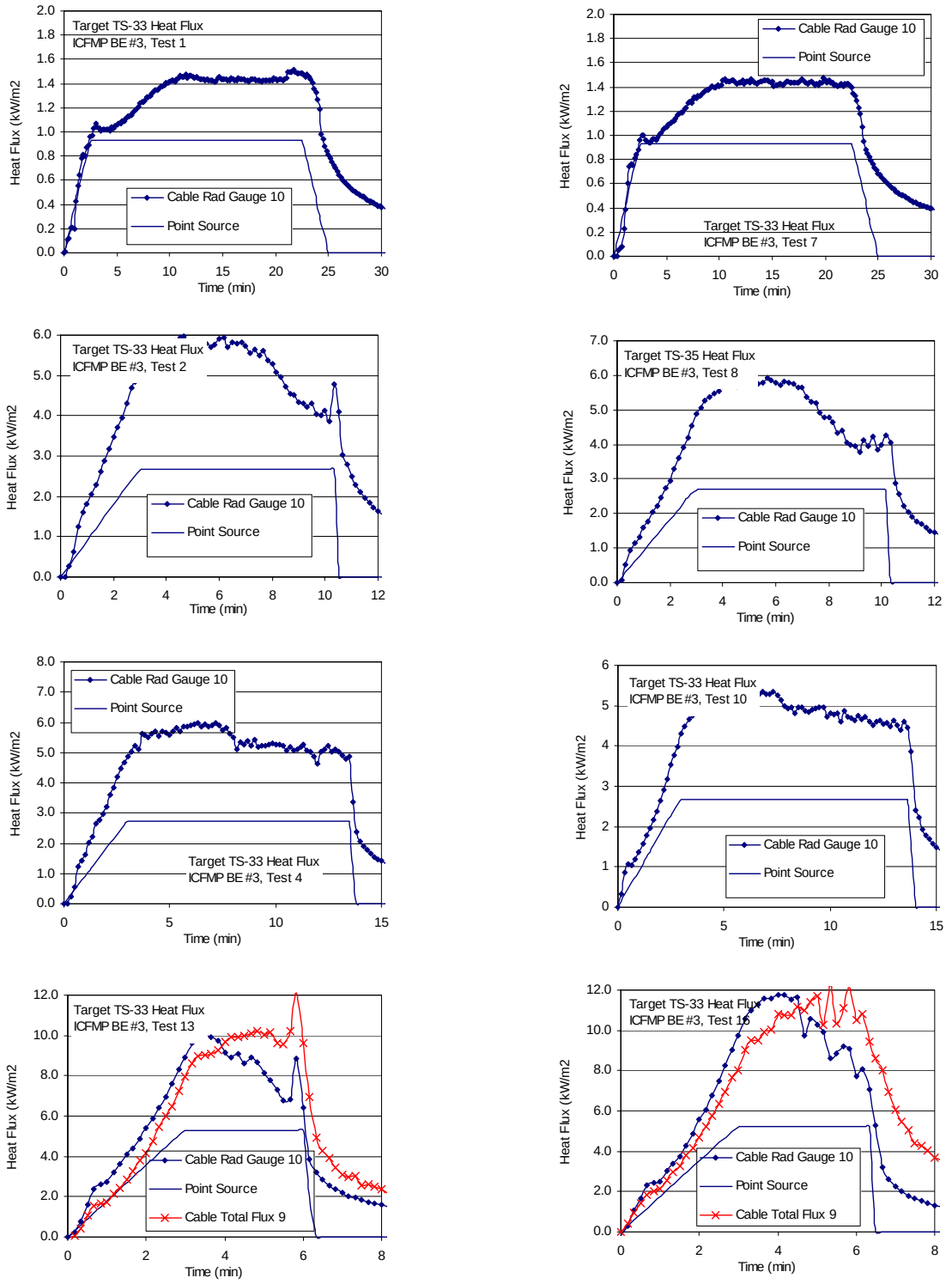

Figure A-30: Radiative heat flux to cable G

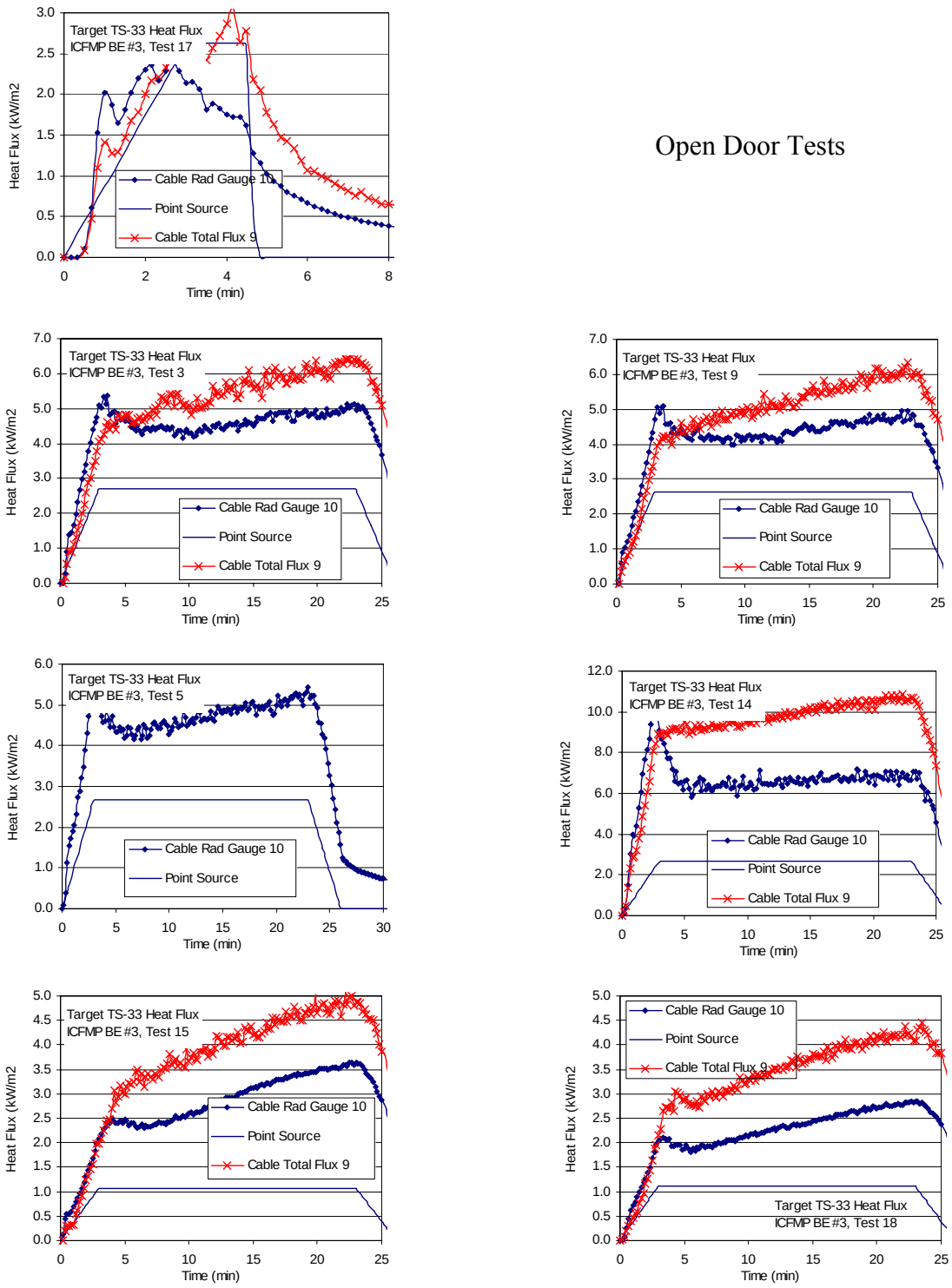

Figure A-31: Radiative heat flux to cable G

Table A-22: Relative differences for radiative heat flux

Gauge 1	ΔE (kW/m^2)	ΔM (kW/m^2)	Relative Difference	Gauge 3	ΔE (kW/m^2)	ΔM (kW/m^2)	Relative Difference
Test 1	0.87	0.95	10%	Test 1	1.12	1.09	-3%
Test 7	0.82	0.95	16%	Test 7	1.21	1.09	-9%
Test 2	1.99	2.76	39%	Test 2	2.88	3.17	10%
Test 8	1.93	2.76	43%	Test 8	2.91	3.17	9%
Test 4	2.02	2.80	38%	Test 4	2.92	3.21	10%
Test 10	2.73	2.72	0%	Test 10	2.69	3.17	18%
Test 13	2.90	5.42	87%	Test 13	4.77	6.22	30%
Test 16	2.76	5.35	94%	Test 16	4.12	6.14	49%
Test 17	0.88	2.70	206%	Test 17	1.30	3.10	138%
Test 3	2.95	2.76	-6%	Test 3	4.45	3.17	-29%
Test 9	1.93	2.76	43%	Test 9	4.29	3.12	-27%
Test 5	2.65	2.76	4%	Test 5	3.88	3.17	-18%
Test 14	2.12	1.41	-34%	Test 14	2.84	1.67	-41%
Test 15	18.29	7.88	-57%	Test 15	46.49	5.77	-88%
Test 18	5.18	4.93	-5%	Test 18	5.23	4.22	-19%

Gauge 7	ΔE (kW/m^2)	ΔM (kW/m^2)	Relative Difference	Gauge 10	ΔE (kW/m^2)	ΔM (kW/m^2)	Relative Difference
Test 1	1.44	1.11	-23%	Test 1	1.51	0.93	-39%
Test 7	1.35	1.11	-18%	Test 7	1.47	0.93	-37%
Test 2	4.16	3.21	-23%	Test 2	5.97	2.69	-55%
Test 8	3.55	3.21	-10%	Test 8	6.03	2.69	-55%
Test 4	3.26	3.24	0%	Test 4	6.00	2.72	-55%
Test 10	2.91	3.21	10%	Test 10	5.42	2.69	-50%
Test 13	6.58	6.29	-4%	Test 13	10.06	5.27	-48%
Test 16	4.83	6.21	28%	Test 16	11.96	5.20	-57%
Test 17	1.52	3.13	106%	Test 17	2.42	2.62	9%
Test 3		3.21		Test 3	5.36	2.69	-50%
Test 9	5.26	3.16	-40%	Test 9	5.15	2.65	-49%
Test 14	3.32	1.90	-43%	Test 5	5.45	2.69	-51%
Test 5	4.78	3.21	-33%	Test 14	10.50	2.67	-75%
Test 15		3.81		Test 15	3.73	1.07	-71%
Test 18		3.18		Test 18	2.85	1.10	-61%